POLITECNICO DI MILANO

Research Doctorate course in Bioengineering

XXIX cycle

POLITECNICO
MILANO 1863

PhD Thesis

New clinical indexes for the automatic management of the dialysis treatment

PhD Candidate

Domenico Vito

Supervisor: Maria Laura Costantino

Co-supervisor: Giustina Casagrande

Tutor: Anna Maria Bianchi

Quelli che ballavano erano visti come pazzi
da quelli che non sentivano la musica.

F.NIetzche

“Stranamente, non abbiamo mai avuto più informazioni di adesso, ma continuiamo a non sapere che cosa succede.”

PAPA FRANCESCO

Abstract

End stage uremic patients number continues to increase involving high percentages of elderly, predisposed to comorbidities. Considering the high number of functions carried out by the kidneys, it can be easily understood how a kidney impairment could involve the whole body and in its most severe form becomes incompatible with the survival. Dialysis is the elective treatment for chronic kidneys diseases: it artificial substitutes the renal functions of removing waste and excess water from the blood. The tolerance to the treatment can vary among different individuals, also in the presence of similar prescriptions due to the peculiar patient-machine interaction. Intradialysis hypotension (IDH) is one of the main short – term hemodialysis complications, occurring in 25-30% of cases and there are no standardized clinical protocols that provide an accurate blood pressure monitoring and the preventive

The goal of the research is to develop new instruments for the evaluation of the dialysis treatment in order to enable its automatic management. The study has been developed in collaboration with four clinical centres between Italy and Switzerland inside the DialisYS project. The development of innovative indexes has been based data on recorded during real hemodialysis treatments. A Federated DataBase System (FDBS) approach has been adopted to construct a common data repository. The storage system has been built by the Dialysis Data Infrastructure (DDI), a unique multilevel standardized data structure supported by the Dialysis MATlib (DM), an embedded Matlab® library, that's able to threat and manage data in the different formats collected from 4 different clinics. The Dialysis Data Infrastructure currently contains the acquisition of 1020 dialysis sessions performed on a total of 145 patients A statistical analysis has been conducted on the collected data in order to find the potential risk factor related to IDH onset. both at early stages and during the treatment. A predictive index, J, in two version J1 andJ2 was defined as a weighted patient-specific combination of potential risk factors in order to predict the IDH onset at the early stage of the treatment. The indexes has been also tested in their predictive ability, experimenting also different threshold for the prediction.

The statistical analysis performed considering the intra-treatment period has also a multiparameter criterion, for the intra-treatment identification of IDH onset has been also developed Besides the inferential statistical analysis a machine learning approach has been tested to predict IDH event from pre-dialysis conditions and considering the IDH prediction as a binary classification problem. Three different algorithm has been explored for the prediction of IDH event as result of a binary classification problem: Random Forest, Artificial Neural Networks and Support Vector Machines. The considered dataset presented unbalanced classes: the class of interest (i.e. sessions with hypotension events) was only about the 10% of the total. In order to get effective learning from the data, minority class oversampling was required. Different techniques (e.g. bootstrap, SMOTE) combinations were tested and compared. The results show that J1 index allow predicting

the 77% of the IDH events, when the threshold is set equal to 1. The use of center specific thresholds allows slightly improving index specificity and sensitivity, but does not substantially alter the results. Indeed the multiparameter criteria allows to identify the 75,56%of sessions with hypotension as defined by IDH-D, with the 24,44% of false positives. Among the tested machine learning algorithm, the SVM model balanced with high minority class SMOTE and no majority class down sampling techniques, shows the best performance and the smallest variability interval (e.g. overall accuracy: 88.26% ± 2.80%). In conclusion this work provides a set of indexes and alghorithms for the prediction of the IDH onset during the dialysis treatment. They represent a first step in the direction of a better an more personalized dialysis treatment.

Acknowledgments

It's been a path, a catharsis between heavens and hells joys and sorrows. A purification in the blood. All set off by a sound, the will not to give up the hold on that life which makes us unique, but that sometimes escapes us. Beyond our will It accompanied 'been a path, as in a fantasy saga by squires friends, fairies and tales. A run in the woods. But it was great and tragic, like any training. Fears and hopes on this trip in the know and in whether. And like every experience every trip with the go due.

Thanks first and foremost to my family, always beside my headlamp for better or for worse Mamma, Papà, Giovanni how to thank you? Not just no words. My supervisor and my team, alongside of su(o)pport me Maria Laura, Thanks Giustina, ubiquitous Camilla, Francis and Luke, Thanks to you first Thanks to the guys I've met during this path Giulia, Stefania, Elena, Alessandro, Andrea, Stefano, Alessandro, Giada e Paolo. Thanks to my dearest friends Giacomo, Chris (Luke), Debbie, Claudia Thanks to my cousins - Thanks to Stephen, Vale, Matt, Samu, Thanks to Gabi, and to all Thanks to the friends of Ema LaBS, prof. Migliavacca, Dubini, Claudio, Monica, Gigi, Gigi, Iron, Lele, and Elena C. Elena, thanks to Eros Thanks to the Faculty of bioengineering all it was a nice trip, intense, cathartic .... Thank God I hope I did not forget anyone If not

Thank you all

Ringraziamenti

E’ stato un percorso, una catarsi tra paradisi e inferni gioie e dolori. Una purificazione nel sangue. Il tutto partì da un suono, dalla volontà di non mollare dal tenersi stretti quella vita che ci fa unici ma che a volte ci sfugge. Al di la della nostra volontà E’ stato un percorso accompagnato, come in una saga fantasy da amici scudieri, fate e racconti. Una corsa nel bosco. Ma è stato bello e tragico, come ogni formazione. Paure e speranze in questo viaggio nel sapere e dentro se. E come ogni esperienza ogni viaggio i grazie vanno dovuti. Grazie in primis alla mia famiglia, sempre accanto mio faro nel bene e nel male Mamma, Papà, Giovanni come ringraziarvi? Non basta nessuna parola. La mia supervisor e il mio team, accanto a su(o)pportarmi grazie Maria Laura, grazie Giustina, onnipresenti Camilla, Francesco e Luca, Grazie Grazie ai ragazzi che ho incontrato in questo percorso Giulia, Stefania, Elena, Alessandro, Andrea,**Stefano e Alessandro, Giada e Paolo Grazie ai miei amici piu cari Giacomo, Chris (Luca),Debbi Ai miei Cugini Grazie a Stefano,Vale, Matt, Samu, Grazie a Gabi, e a tutti Grazie agli amici del LaBS Ema, prof. Migliavacca, Dubini, Claudio, Monica, Gigi, Gigi, Ferro, Lele, Elena C. e Elena, Grazie a Eros Grazie alla facoltà di bioingegneria tutta è stato un** viaggio bello, intenso, catartico.... Grazie a Dio
Spero di non aver dimenticato nessuno
Se non,

Grazie a tutti

Domenico

Contents

CONTENTS

Chapter 1 – Anatomy and Physiology

1.1 The urinary system

1.1.1 The kidneys

The urinary system (Figure 1.1), whose main function is the elimination of waste and excess fluid, consists of two kidneys connected to the bladder by the ureters, which carry urine produced there.
The kidneys are two symmetrical organs located in the back-peritoneum at the level of inner coast and in the adult each has a weight of about 250g[2].
Each kidney is about 12cm long and weights about 150g and it is situated at the level of the twelfth thoracic vertebra.
Kidneys work by filtering blood: their key role is to maintain homeostasis.
Homeostasis mean the maintenance of nearly constant conditions in the internal balance of water and metabolites [3].
The principal kidneys functions are:

- water content regulation;
- electrolyte balance in body fluids by controlling the concentrations of [Ca $^{2+}$], [Na $^{+}$],[K +], [Cl $^{-}$], [HCO 3 $^{-}$], [H +], [Mg 2+], [$PO^4{}_3$ $^{-}$], glucose, amino acid uric acid and urea by means of integration of processes of filtration, reabsorption and secretion at the level of the nephron;
- acid-base equilibrium maintenance;
- metabolic catabolites excretion;
- hormones synthesis and secretion

They are also responsible for toxic materials (e.g. protein metabolism catabolites such as urea, creatinine and uric acid) elimination from the body through the urine.

As the main function of kidneys is regulating concentrations of substances in the blood, a high blood flow to the kidney is essential. Renal blood flow usually amounts to about 1200 ml / min, accounting for approximately 21% of cardiac output [9].
The rate of cardiac output through the kidney is called the renal fraction [5].
The renal artery within the kidney is divided into smaller and smaller vessels as they sink into the renal cortex-giving rise to afferent arterioles and further branch into the glomerular capillaries.

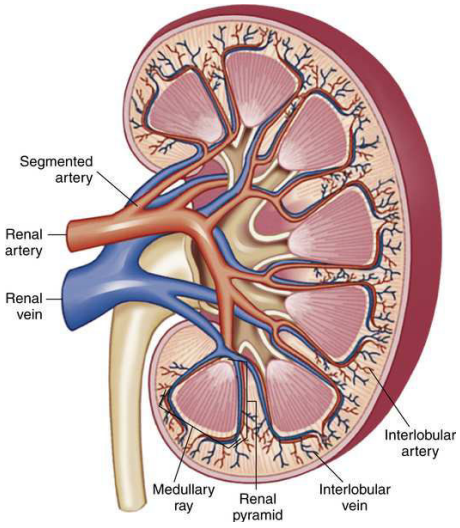

Figure 1.1. Kidney longitudinal section, showing the major blood vessels arrangement

Kidneys are placed on either side of the abdominal aorta.
There are two main branches of the abdominal aorta called the renal arteries (Figure 1.1). The renal artery branches out to form the afferent arterioles, which then form the glomerular capillaries of individual glomeruli. The glomerular capillaries then join to form the efferent arterioles, which in turn diffuse into peritubular capillaries and the vasa recta.
The blood leaves the kidney through two renal veins, one from each kidney, which carries the blood back to the vena cava and then back up to the heart.
Blood flow to the kidneys is dependent on hydration and cardiac output.

1.1.2 The nephron

The kidney is composed of about 1,000,000 to 1.2000000 of nephrons, which constitute the functional and structural unit of the renal system.
The nephron, in Figure 1.2, is constituted by a spherical structure, called the Malpighi corpuscle, where it is produced the glomerular filtrate, and a tubular part, the renal tubule, responsible for the reabsorption and processing of the filtrate up to the production of urine.
The corpuscle is constituted by the glomerulus, which is a dense network of capillaries that filters the plasma, and the Bowman's capsule, which surrounds the glomerulus and collects the filtrate [3].

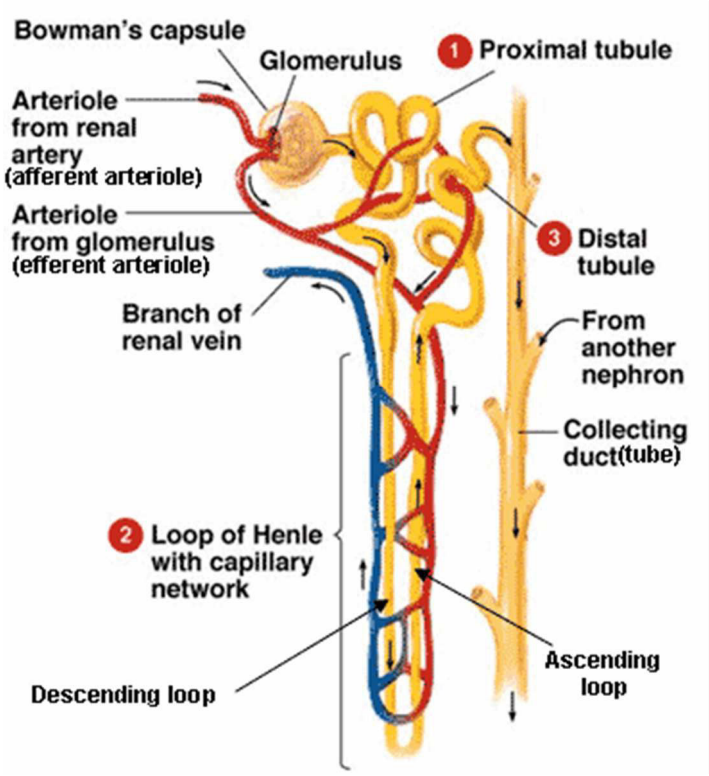

Figure 1.2. Structure of the Bowman's capsule

The glomerulus is the part of the nephron responsible, through pressure of gradients, of the ultrafiltration of plasma.
The glomerulus filters all the molecules below the molecular size of albumin (64 kDa), pass the filter and enter the into the tubule where It is converted into urine [4].
The peritubular capillaries in turn feed into the venous system of vessels to form the renal vein-protruding organ always through the hilum.
Renal circulation is the only one in the body that it has two capillary networks, glomerular and peritubular, arranged in series.
The afferent and efferent arterioles help regulate hydrostatic pressure in both capillary networks; adjusting the resistance, the kidney controls the speed of filtration to glomerular capillary level and / or reabsorption of the peritubular capillaries in response to the needs of homeostasis of the body.
Due to the pressure in its capillaries, the glomerulus works by determining a continuous filtration; the peritubular capillary system, by virtue of its low pressure, runs continuously attracting liquid in the capillary [2].
All molecules below the molecular size of albumin (that is, 68 kDa)[4] passes into the proximal tubule and the loop on Henle the filter and enter a long tubule in which the filtered fluid is converted into urine on its way to the pelvis of the kidney called 'distal tubule'.
The 'distal tubule' consists in the proximal convoluted tubule, the loop of Henle and the distal convoluted tubule.
The tubular epithelial cells reabsorb water, small proteins, amino acids, carbohydrates and electrolytes, thereby regulating plasma osmolality, extracellular volume, blood pressure and acid–base and electrolyte balance [3].
Non-reabsorbed compounds pass from the tubular system into the collecting ducts to form urine.
The space between the tubules is called the interstitium and contains most of the intrarenal immune system, which mainly consists of dendritic cells, but also of macrophages and fibroblasts (Figure 1.2)[4].

1.2 Renal Failure

Any deficit in kidneys power to eliminate toxic substances (e.g. urea, creatinine, phosphates and other corporeal acids) or to correctly re-absorb water and nutrients, resulting in the inability to maintain constant the composition of blood and fluid balance, is definable as renal failure [12].
Renal failures can be classified as acute (ARF) or chronic (CRF).
The main consequences of renal functionality loss are alterations to:

- Blood acidity and composition: lower concentration of red blood cells platelets determines anemia and tendency to bleeding;
- Peripheral nervous system: lower arts pain and burning sensations; Digestive system: xerostomia, gastritis;
- Cardiovascular system: arterial hypertension, heart failure;
- Hydroelectric and bone metabolism: hyperpotassemia, hypocalcemia, hyperphosphatemia, bones decalcification;
- Carbohydrate metabolism: hyperglycemia and, therefore, diabetes propensity;
- Lipid metabolism: fat cells increasing concentration in blood;
- Immune system: lower metabolic defenses.

1.2.2 Acute Renal Failure

The acute renal failure causes can be grouped into three main categories:

- *prerenal acute renal failure*, resulting from reduced blood flow to the kidneys. It can be caused by heart failure with reduced cardiac output, low blood pressure, or by conditions associated with decreased blood volume (eg severe hemorrhage);
- *intrarenal acute renal failure*, caused by internal damage to the kidney itself;
- *postrenal failure*, which involves the obstruction of the urine collection system and can occur anywhere, from the cups to the exit routes from the bladder, whose main causes are kidney stones,.

In the presence of acute renal failure, the primary physiological effect is the retention of water into the blood and the interstitium, altered electrolytes and metabolic waste products concentration, with consequent hypertension and edema due to the overload of water and salts.
It is to notice that a high potassium concentration can cause such an arrhythmias that compromise the cardiac function.
Since the kidneys are not able to eliminate the necessary quantity of hydrogen ions, patients with acute renal failure develop metabolic acidosis, which may worsen hyperkaliemia and even be lethal. In severe cases of acute renal failure the total anuria, if not corrected by dialysis, can lead to death within few days [1,7].

1.2.3 Chronic renal failure

Chronic kidney failure stands for a loss of kidney function that occurs over a prolonged time [14].
The loss of renal function may be due to previous episodes of acute renal failure with subsequent long-term kidney damage or to diseases that lead to the progressive deterioration of the kidney such as primary kidney diseases (glomerulonephritis) or secondary disorders such as diabetes, hypertension, or auto-immune disorders [11].
Chronic kidney disease is common and may go undiagnosed until the process is advanced. CKD is more frequent in the elderly patients.
However, while younger patients with CKD are typically affected by a progressive loss of kidney function, 30% of patients over 65 years of age with CKD have stable a disease [11]. Unfortunately, many patients with chronic kidney disease, will progress to the stage of end stage renal disease (ESRD).
The possibility to early diagnose the kidney disease is very helpful preventing the progression of the patient's kidney deterioration.
Chronic renal failure in its final stage is identified as end-stage renal failure, a condition in which kidney function is reduced to less than 10% [15].
People with permanent kidney failure need dialysis or a transplant to substitute the functions of their failed kidneys.
Renal pathologies are one of the main causes of death and invalidity in all the developing countries, all over the world considering that about 1 in 10 people have some degree of chronic kidney disease (CKD)[5].
Nephrons cannot regenerate, hence with renal injury, disease or normal aging, their number decreases [1].

1.3 Replacement of renal functions

The replacement therapy of renal function is generally based on two treatments, the transplant and the dialysis.
In general, the choice of the treatment can be the result of various factors, as affect the decision-making process in which the economic clinical and organizational aspects should be considered.
The new kidney is placed in the front of the abdomen and the artery, vein and ureter of the kidney are respectively connected to an artery, a vein and bladder of the recipient.

1.3.1. Kidney Transplantation

The kidney transplant replaces all kidney function, and corrects the CKD better than any type of dialysis, with a high success rate (graft survival at one year after transplantation is 92% in Italy and 96.3 % in Europe).
Also organ functions are maintained for many years. The kidney to be transplanted can be removed from a living donor (usually a family member, even unrelated as in the case of married couples) or from a deceased donor. In the first case it is easier to plan and carry out the operation, also getting a better survival of the transplanted kidney (organ with a half-life of 27 years for patients with HLA-identical donor compared to 13 patients with a cadaveric transplant) [20].

1.3.2. Dialysis therapies

Dialysis is a therapy that allows purifying the blood from harmful substances and rebalances the body's fluids.
This treatment tries to mimic what happens physiologically in the human body.
Dialysis has two main objectives:

- **the elimination of toxic substances**, such as potassium and urea from the patient's blood or adding solutes, such as bicarbonate to the patient's blood;
- **the removal** by ultrafiltration **of the excess fluids** that are accumulated in the body.

The details of the dialysis treatment are exposed in the next paragraph.

1.4 The dialysis therapy

Considering the high number of functions carried out by the kidneys, it can be easily understood how kidney impairment should involve the whole body and in its most severe form becomes incompatible with the survival.
For this reason when the renal function is reduced, it is necessary to act with a therapy which allows the purification of the blood with the use of an artificial kidney.
If the loss of renal function is irreversible it is necessary to perform dialysis periodically to keep the patient alive.
In broad terms, the process of dialysis involves bidirectional movement of molecules across a semi-permeable membrane.
Clinically, this movement takes place in and out of blood, across a semipermeable membrane.
The two main mechanisms underlying dialysis are the diffusion and the convection, which opposes the oncotic pressure of the blood proteins.
The physiological and physiochemical principles that regulates the process of dialysis are:

- **Diffusion:** is the process of solute movement on a concentration gradient and is caused by the random movement of the solute molecules striking and moving across the membrane. It regard lo molecular weight solutes

$$jdiff = PL\Delta C = n\pi r2\Delta XDm\Delta C \quad (1.1)$$

where the solute flux j_{sol} is proportional to the membrane permeance P_L and to the concentration gradient ΔC. The permeance is directly proportional to membrane diffusion coefficient D_m and to the total pores area $n\pi r_2$. It is inversely proportional to the diffusion distance ΔX;

- **Convection:** is the movement of solute molecules dragged by the solvent movement due to pressures gradient.
  The transport of any solute molecule is dependent on the ratio among the size of the molecule and those of the pores.
  Similarly, the electrical charge and the shape of the molecule also determine the rate of transport across the membrane.
  The equations that regulated convection are:

$$jconv = Lp\Delta p = n\pi r48\mu\Delta X\Delta p \quad 1.3$$

$$jsolv = -LP(\Delta p - \sigma\Delta\pi) \quad 1.4$$

  where the convection fluxes j_{conv} and j_{solv} are defined as the product of the membrane filtration factor L_p and the pressure gradients.
  The filtration factor is directly proportional to the pores number (n) and size (r) while it is inversely proportional to the fluid viscosity μ and the convection distance ΔX.

Solutes convection is determined only by hydraulic (p) pressures, solvent convection is given by the balance between hydraulic and osmotic (π) pressures. The coefficient σ , is the Staverman coefficient that considers that the membrane is not fully permeable at certain solutes by which there will be a different osmotic gradient [21]. The total pressure acting over the fluid is the result of osmotic force and mechanical hydrostatic pressure: the solvent is forced across a semipermeable membrane leading to a partial fluid removal.
This phenomenon is called ultrafiltration and is commonly accomplished by lowering the hydrostatic pressure of the dialysate compartment of a dialyzer, thus allowing fluids to move from the plasma to the dialysate.
All the dialysis systems currently available on the market are able to only partially replace the purifying function of the kidney, not the production of hormones for which it is often necessary to provide with drugs (vitamin D, erythropoietin).

1.3.1. Peritoneal Dialysis

The peritoneal dialysis instead exploits the semi-permeability of the peritoneum and the difference of osmotic pressure that is created between the blood and dialysate (Figure 1.5).
The dialysis solution is injected into the abdomen of the patient via a peritoneal catheter, placed under local anesthesia side navel.
The substances presents in the blood migrate through the peritoneum to the dialysis solution that, after a contact period of 4-6 hours, is replaced.
This process takes place from 4 to 6 times per 24 hours.
The peritoneal dialysis attenuates symptoms of uremia and has less stressful effect on the organism, because the patient performs it daily and autonomously. At the same time, however, it requires particular care and attention of the catheter, to avoid contamination of the peritoneum and consequent peritonitis.

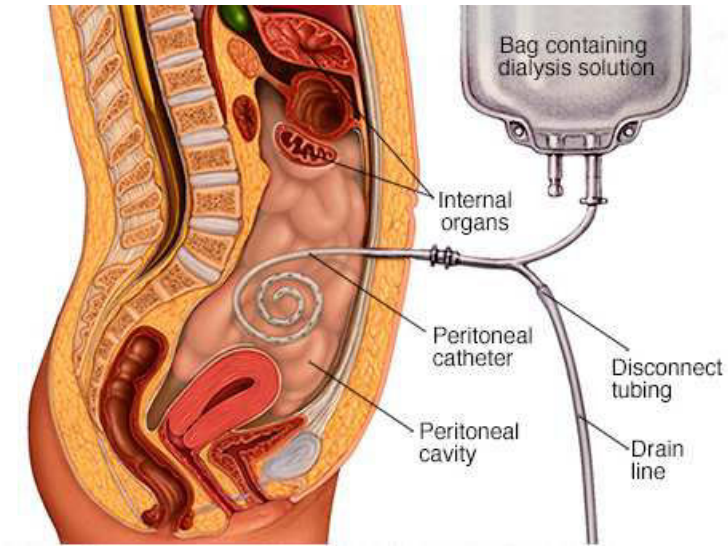

Figure 1.5 Peritoneal dialysis

1.3.2. Hemodialysis

Hemodialysis is currently the most widely used substitution treatment in the world. The therapy is usually performed thrice a week for 3-4 hours/each session.

This method meets the clinical needs of both the acute and chronic patients, but usually has a higher cost with respect to other methods.

Hemodialysis is performed by the dialysis machine, to which the patient is connected during a hemodialysis session. Hemodialysis system is made by the components [18], shown in Figure 1.6:

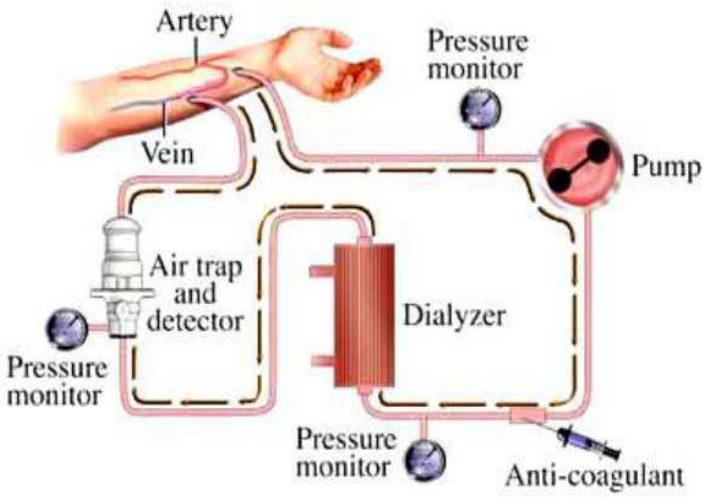

Figure 1.6 Hemodialysis Circuit

- a blood circuit: where flows the patient's blood;
- a pump to extract the blood from the patient
- a dialysis fluid circuit;
- a monitor for the setting-up and the control of the treatment parameters;
- a mass exchanger: the dialyzer or dialysis filter.

Hemodialysis is usually performed in the hospital (on the contrary of peritoneal dialysis) or from specialized (public or private) centers, with a scheduling of 3 weekly sessions, during an average of 4 hours (3 to 5 hours) each.

The blood and the dialysis solution are pumped by the dialysis machine inside the filter, composed of two compartments. The *blood compartment* that

consists of several thousand hollow fibers (from six thousand to twelve thousand), with a diameter of just over a hair, said just capillaries, all 'inside of which flows the blood; the high number of fiber is needed to guarantee a large exchange surface;
The dialysis solution is flowing all around the capillaries, forming the *compartment of the dialysis fluid.*
This means that the membrane formed by the walls of the capillaries always separates the two fluids and the molecules pass from one compartment to another by virtue of the difference in concentration between the two compartments.
During dialysis blood is drawn from the body and is continuously purified with a speed of roughly 300 mL / min; to avoid blood coagulation, heparin is infused, before the blood enters the dialyzer.
To connect the patient to the machine a specific vascular access is required.
The vascular access is usually achieved through arteriovenous fistula (FAV), shown in Figure 1.3, an anastomosis between vein and artery generally performed in the brachial area between radial artery and cephalic vein.
This strategic surgically allows the arterialization the vein in order to make possible a greater flow sampling in an easily accessible vase and more resistant to frequent needle insertions (Figure 1.7)

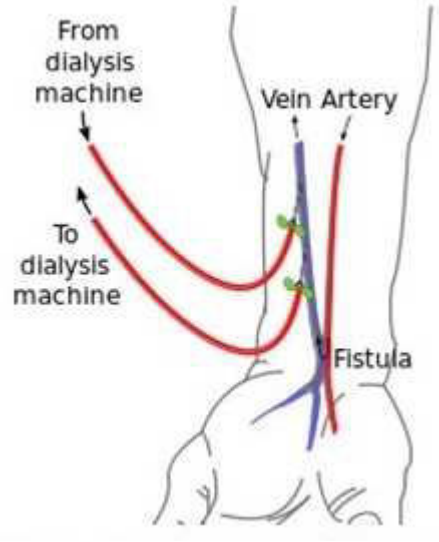

Figure 1.7 Arterio-Venus Fistula

There are different types of hemodialysis therapies, among them:

- **Standard hemodialysis** (HD): the purification process is mainly based on diffusion, with higher efficiency in low molecular weight catabolite (Es. urea, creatinine) removal.
  The convection, is present even if it is not the prevailing phenomenon. Standard hemodialysis is currently known as bicarbonate dialysis, as a dialysis solution containing sodium bicarbonate is used.
- **Hemofiltration** (HF) technique exclusively convective rarely used. High porosity membranes were here used and applying an adequate trans-membrane pressure it is possible to remove a high volume of water, in the order of tens of liters per session, together with the in it dissolved substances. Since such a high fluid loss is not sustainable by the human body, it is necessary to reinfuse the most of the volume filtered with an adequate flow of substitution fluid. It is indicated in hemodynamically unstable patients.
- The **Hemodiafiltration** (HDF) is a mixed dialysis method, obtained by the balanced combination of diffusion and convection. The diffusion allows the purification from low molecular weight catabolites, while

the convection allows the purification from the medium-molecular weight substances.
Reinfusion can be performed, as for hemodiafiltration, both pre-filter and post-filter.
It is thus possible to distinguish two types of HDF: the *HDF with pre – dilution* where the infusion of dialysate is made upstream to the dialyzer: this technique is generally prescribed for patients with reduced blood flow or high hemoconcentration so as to limit the increase in the transmembrane pressure to avoid intradialytic complications.
The other type is the *HDF with post – dilution*: this is the case by which the substitution fluid is mixed with the blood just before being released back into the patient.
The high ultrafiltration can induce clots or hemolysis within the capillaries of the filter, with consequent increase in the transmembrane pressure and risk of clogging of capillaries and of loss of the membrane proteins with impaired osmotic balance.
With the pre-dilution in the convection-diffusion ratio it is privileged before removing macromolecules but the blood is more diluted, making the process of diffusion less effective.
With the post-filter reinfusion instead the spread since the blood reaches the filter undiluted and clearance of low / medium molecular weight is greater than hemodialysis. The risk is, however, that the blood can clot into the dialyzer.
The HDF allows removing not only low molecular weight solutes, as happens for hemodialysis, but also medium / high molecular weight, such as beta-2-microglobuline (11, 8 kDa) [22].
The term On-Line indicates the production in situ of the reinfusion liquid for the patient. The dialysis solution is online prepared by the machine by dilution of a concentrated bag.
This technique is very useful in patients requiring a high purification.

- **Acetate free biofiltration** (AFB) is a dialysis mixed diffusive-convective method characterized by the use of a dialysis solution swabs-free (or acetate or bicarbonate) [21,23].
  AFB is the analogous of hemodiafiltration, regarding the purification principles, the main difference compared to HDF is that in this technique is sub-ministered intravenously [23]. The dialysis bath is completely free of buffer and involves the separation of the mechanisms for the acquisition and transfer of the bicarbonate.
  In particular sodium is acquired from the blood only through the infusion after dilution. There is a control system of the bicarbonaturia.
  This technique allows two different types of treatment: constant potassium or potassium profile [23].
  .

1.4. Complications during dialysis therapies

Although hemodialysis is the most widely used therapy to treat the end stage renal failure, and technology advances have improved the quality of dialysis sessions, this type of treatment is not without risk and can have numerous symptoms intra- and inter-treatment, mostly related to subtraction of liquids and to the electrolytic rebalancing.
The most prevalent dialysis complication are related to pressure imbalances (whether hyper- or hypotension), which brings to severe damage to the body, especially the cardiovascular system, increasing patient mortality and morbidity.
The inter-dialysis blood pressure affects about 50% of patients on dialysis and while it has multifactorial pathogenesis, the dominant cause is the increase in blood volume from one session to the other [25].
There might be may be hypertensive episodes during the session due, for example, to the incorrect concentration of the dialysate (not patient specific).
The intra-dialysis hypotension (IDH) affects 20% - 30% of the sessions [24] [25] and consists of a reduction of excessive blood volume compared to the adaptability of the cardiovascular response [27] [25].
The IDH is accompanied by symptoms such as sweating, nausea, vomiting, epigastric pain, yawning, blurred vision, and convulsive events [26], leading to the premature end of the session.
This lead to a not complete removal of excess fluid.
Despite pressure control mechanisms, dialysis can lead to complication during the treatment as severe intra-dialysis hypotension and hypertension and hypertensive crisis in the inter-dialysis period.
In addition to these problems the onset of fever (due to bacterial infections) or bleeding (often caused by the administration of heparin to prevent thrombus formation in the catheter) is not uncommon, especially in patients who have central venous catheter[27]
During a hemodialysis session, destabilizing events could occur such as:

- *Arterial hypotension* is the most frequent complication.
  Hypotension is the consequence of the failure to adapt to the reduction of the vascular circulating blood mass, if the dehydration is too rapid or excessive. The pressure drop is often preceded by repeated yawning, decreased blood flow provided by the vascular access, accompanied by cramps, nausea, vomiting.
- *Hemorrhage:* the uremic patient shows an increased risk of spontaneous bleeding, more frequently borne in the gastrointestinal tract. There could be also not uncommon blood losses caused by technical problems on the dialysis monitor (lines or filter rupture), or from the point of insertion of needles.
- *Muscle cramps:* it affects more frequently in the legs, with painful contractions of the calf muscles They are caused by very high ultrafiltration or by low concentration of sodium in the dialysate
- *Air embolism:* caused by penetration of air in the blood circuit. This are rare complication but also the most dangerous for the patient.

During the dialysis treatment also technical incidents can occur on equipment such as clots in the circuit, breaking in hemodialysis filters.

Chapter 2 – Hypotension during dialysis

2.1 Introduction

Despite notorious technological progress that improved dialytic-treatment's safety, the operation is never risk-free and Intra-Dialysis Hypotension (IDH) is one of the most relevant short-term complications of hemodialysis, which occurs in 25-30% of the cases [28].
The intra-dialysis hypotension consists of a significant drop in pressure during the dialysis session, often accompanied with symptoms such as cramps, weakness and vomiting [29].
In the long-term chronic fluid accumulation, caused by the interruption in advance of dialysis sessions due to IDH, can lead to IDH and increase cardiac output, leading to hypertrophy of the left ventricle [30].
The IDH can also cause a reduction in diastolic blood pressure and heart perfusion, which in turn can lead to myocardial ischemia.
The chronic IDH has been also linked to the development of cardiac fibrosis, which predisposes to the onset of arrhythmias.
IDH onset is more frequently found in the standard thrice-weekly hemodialysis treatment rather than in short daily or nocturnal treatment because the former type of treatment requires a higher dose of ultrafiltration [29].
On the long-term, frequent hypotension episodes may lead to permanent damages to heart and intestines, in addition to risk of arteriovenous fistula occlusion [32].
In most cases IDH events entails early discontinuation of treatment, resulting in failure to achieve the dry weight of the patient and bad blood purification [33].
In recent years, IDH prevention has been highly investigated.
This highlighted the necessity of a better evaluation of patient's dry weight, a correct regulation of dialysate temperature, a particular dialysate sodium concentration (DSC) and an online monitoring of blood volume (BV).
One of the open challenges is to determine, before the hemodialysis session, the probability that the patient will suffer intra-dialytic hypotension.
The main obstacle in reaching this goal lies in IDH onset, that is not always observable through external manifestation, because some patients do not show any precursor symptoms.
In general, IDH clinical treatment procedures consider the reduction of hematic flow in the extracorporeal circuit, the reduction of ultrafiltration rate and the increase in volemia.
This is achievable either through the administration of liquids or the infusion of a hypertonic solution able to facilitate the fluid's osmotic flow from extravascular to intravascular compartment, in order to increase blood volume and pressure [32].
These actions are necessary when symptoms are manifest, although it is desirable to prevent hypotension episodes rather than correct them.
The patient's peculiar reaction to the treatment implies difficulties in preventing IDH episodes.
Hypotension short-term consequences are general malaise, nausea, vomit and fainting; such symptoms are not only draining for the patient but also tough to be managed by clinicians.
Moreover, given that IDH often causes premature interruption of dialysis session, patient's blood may not be adequately purified.

All this increases the risk of cardiovascular morbidity and mortality.
An inadequate cardiac filling, due to a reduction in the central blood volume, it's considered to be its most etiological factor.
Koch and Ritz et al [33] reported that the risk of cardiac death is increased when two or three hypotensive episodes occurred per week, but their relatively small study failed to show significant differences in BP during hemodialysis between patients who died of myocardial infarction and survivors.
IDH prevention indeed stands in a great effort in order to decrease mortality during the session.

2.2 Clinical Definition of hypotension

Despite hypotension is still one of the most common acute complication that occurs during hemodialysis, there is currently a strong lack of clinical techniques to detect its onset during the conventional treatment. .
There isn't a universally recognized clinical definition of IDH.
Mancini et al. [32] proposed a definition of hypotension, based on the following three conditions on arterial pressure and clinical records:
Standing to Mancini, IDH can occur by one of the following conditions:

- if the predialysis systolic arterial pressure (SAP) is greater than 100 mmHg, each episode with SAP less of 90 mmHg, without any associated clinical event;
- if (SAP) predialysis is less than 100 mm Hg, each reduction of SAP of at least 10% with reference to the associated disorders; any reduction of SAP of 25% or more compared to the predialysis value with typical symptoms, specific for the interventions to the applicants.

There are simple definitions of IDH, given by Bayya et al., as the reduction of SAP by 20% [33].
The methods should differ depending on whether the target is to predict an acute episode or not IDH.

2.3. Pathophysiology of IDH

The factors involved in the onset of hypotension in patients undergoing dialysis are due both to clinical conditions (e.g. presence of vascular or cardiac diseases, neuropathology, anemia) and treatment settings
In particular the causes of hemodialysis-induced hypotension are multifactorial and related to the interaction between the patient and the dialysis procedure [34] [36].
Indeed, the rate and amount of ultrafiltration will influence the patient's fluid status; on the other side, the patient's compensatory response to hypovolemia will determine the clinical manifestations of IDH[41].
The mechanisms of IDH are complex.
Several agents are involved in the pathogenesis of dialysis discomfort, that interfere with optimal fluid removal and reducing the efficacy of the treatment [40]; a decrease in intravascular circulating blood volume caused by imbalanced ultrafiltration rate (UF) and plasma refilling rate (PR) is the most important one [41].
An alteration in cardiovascular regulatory mechanisms, such as increased heart rate, contractility and peripheral vascular tone, that controls the blood volume balancing could led to hemodialysis-induced hypovolemia [42].

2.4. Body Fluids Dynamics during hemodialysis

The body fluids are distributed in two main compartments:
- Extracellular -

- Intracellular

The extracellular compartment in turn comprises the interstitial liquid and blood plasma.

In a normal adult of 70 kg of weight, the total amount of liquid is on average 60% of body weight [2].

This percentage may vary with age, sex and degree of obesity.

The extracellular fluid compartment includes:

- *the interstitial fluid*, which it makes up about three-quarters of the extracellular fluid ;and it's the fluid external to the cells
- *the plasma*, which constitutes about one quarter of the extracellular fluid: it is in dynamic equilibrium with the interstitial fluid, by which exchanges solutes through the pores of the capillary membranes.

These pores are permeable to almost all solutes present in the extracellular fluid, except that the protein.

In this way the liquid of the extracellular compartment are mixed continuously, so that the plasma and interstitial fluid compositions remain similar, with the exception of the proteins that are more concentrated in the plasma.

The extracellular fluid also contains large amounts of sodium and chlorine ions, discrete quantities of bicarbonate ions, but only small amounts of potassium, calcium ions, magnesium, phosphates and organic acids.

The intracellular compartment instead is constituted by the liquid contained within the body's cells and corresponds to approximately 28 of the 42 liters of total body water. The two compartments are separated from highly selective membranes highly permeable to water and impermeable to most of the body electrolytes.

The extracellular volume and blood volume, that is, the hemodynamically active part of the extracellular volume, are normally maintained rigorously constant by fine adjustments in renal excretion of water and catabolites.

In hemodialysis these volumes depend, by the water and solutes and on the other by the dialysis procedure.

Particularly blood volume subtraction in uremic patients evoke a series of cardiovascular reflex in response to the changes in fluido-dynamic and osmotic equilibrium.

The most important mechanism is the increase in arteriolar tone.

This increase on the one hand helps to prevent an excessive lowering of blood pressure and on the other reduces the venous pressure, favoring by elastic "recoil" elastic the venous return to the heart and the maintenance of the cardiac output.

On the other hand the reduction of the pressure in the capillaries (direct consequence of arteriolar vasoconstriction) alters Starling of forces facilitating the vascular refilling.

It is intuitive that the time factor, that is, the ultrafiltration rate, assumes a fundamental importance in the tolerance of the volume subtraction.

That's why the intervention of the compensation factors will be more effective as smaller the hemodynamic stress imposed by the dialysis procedure will be.

A too high ultrafiltration rate can induce hypotension phenomena [22].

2.4.1 Cardiovascular response and the plasma refilling (PR)

Blood pressure regulation in the human body, is controlled by the autonomic nervous system, by the cooperative action of receptors, nerves, and hormones to balance the effects of the sympathetic nervous system, which tends to raise blood pressure, and the parasympathetic nervous system, which lowers it [41].

Low-pressure volume's receptor resides in the heart atria and in the vena cava: they are sensitive to variations of blood volume filling of the central venous system.

Baroreceptors are instead sited on the carotid bifurcation and on the aortic arch:

they are sensitive to a variation in the pressure of the central arterials system.
Both the receptors, in rest conditions, have an inhibitory effect on the cardiovascular centre that modulates sympathetic system and vascular resistances activity [42].

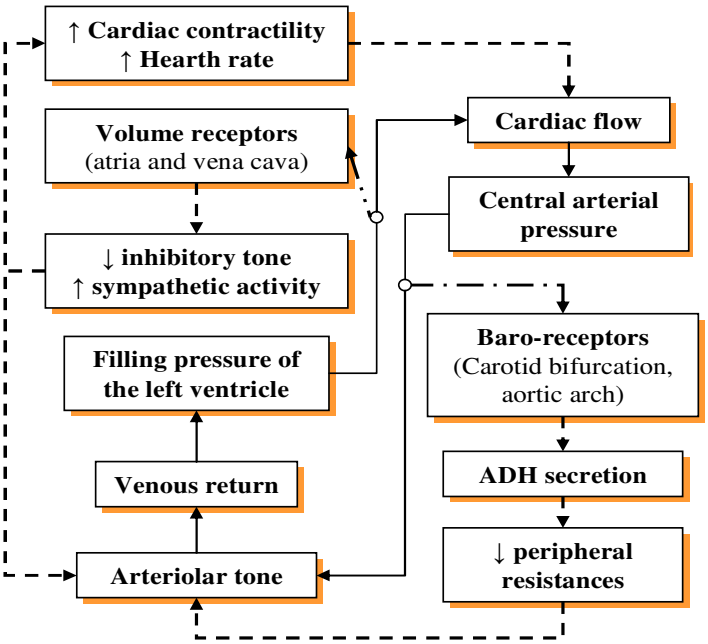

Fig.2.1 mechanisms involved in the body response to the decrease in blood circulating volume, as a consequence of high ultrafiltration during dialysis[41].

So the body reacts to blood uptake with a series of reflex control, to compensate the decrease in blood volume. Particularly these controls acts on three fundamental and correlated mechanisms [43].
Support of the venous return to fill the cardiac cavity.

- Increase of the hearth rate and of the fibre's contraction force, with the aim to increase the cardiac output, even in reduced ventricular filling conditions.
- Increase vascular resistances, so to reduce venous capacity and to fill the cardiac output between the vascular districts, with attention to critical organs (e.g. the brain) perfusion [40].

The most important consequence of the described strategies is the onset of a plasma refilling flux from the interstitial to the vascular compartment.
During HD, the fluid is removed by UF from the intravascular compartment. Thus the capillary pressure is going to reduce altering the Starling equilibrium (Figure 2.2).
The fluid transfer between the interstitial to the vascular compartment is called plasma refilling (PR)[46]
The flow intensity depends on the hydration status and on arteriolar tone, which determine the hydraulic pressure's values at the vascular level.
Vasoconstriction set a pressure drop into the capillaries that determines the fluid reabsorption, while the vasodilatation has the opposite effect.
At the same time a high plasmatic osmolarity and a consistent presence of proteins can influence the plasma refilling [46].

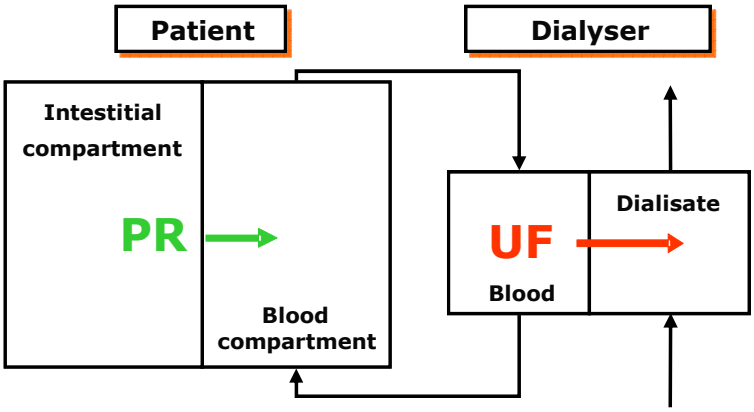

Fig.2.2 HD fluid removal by compartment models. During HD, the fluid is removed by UF directly from the intravascular compartment. The consequent fluid transfer from the interstitial to the blood compartment is called plasma refilling (PR)[41].

The failed activation of the mechanisms aimed at compensating the decrease in circulating volume affects the hemodynamic conditions of the patients during the sessions, exposing him/her to hypotension episodes.
Cardiac underfilling and impaired cardiovascular compensatory mechanisms may trigger the sympato-inhibitory cardiodepressor Bezold–Jarish reflex[47]. The Bezold-Jartsch reflex originates in cardiac sensory receptors with non-myelinated vagal afferent pathways [47] in the left ventricle, in- creasing parasympathetic activity and inhibits sympathetic activity. These effects promote reflex bradycardia, vasodilation and hypotension.

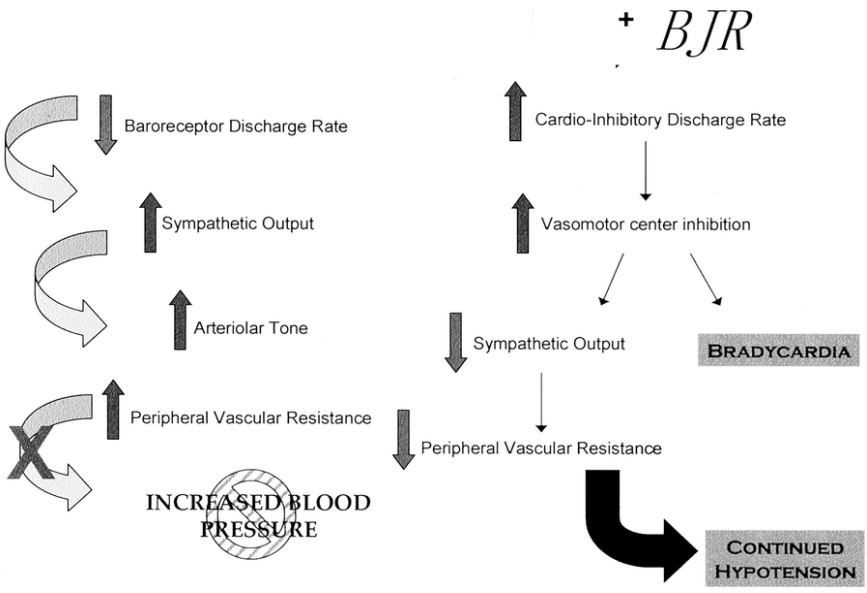

Fig.2.3: Schema of the Bezold–Jarish reflex.

The first receptors that intervene to contrast a blood volume decrease due to ultrafiltration are the low pressure-volume receptors, which increase the sympathetic activity. A higher reduction in volume activates also the baroreceptors, that over to exert a concurrent sympathetic activation, influence also the secretion of vasopressin (ADH).
ADH induces an increase in vascular peripheral resistances so to reduce the pressure and the blood flow in the venous compartment where a consistent part of the total blood volume is contained.

The elastic force of venous walls prevails and, reducing the venous system capacity, supports the venous return and the cardiac output preservation [42].
The reduced circulating volume activates as well the normal cardiac response to hypovolemic that consists in a tachycardia followed by a reduction of hearth rate since new rest conditions will be reached, and on the other side in an increase in cardiac muscle contractility, aimed to increase the ejection volume and consequently the cardiac output.
Hypotension during dialysis could be directly related to a reduction in blood volume or to a decrease in cardiovascular activation as a response to decreased cardiac filling.
Patients may have inefficient compensatory mechanisms, such as sympathetic autonomic failure and increased parasympathetic activity, and thus be more sensitive to hypovolemia [45].
Under conditions of hypovolemia, increased sequestration of blood in veins reduces cardiac filling, cardiac output, and blood pressure too.
Adenosine release due to tissue ischemia may concur in the activation of the Bezold-Jarisch reflex, by a local reduction of norepinephrine [49].
Intradialytic hypotension is therefore more common in patients with cardiovascular disease and diabetes mellitus, because of their limited capability of physiological compensatory response.
In conclusion, during a hemodialysis session, events like eating and changing the body position can be triggers for hypotension episodes that alter the blood pressure and sympathetic/parasympathetic balance.

2.4.2. Risk connected to IDH in dialysis therapy

Between two subsequent treatments, the uremic patients accumulates fluid, the entity of fluid weight increase depends on the patient's diet and the renal residual function. During hemodialysis, these accumulated fluids (usually from 1 to 4 liters) are removed by ultrafiltration.
The long-term chronic fluid accumulation, caused by the interruption in a dialysis session, due to IDH, can lead to interdialysis hypertension and to an increased cardiac output, leading to hypertrophy of the left ventricle.
This increases the risk of cardiovascular morbidity and mortality.
IDH determines also a reduction in the diastolic blood pressure and heart perfusion, and consequently could lead to myocardial ischemia.
Chronic IDH has also been linked to the development of cardiac fibrosis, that predisposes to the onset of arrhythmias and then cardiovascular death (Figure 2.4).
Sudden cardiac death is a major cause of mortality of patients on dialysis (15% approximately) [50].

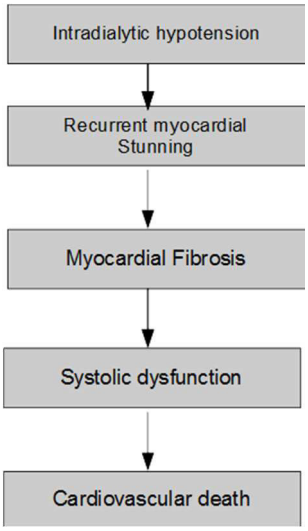

Fig.2.3 Mechanism of vascular instability related to IDH onset

2.5. Clinical Management of hypotension

An efficient treatment of IDH currently a great challenge in nephrology.

Due to its multifactorial nature, an adequate therapy requires a multilevel strategy.

In many hospitals, the IDH clinical management is done by Trendelenburg position, by which the body is set in a supine position with the feet higher than your head [36].

Other methods of IDH treatment are mostly related to hemodialysis procedure.

Particularly the use of sodium modelling profiles, higher sodium concentration in dialysate–especially at the beginning of the procedure and lower dialysis temperature are first therapeutic option for hypotension-prone patients [43].

Common strategies of long-term treatment and prevention of IDH include an accurate assessment of 'dry weight' [43] and patient education to avoid excessive intra-dialysis weight gain and no heavy meals during or just before the dialysis, adequate hypertension management sometimes it is necessary to skip or reduce drug dose on the day of dialysis session, use of bicarbonate dialysate buffer and biocompatible membranes.

2.5.1 Ultrafiltration Rate Modulation

Since the removal of body fluid during the dialysis procedure is often faster than the body ability to draw fluid from the interstitial space, the change of the rate and frequency of ultrafiltration (UF) may decrease the incidence of IDH[51].

In particular, the treatment is more effective if greater quantities of blood volume are removed at the beginning of the session, when there is the greatest accumulation of fluid available to facilitate the "plasma refilling" phenomenon, and gradually the extracted quantity is reduced.

An impulsive step indeed produces an opposite effect, encouraging hypotension. [49] [50].

2.5.2 Sodium Profiling

At the beginning of dialysis, the removal of the blood volume and solutes leads to a fall of plasma osmolality, with a negative repercussions in the transition of the fluid from the intracellular to the extracellular space.
The Dialysate Sodium Concentration (DSC) is closely related to the conductivity of the plasma [52] and has an indirect influence on the RBV, because it changes the osmolality of the plasma, which in turn controls the plasma refilling process [53].
The sodium content in the dialysis fluid can be varied during the session to minimize the plasma osmolality decreases and the correlated (disequilibrium syndrome), and to facilitate the plasma refilling, allowing to better tolerating the ultrafiltration.
The "sodium profiling" technique allows to vary the sodium concentration in the dialysis fluid during the session: at the beginning of treatment high sodium concentrations are maintained (> 145 mEq / L), to increase the osmolality of plasma and the passage of water from the interstitial space.
Subsequently the sodium present in the dialysate is reduced, allowing the removal of the solute from the blood by a concentration gradient [31].
The difficulty of this method stands the correct choice of the profile to be adapted to the patient.
A wrong profile, results in an accumulation of the solute in the blood.
A high imbalance of the sodium concentration in the dialysate determines a significant increase in post - dialysis plasma sodium concentration and, consequently, can lead to a greater increase of weight intradialytic and thus to hypertension [54]. In particular the combination of sodium modulation monitoring and ultrafiltration rate has been shown to be particularly effective in different studies [28].
The increase in the sodium concentration in the dialysate can be particularly useful in preventing hypotensive episodes, when used combination with a high rate of ultrafiltration.
This approach optimizes the plasma refilling when the reductions in plasma volume induced ultrafiltration are excessive, but it requires the ability to predict the final concentration of sodium in plasma determined by each particular profile [52]. Even thought, the reduction of the frequency of IDH thanks to the use of sodium profiles is not universally recognized: in a study of 2006, Moret concluded that the IDH can be reduced by 15% using the sodium profile [54], while another of Selby and colleagues in 2007 found no difference [59].

2.5.3 Dialysate Temperature Monitoring

One of the most common ways to decrease the onset of hypotension and improve cardiovascular stability is the use of the dialysis liquid at 35 ° C, instead of at the standard temperature of 37 ° C.
This correction reduces the onset of IDH at least 7.1 times than conventional hemodialysis. [57]
During the dialysis treatment, in fact, the reduction of blood flow in the skin and muscles contributes to preserve the volume of the central plasma, which can result in an increase the in core temperature of the body, and in a consequent vasodilation. [58]
Biofeedback systems have been developed to measure the temperature of the blood and transmit the information to the machine thermostats [34].
The goal is to modulate the temperature of the dialysate, keeping constant the body temperature.
However, the working temperature must be adjusted and controlled in relation to the symptoms of hypothermia that the patient might show.
A disadvantage in dialysate temperature monitoring is the increased risk of chills and cold feeling [59], which could generate discomfort for the patient during

treatment.

2.5.4 Blood Volume Monitoring BVM

The BVM has been developed to improve the attainment of the dry weight after the session and for the prevention of hypotensive episodes.
The blood volume is calculated from the measurements of hematocrit or hemoglobin in the blood, it is lower for higher concentrations.
The relative blood volume (RBV) is the measure of blood volume in a moment of time, and is expressed as a percentage of the predialysis volume. Several studies have shown that the RBV Profile rapidly decreases in sessions with IDH, and these changes can be used to prevent it [53,59].

2.5.5 "Fuzzy" Logic Automatic Monitoring

Mancini and colleagues [52] studied the efficacy of an automatic control system for the stabilization of blood pressure (BP) by means of biofeedback (ABPS - automatic blood pressure stabilization).
The system, based on the use of "fuzzy", is directly installed on the dialysis machine, and uses the instantaneous values of BP as input variables to adjust the rate of ultrafiltration rate (UFR)
The machine requires to work two patient-specific data: the critical pressure value, that's the maximum value that it's supposed may arise IDH, and the maximum ultrafiltration rate that can be applied to the subject.
In the case by which the threshold pressure is reached, the UFR is automatically stopped, to resume the situation of hemodynamic instability.
This system, is a result of a multicenter study, and was effective in preventing IDH in subjects prone to hypotension, with a 25% of reduction of hypotensive episodes, that rises to 40% in the case of severe hypotensive crisis.

Chapter 3 – Clinical Variables related to Hypotension

3.1 Introduction

A condition of hypotension during the treatment could be usually associated to a particular physiological state of the patient and thus to a variation in different clinical variables.
Nowadays, the clinical monitoring of the patient by sensors and electronic equipment connected to the machine allows having continuous real-time measurement of physical and chemical signals coming from the dialysis patient. On-line monitoring is thus possible for different clinical variables such as blood volume that characterize the circulatory system about IDH, in particular the temperature of blood, blood volume and bio-impedance, with the ultimate aim to find "actuators" variables to reduce the incidence of hypotension during the dialysis session [66].
This could allow the automatic control of dialysis machine settings in order to guarantee a better management of dialysis IDH.

3.2. Clinical Variables related to hypotension

Numerous studies have analyzed the relationship between the variables that characterize the circulatory system and IDH [63].
Particularly blood pressure, blood temperature, relative blood volume (RBV), bio impedance, ECG and fotoplethismography (PPG).
Furthermore, in addition to the baroreflex sensitivity, other cardiovascular variables, that reflect the variability and the turbulence of the heart rate, have been used to study the feedback control of hemodialysis systems, in order to improve their performance [67].

3.2.1 Blood pressure P

Blood pressure is the first natural starting point to develop an algorithm for the on-line prediction and prevention of hypotension.
Blood pressure is thus the eligible variable to be monitored during the sessions to understand the evolution of IDH onsets during the sessions.

3.2.2. Blood temperature T

The patient's temperature increases during hemodialysis.
The hemodialysis increases body temperature as the blood, which normally flows on the body surface area to dissipate heat, remains in the central circulation to preserve the core of the plasma volume that is reduced after ultrafiltration.
The sympathetic activity consequentially increases in response to ultrafiltration and leads to peripheral vasoconstriction, which reduces the heat dissipation resulting in an augmentation in body temperature [68].

3.2.3. Relative Blood Volume

The loss of blood volume that occurs during hemodialysis is a determining factor for the development of IDH [63]. The blood volume decreases as a result of ultrafiltration (UF) and, if the ultrafiltration rate (UFR) is greater than the plasma filling rate (PRR) and the cardiovascular compensatory mechanism that counteracts the hypovolemia is insufficient or compromise, IDH may arise. Thus, the calibration of the decrease in blood volume during the HD is an important target to prevent complications. Several non-invasive techniques that measures changes in the relative blood volume (blood relative value change, ΔRBV) during dialysis due to UF are based on the analysis of changes respectively of hematocrit (Ht), hemoglobin (Hb) or the concentration of the total plasma proteins.

The changes of the concentration of blood constituents can reflect changes in the volume of blood if the total quantity of the blood components in the circulation is constant and the mix of the constituents is uniform throughout the vascular space [81]. During the ultrafiltration a compensatory mobilization of poor blood hematocrit from the microcirculation to the central circulation occurs and this dilution effect reduces the degree of hemo-concentration, causing a possible underestimation of the total ultrafiltration volume [28].

When hematocrit and hemoglobin are measured at the beginning of a session, the patient usually passes from a prone to a supine position, then the recorded values are not stationary.

Even postural changes during the session have a big effect on hematocrit and hemoglobin, but this effect cannot be prevented during a patient movement contemporary to the treatment.

Given the many factors that affect hematocrit, hemoglobin and protein concentration during dialysis, it is not surprising that the RBV trends vary considerably patient to patients.

Hemodynamic stability is not only determined by the performance of blood volume but also by the response of hypovolemia compensatory mechanisms.

Such response is influenced by various factors that may differently affect the various dialysis sessions for the same patient. All these elements explain the little predictive power of RBV for dialysis hypotension.

At the current state of art, the conducted studies have not been able to establish a close relationship between IDH and hypovolemic-induced UF: the reduction of blood volume at the time of symptomatic IDH does not differ significantly from what in the sessions without IDH [83].

This suggests that hypotension cannot be predicted simply by checking if the relative volume of blood falls below a predetermined threshold.

Rather, the threshold value is closely patient-dependent and therefore particularly difficult to be estimated.

Best predictions have been obtained when the shape of the trend of RBV was analyzed in relation to certain features such as the decrease of the long-term variability [41]. In the individual patient, the continuous measurement of RBV would be a perfect tool for the prevention dialytic hypotension if the critical lowering of the pressure happen the increase of irregularities [87] and the increase in the time needed to switch from a linear decay to one exponential [78].

3.2.3. Bioimpedance

The bioelectrical impedance measurements are non-invasive techniques to assess [71] the body hydration status.

Impedance is decomposed into resistance (opposition to the intra and extracellular current flow) and reactance (capacitive component of cell membranes).

Changes in body fluid volume (whole-body fluid volume) can be estimated by

measuring changes in impedance.
In particular, an increase of impedance corresponds to a decrease of fluid volume. The contribution of the trunk and limbs to the body impedance is respectively 10% and 90% [72].
Impedance is measured by applying an alternate current, traditionally with a single frequency of 50 kHz, and using electrodes placed on the head and foot.
Before being analyzed, impedance is normalized with respect to the height of the patient.
Several studies have shown how impedance has been used for dry weight assessment, while very few studies have considered this method to predict the IDH.
In early studies, the impedance has been associated with a very low predictive value (42%) and low sensitivity (66%).
More recently, the bioelectrical impedance vector analysis has been suggested as a prediction method, but the potential of this method has not been investigated in detail [72,73].

3.2.4. Electrocardiographic variables

Cardiac function in hemodialysis patients has been extensively studied, since cardiovascular problems cause about 50% of the deaths on the treatment [70].
Sudden cardiac death, ischemic heart disease and heart failure are the main causes of mortality.
A deeper understanding of cardiac events is critical to improve patient management and may lead to the modification of the hemodialysis prescription in order to reduce the worsening of the disease.

3.2.4.1 Hearth Rate Variability

The analysis of HRV (heart rate variability, HRV) has proved to be a powerful noninvasive tool to quantify the neural mechanism that controls the cardiovascular system.
The dynamics of HRV can be generally analyzed in the time domain or in the frequency domain, where the resulting power spectrum, by convention, is divided into a low frequency band (LF, 0.04 -0.15Hz) and high frequency (HF, 0:15 to 0:40 Hz).
These two bands are related respectively sympathetic and parasympathetic autonomic nervous system activity and the power ratio LF / HF is a spectral parameter, reflecting the sympatho-vagal balance [81].
The literature shows that the LF components plays a dominant role as they represent of the compensatory autonomous mediated response [80].
The insufficient cardiovascular compensatory mechanisms that counteract the reduced blood volume, arterial and cardiopulmonary baroreceptor reflex lead to sympathetic and parasympathetic inhibition.
As a consequence of these reflex, the LF component tends to dominate on the HRV spectrum during the analysis in the time domain) and the frequency domain, in which the resulting power spectrum, for convention, is divided into a low frequency band (LF, 0.04-0.15Hz) and high frequency band (HF, 0:15 to 0:40 Hz).
These two bands are related respectively to sympathetic and parasympathetic autonomic nervous system activity and the power ratio LF / HF is a spectral parameter for the sympathetic/parasimpathetic balance[81].
Studies carried out on HRV uremic prone (hypotension prone, HP) or resistant (resistant hypotension, HR) patients to hypotension, have concluded that the spectral parameters can distinguish between these two groups of patients using the power of LF/ HF power ratio [93].
High values of this parameter have been reported in sessions without hypotension, conversely lower values correspond to hemodialysis sessions with

hypotension [68].
There is a statistical difference in the LF / HF ratio among patients HR and HP and a plausible threshold to distinguish between the two groups can be a value around 1.
The HRV parameters alone, are not powerful enough to predict IDH, with acceptable clinical accuracy, they are still part of the physiological parameters that must be considered as online predictor.
Although the frequency domain analysis seems to be the predominant approach for the HRV characterization, the analysis in the non-linear time domain represents an important approach that typically is based on entropy measures [80]. It has been shown that the Shannon entropy is strongly correlated to a change of the SAP during the hemodialysis session; leading to the conclusion that entropy measures maybe suitable predictors of propensity to hypotension during dialysis [90].

3.2.4.2 Premature Ventricular Beats (PVB)

The analysis of heart rate variability is not, able to treat the ectopic beats common in dialysis patients, and this makes this instrument not suitable to be elected as a marker for hypotension
Premature ventricular beats (PVBs) are common in dialysis patients and increase during hemodialysis as potassium is removed [84].
The results show that ventricular arrhythmias appear much more frequently during hemodialysis that in the post dialysis period [85].
The presence of occasional VPBs can be detected by the HRV analysis, [97] coupled with the EBC (ectopic beat count), based on the time of onset of ectopic beats [96].
The EBC analysis tracks the average change in intensity of ventricular ectopic beats and "missing beats".
The intensity of ectopic beats appears to greatly increase during acute symptomatic hypotension. This increase has been not observed in patients with stable blood pressure. It will not possible to establish an absolute threshold, since the number of these beats is patient - dependent and differs between different treatments.
The acute symptomatic hypotension requires a relative threshold, since the interesting thing is the change in intensity. The frequent presence of VPBs in dialysis patients gives the possibility possible to calculate parameters that characterize the turbulence of the heart rate (heart rate Turbulence, HRT), that is, the fluctuation in frequency triggered by a single VPB.
Such turbulence is considered a blood pressure regulation mechanism, which in healthy subjects compensates hypotension induced VPBs, due to an accelerated of the breath rate.
Several studies have claimed that HRT is one of the most powerful predictors of mortality and sudden cardiac death due to acute myocardial infarction [88].
For patients on hemodialysis, there are good reasons to believe that HRT could give significant clinically information because the autonomic neuropathy is associated with a marked drop in blood pressure.
To date, only one study has addressed the question of whether a greater propensity to IDH is reflected in the HRT parameters [93].
The results showed that the acceleration of the heart rate that follows a VPB is significantly lower in patients prone to IDH rather than patients not subject to hypotension, and both groups of patients showed a smoothed HRT according to standard criteria [99].

3.2.4.3 Baroreflex analysis

The sensitivity of the arterial baroreceptor heart reflex (cardiac-arterial Baroreceptor Reflex Sensitivity BRS) is generally estimated using techniques that are based on non-invasive measurements of cardiac activity, such the

measurement of SAP [71].
The slope of the regression curve between the measurements of the SAP and RR intervals is calculated in each one of the baroreflex sequences and the resulting gradients of all the sequences are averaged to produce an estimate of BRS.
The evaluation of spontaneous BRS is interesting in IDH prone patients as the baroreflex arc is under the control of the autonomic system and sets the short-term dynamics of blood pressure.
Two studies in particular, have focused on the role of BRS in this group of patients.
At first Chesterton [93] showed that the cold dialysate reduces the IDH asymptomatic and the absolute values of BRS not change significantly.
Greater variability in BRS during the cold hemodialysis may suggest a better hemodynamic stability.
Therefore, early identification of patients with reduced BRS variability may reduce the incidence of IDH individualizing therapy.
Another study on BRS [94] investigated the contribution of a compromised BRS in the pathophysiology of IDH.
The main result is that the BRS, measured at rest immediately before the start of session, is extremely heterogeneous and, therefore, cannot be identified individual hemodynamic response pattern, even in patients prone to 'IDH'.
The baroreflex sensitivity may also be evaluated at different frequencies, based on a spectral coherence measure between the variability in the heart rate and the systolic blood pressure [87]. Using the LF and HF bands, as defined for the HRV analysis, BRS show significant differences in the HF band in HP prone and HR resistant patients [95].
What can be finally considered is that the failure of the baroreflex function is a possible trigger of IDH element.
Arterial and cardiopulmonary BRS can lead to the arousal of sympathetic and parasympathetic inhibition, resulting in higher LF power on the HRV spectrum.

3.3. Electrolytic imbalances and dysrhythmias

During a dialysis session hypotensive episodes can be induced by electrolyte homeostasis aberrations.
Electrolyte homeostasis aberrations are often associated with alterations in cardiac conduction, which can cause, clinically relevant electrocardiographic changes. [97, 96].
The changes could reflect as dangerous cardiac dysrhythmias.
Several author have studied the effects on the dialysis treatment of alterations in electrolyte unbalances.
Particularly, the sudden decrease in potassium, in addition to an increase of ionized calcium in plasma [109], may increase the susceptibility to ventricular arrhythmias. In fact, the intra and extra-cellular concentrations of magnesium, calcium and potassium are important factors for the electrical stability of the myocardium.
They are indeed involved in the determination of the normal cellular excitability, pulse propagation and regular ventricular recovery.
Furthermore during the treatment the solutes in the blood affect the oncotic pressure of the plasma.
This affects in the plasma refilling phenomenon, conditioning the exchanges between blood and dialysis liquid through the phenomena of diffusion and ultrafiltration.

3.3.1 Potassium Ion unbalances

Potassium is the major cation of intracellular fluid.
Most of the potassium ion is allocated in the intracellular space (98%), while the remaining 2% is in the extracellular compartment.
Potassium is a key electrolyte that helps maintaining the acid-base equilibrium, the osmotic pressure of the intracellular volume status and that promotes the action of the enzymes involved in cellular metabolism.
It also plays a key role in the excitability of some cell types, including cardiac myocytes [97].
A reduction of extracellular potassium makes the cells less excitable, while its increase makes them more excitable up to a threshold value beyond which the excitability decreases rapidly.
Potassium physiological levels in the blood are between 3.5 mmol / l and 5.0 mmol / l [98]. So the abnormal blood concentrations of potassium could be classified as hypokalemia and hypekalemia
It is usually considered hypokalemia a $[K^+]_b$<3,5 mmol/l, mild hypokalemia between 3.0 and 3.5 mmol / l and moderate hypokalemia on $[K^+]$ between on 2.5 and 3.0 mmol/l.
Severe hypokalemia is defined for $[K^+]_b$<2,5 mmol/l.
Such changes may cause dangerous arrhythmias, in particular: tachycardia / ventricular fibrillation; and torsades de pointes[108].
The hyperkalemia is reached when the serum potassium concentration is greater than 5.0 mmol / l .
It is classified as mild hyperkalemia for $[K^+]_b$ between 5.0 and 5.9mmol/l, moderate between 6 and 6.4 mmol / l, severe than 6.5 mmol / l, hyperkalemia incompatible with the life of 10 mmol / l).
Hyperkalemia modification could be registered on ECG changes [98].
All clinical manifestations related to hypo/hyperkalaemia are conditioned by the velocity by which the alteration is established, the presence of underlying diseases, by co-administration of drugs.

3.3.2. Calcium ion unbalances

Ca^{++} serum physiological values are in the range 1.15 to 1.29 mmol / l [100], although currently there is a tendency to consider hypocalcemia a ionized calcium concentration of less than 1.09 mmol / l [100].
It is classified as a severe hypercalcemia level of Ca^{++} serum greater than 3.5 mmol / l.

3.3.3 Magnesium ion unbalances

In general, hypomagnesemia is associated with far-reaching adversities during HD, including effects on the central nervous system (CNS), such as mental confusion, dysrhythmias and vasospasm, endocrine dysfunctions and muscular effects as weakness and bronchospasm.
Lack of magnesium can also cause supraventricular or ventricular dysritmias. Hypomagnesaemia is often associated with hypocalcemia.
The hypermagnesaemia occurs mainly in patients with renal failure whom are more usual to consume magnesium in diet [97].
For the electrolyte homeostasis equilibrium during the treatment, the magnesium and calcium concentration in the dialysate are important.
Kyriazis et al. [75] reports that a dialysate solution with 0:25 mmol / L of Mg to 1.25 mmol / L of Ca increases the risk of IDH, while use a solution with 0.75 mmol / L of Mg (often accompanied 1.25 mmol / L of Ca) may instead decrease it.
However, further studies are needed to confirm the role of magnesium on the hemodynamic stability.

3.3.4. Potassium and calcium removal during hemodialysis and effects on the QTc wave

Dysfunctions in electrolyte homeostasis determine cardiac problems that can be detected by the analysis of ECG signal due to a modification of the shape of the action potential wave.

In particular, several studies have shown that durings hemodialysis treatment, a dilation of the QTc interval is registered by a 12-lead ECG This is called QTc dispersion [104-107].

The dispersion of the QTc interval is therefore considered a marker of risk of ventricular arrhythmia and its prolongation has been linked in general to an increase of risk of sudden death [104,105].

The increase in QTc dispersion during HD is primarily related to the diffusion process, in particular the removal of potassium, which must therefore be given special attention in the case of uremic patients with heart problems.

The HD introduces a number of factors that can affect the QTc interval duration: the composition of body fluids, tissue hydration, electrolyte balance and adrenergic activation. Electrolytic disorders are one of the main factors that determine hemodialysis dependent QTc interval changes and ventricular arrhythmias, due to their involvement in the genesis, life, morphology and propagation of the action potential [104].

In particular, the sudden decrease of potassium, in addition to an increase of ionized calcium in the plasma [109], may increase susceptibility to ventricular arrhythmias. In fact, the intra and extra-cellular concentrations of magnesium, calcium and potassium are important factors for the electrical stability of the myocardium, being involved in the determination of the normal cellular excitability, pulse propagation and regular ventricular recovery. Consequently, the imbalance caused from a hard drive is probably the main cause of the increase in QTc dispersion [105].

Cupisti et al. have observed an increase in this dispersion against a decrease in potassium and magnesium, and an increase of calcium and that the increase of QTc dispersion seems limited to the hemodialysis session, occurring in the first hour of treatment (abruptly reaches its maximum value is twice that of session end), when the removal of potassium is more rapid, and returning to baseline after two hours from the end of therapy [105].

For patients on HD, the QTc prolongation is inversely related to the change of Ca^{2+} in plasma, suggesting that patients with the greatest variation of Ca^{2+} at the end of the session will have the greatest increase in QTc interval [110, 112].

On the other hand, several authors have reported the removal of K^{+} as a fundamental factor in the induction of arrhythmia, associated with hemodialysis.

Numerical simulations have predicted an action potential and a long QT critically when simultaneously considering a low level of K^{+} and Ca^{2+}, suggesting that concurrent decrease their electrolytes have an arhythmogenic potential factor [104].

The Ca^{2+} content in the dialysate should be designed not to critically lower the level of Ca^{2+} serum, especially in patients at risk of hypotension.

Chapter 4 – Data Management and Personalized medicine

4.1 Personalization of the dialysis therapy

Patient-centered care is a crucial point for the chronic kidney disease management [115].
The clinical practice shows a great variability of tolerance to the treatment, even in the presence of similar prescriptions due to the peculiar patient-machine interaction
The heterogeneity of the treatment approach among different dialysis centers, and the not homogeneous criteria for the choice of the therapy and for the IDH management is also an important point that address the fact that the dialysis therapy should be provided in the most personalized and patient-compliant way possible [116].
This problem is emphasized in border areas where different National Health Systems adopts specific rules to guarantee the access to the treatment, make moreover difficult the mobility of the patients, with high negative impact on their quality of life.
Not less important, it has to be underlined that patients on dialysis face a significant number of restrictions in daily life, as well as the physical and substantial time needed to follow dialysis treatments [115].
A significant improvement in the dialysis care provision, stands in the provision of a customize therapy for each patient toward a personalized approach.
Due to rapid evolution of new technologies the concept of personalized medicine has evolved [117].
The availability of several new generation digital instruments and sensors make nowadays easier to produce and gather large number of clinical related data, not only referred to longitudinal trend in the pathology evolution, but also addressed to single treatments.
Thanks to the use of large amounts of data, standard medical practice is moving from relatively ad-hoc and subjective decision making to evidence based and personalized healthcare [116].
The expansion of the medical record as well as the development of new methods for creating disease profiles constitute a challenge in the information technology filed.
Over the past few decades, computers have been increasingly used in most areas of services and clinical business, with no exception for hospital management systems and sometimes renal units[116].

4.2 Patient mobility

Patient mobility has only slowly emerged on the European health policy agenda. With the growing awareness of on well-being and the availability of several, easy to access, medical information's (even if not always proper and appropriate, rather often partial), patients, when in need of medical treatment, increasingly act as informed consumers who claim the right to choose their own provider, including beyond their national borders.
They are supported and encouraged in this by several factors and actors, the availability of internet on one side, and internationally trained health professionals on the other side. "Cross-border patient mobility" is the most commonly used expression within the EU to describe a social phenomenon that involves people crossing a border to receive health care [121].

Patients are often unwilling to travel significant distances for care, but in some border regions in the EU the most accessible care happens to be in another Member State. European cross-border health care is the key to unlock this great potential, by facilitating the transfer of expertise and knowledge, by improving choice for patients, and by enabling greater efficiency in providing health care through cross-border cooperation [123].
In 2011, the European Parliament and Council adopted the Directive on Patients' Rights in Cross-border Healthcare, which sought to provide a clear legal framework and resolve ambiguities about the mechanisms involved in providing cross-border care (European Council, 2011) [123].
In such a way the goal is to obtain "personalized therapies" that could act "over the places".

4.3 Data sharing in renal facilities

The technological evolution and production of data in the healthcare field has lead to the storage into public or private repository of even higher quantities of data related to patients and their pathological evolution.
The public databases were usually shared through the web to be used by other scientists.
The national and international renal registries use data collected by the renal medical centers and publishes annual data report based on this very large data set, but the majority of the data representations we see in nephrology today are simply visual representations of historical data [138].
Biomedical research when coupled with the high speed processing technologies results in highly detailed datasets.
Using data for decision-making is a key way to personalize medical treatments; the promise of data-driven decision-making could allow an improvement in kidney disease diagnostics and therapy and there is fast-growing enthusiasm for the notion of ``Big Data''[139].
Big Data is an "information assets characterized by high volume, velocity and variety" that requires "specific technology and analytical methods for its transformation into value" (De Mauro et al) [133].
Big data analysis is an innovative approach in medical research, that try to infer knowledge from complex heterogeneous sources, by the analysis of patient/data correlations in longitudinal records trying to understanding unstructured clinical notes in the right context.
The potential benefits of the analyses of large amount of data are real and significant; even if some initial successes have already been achieved, several technical threads must be overcome to fully show their potential.
Main problems were indeed directly related to the data storage.
Heterogeneity, scale, timeliness, and lack of proper common standards are typical problems that impede the extraction of the information from the data.
This is particularly true dealing with data coming from dialysis unit, where the lack of proper exchange protocols between concurrent software vendors, results in a lack of interoperability within data coming from different dialysis machines [134].
For these reasons, the development of a common framework to store the large amount of available clinical data related to treatment performances, could be complex and not straightforward.

4.4 Privacy Issues related to medical data

The diffuse access to cheap data collection and processing technologies has allowed the availably of large volumes of but at the same time has raised several privacy problems.
Considering the very sensitive nature of medical data and easy dissemination of information on electronic format, clinical data from electronic medical records EHRs need a special attention[124]
As nowadays medical data are available by the EHR to be shared in common repository the HIS systems need to satisfy certain requirements in term of and the consistency of security policies [129].
The protection and security of personal information has thus became a critical point in the health sector.
Several technique are nowadays available to grant clinical data security.
De-identification and anonymization are two of the available strategies that remove any connection to the data and patient identity in electronic health record (EHR)[125]
In particular:

- *De-identification* is the removal or replacement of personal identifiers in order to make difficult any possible connection to the individual and his or her data
- *anonymization* refers to the irreversible removal of the link between the individual and his or her medical record data

These techniques allow clinical data to be used for research purposes and eventually shared among different center.
Even if they assure a privacy level to the data in order to be share, they had to always accompanied by the informed consent of the patients or a waiver from their IR[125].

4.5 The problem of data interoperability

The possibility to gather and analyze accurate information at the right time from different sources as public healthcare information systems, opened the possibility to better orientate correct clinical assessments and related decisions.
Furthermore, if information is shared across laboratories, and hospitals, patients could benefit of the same focused treatments even in different clinical centers.
Data sharing can also increase public trust in clinical trials and conclusions derived from them by lending transparency to the clinical research process.
Data from medical sources are voluminous, but they come from many different sources, not all commensurate structure or quality [140].
In order to share health information, the HIS systems should grant a minimum level of interoperability.
Rules or guidelines at the national level should mainly aim at achieving essential requirements with regard to semantic, technical, organizational and legal interoperability[124].
While the data gathering at the hospital level is highly keen to provide detailed information about clinical parameters, very often this effort have the intrinsic limit of not being standardized among the different health care providers.
The lack of standardization represents a great barrier to share data and this problem is very common in multicentric initiatives where different health information systems are involved.
Each center in fact, could have various licensed software to produce clinical data and export it. The export formats should be different, and thus the final data cannot be easily merged in unique platforms.
The integration of different data sources in common structures is highly connected to the concept of interoperability.

Interoperability can be defined as"the ability of different information technology systems and software applications to communicate, exchange data, and use the information that has been exchanged"[139].
Interoperability allows the different health information systems to work together and could bring several benefits to effective delivery of healthcare, individuals and communities.
Through health care information exchange and interoperability indeed, clinicians everywhere can have a longitudinal medical record with full information about each patient.
Conversely patient will have better information about their health status across organizational boundaries [140].
The need for interoperating systems is evident in several department of healthcare organizations. This is particularly the case of the dialysis facilities, where a huge gap on interoperable information systems is still present compared with the other medical fields.
The different dialysis machine vendors in fact developed software for physician offices, and even more for hospitals often so customized that did not allow data interexchange between different clinical centres [142].

4.6. The federated database approach

The creation of a shared platform between different health centers is a common problem in clinical data management.
Most of the times, this problem is highly related to the lack data interoperability.
Standing to the classification of Wang et al.[143], data interoperability could be implemented at different levels.
The basic ones are the *technical* and *syntactic* inter-operabilities.
The first is related to the physical connection and network connectivity among different data sources. The second indeed defines the structure or format of data exchange.
If technical interoperability can be usually considered to be covered by the presence of a diffuse internet connection, the syntactical one is several times not granted on health data.
As the clinic information systems produce data in different formats and extension, they have to be converted into a common standard format before being integrated in unique common structures.
An effective shared data platform should definitively grant higher levels of interoperability.
In particular these are the *semantic* interoperability, by which a common meaning of the data is defined and the *pragmatic* interoperability that allows a common utilization of the exchanged information by different users, with an high degree of consistency and easiness in updating.
Such simple considerations show how the process of data integration from different data sources is not trivial and needs a conceptual model to be properly addressed.
To achieve semantic interoperability, the systems involved must refer to an agreed authority, typically a terminology that clearly defines the meanings of the items carrying the information.
In particular semantic interoperability lies into

- syntax, the packaging and transmission mechanisms for data
- semantic, the meaning of the data[147].

Semantic interoperability could be accomplished within different systems and conceptual models.
In computer science a conceptual model can be defined as "the abstract and simplified representation of a system for some specific purpose by languages, figures, tables, or other suitable artifacts"[142].
Several studies on biodata, shows how conceptual models has been applied on

bio-databank by adding data about the data (metadata), linking each data element to a controlled, shared vocabulary (ontology) [147].
An ontology is a formal description of concepts in terms of entities and their relationship within a domain.[148]
By the ontological model is possible to organize complex data in order to be machine readable, connecting of different type and from different sources.
Regarding kidney.
Ontologies in fact, could capture the structure of the domain, through the mechanism of conceptualization. This includes the model of the domain with possible restrictions. Formal specification in fact is required in order to be able to process ontologies and operate on ontologies automatically[148].
Studies in these directions has been conducted in nephrology and dialysis by Goldbreich et al. [149] using the OWL DL and Protégé.
The study showed that OWL DL supports powerful automatic reasoning, but it also arouses some difficulties, propagation of information between the different concepts of the information.
In order to define innovative approaches on data integration and overcome the unsolved problems in dialysis data, the conceptual model that has been adopted to deal with data integration in the Dialysis Project has been the Federated Database System [144,145,146].
The term Federated Database System (FDBS) was coined by Hammer and McLeod (1979)[145] and Heimbigner and McLeod (1985)[145].
It stands for a collection of "cooperating but autonomous component database systems (DBSs)" [146]. Since its introduction, the term has been associated to several different DBS architectures.
A key characteristic of a federation, however, is the cooperation among independent systems, with controlled and sometimes limited integration of autonomous DBSs. Standing to its description it comes intuitive how the FDBS logic can be used to define the structure of a common repository for the data recorded in different dialysis units.
These data have different and peculiar features and act as independent *datapools*.
Their integration into a common storage infrastructure should be managed into different steps.
First of all, an interoperability layer should work to convert into the *common standard format* all the not homogeneous data coming from different source. As a result of this process, a converted database, associated to each dialysis unit is obtained.
Secondly, as each center has its own database, a federation mechanism should acts to merge all the data into a common data infrastructure.
Figure 1 resume in a figure the concept of the common storage infrastructure in FDBS logic.

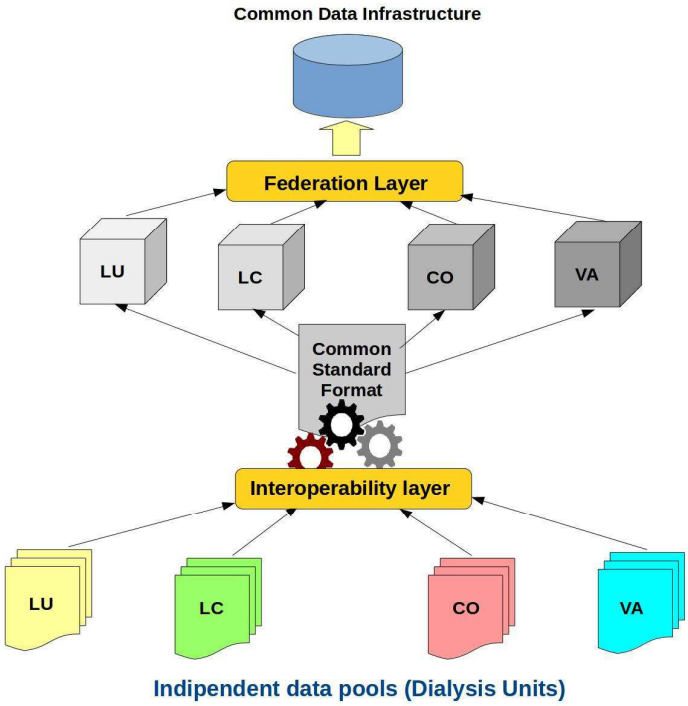

Figure 4.1: Common Storage infrastructure in FDBS logic

4.7. Medical data analysis and mining

The storage of data in commons structures lead to the possibility, to analyse data in a massive way in order to obtain useful information.
This process is commonly known as data analysis or data mining.
Data analysis, or data analytics, implies the inspection, transformation, and model of data
Particularly data mining can be considered an application of data analysis that focuses on modeling and knowledge discovery for predictive rather than purely descriptive purposes [150].
Data mining, also known as knowledge discovery, allows a search, for valuable information, in large volumes of data, in order to find hidden patterns, correlation and useful information [151].
Applied to medical data, the main goal of data mining is to extract unknown information from dataset and transform it into an understandable knowledge for the clinicians [152].
Data analysis has multiple facets and approaches, encompassing diverse techniques.
Standing to Berson et al. [153], these techniques can be classified in:

- *classical techniques*: mainly based on inferential statistics, and statistical predictive models.
- *next generation techniques*: commonly belong to the domain of Artificial intelligence, and Machine learning techniques.

4.7.1 Inferential Statistic Analysis Approach

Inferential statistical analysis are powerful technique that enables a researcher to draw meaningful conclusions from a study in which data are collected through observation, survey or experimentation[154]
In particular in data related medical studies, it is quite reasonable to convert a medical problem into a statistical problem.
On the inferential statistical approach each measured variable can be seen as a sample from a wider population identified by a probability distribution, that describes the physical process.
Generally , biomedical data can be modelled both as variables characterized by normal or Gaussian distribution as well by a not normal distributions.
Inferential statistical analysis, infers properties about these distribution by testing hypotheses and deriving estimators [156].
A hypothesis evidence in a sample of data to infer that a certain condition is true for the entire population.
An hypothesis test examines two opposing hypotheses about a population: the null hypothesis and the alternative hypothesis.
Usually the null hypothesis is a statement of "no effect" or "no difference".
The verification of a hypothesis means its acceptance or rejection, to a predetermined level of probability by a test. The p-value furnishes the level of tolerance by which the null hypothesis could be rejected. Each statistical test has this value has a reference to reject the null hypothesis.
The test depends on the normality of the analyzed distribution that has to be checked by a normality test. In statistic a normality test is able to determine if a data series can be modeled by a normal distribution and thus assumed as a complete random variable.
Depending on the normality of the distributions parametric or non-parametric tests should be applied in order to assess the statistical difference between the two samples [155].
Inferential statistic techniques can help to assess strength of the relationship of cause- effect variables in multivariate datasets.
In particular in the field of medicine and health, they can be used to predict the effects of several factors on a particular disease [154].

4.7.2 Machine Learning techniques

Machine learning, is a branch of artificial intelligence (AI), that focus on finding algorithms capable of learning and/or adapting their structure based on a set of observed data, with adaptation done by optimizing over an objective or cost function [157]. In the past couple of decades it has become a common tool in almost any task that requires information extraction from large datasets [158].
One, of many applications of this approach is to create classifiers that can separate subjects into (usually) two or (rarely) more classes based on attributes measured in each subject.
Machine learning techniques have raised an increasing interest in the biomedical community as they potentially offer the possibility to improve the sensitivity and/or specificity of detection and diagnosis of disease.
Furthermore, the use of machine learning allows to search for patterns and relationships between medical variables and patient physiological states: for this reason the application of machine learning techniques has been highly increased in the clinical field [158].
A range of different problems that can be faced through machine learning is clearly large, and grows as a growing number of templates are discovered to address a large set of situations [159].
Particularly, Machine learning processes could be implied in two important operations:

• *extraction* of salient structure in the data from the simple raw data (*feature* extraction problem);
• *inferring* underlying organized class structure (*classification problem*).

These two mechanisms can be highly useful in the prediction of events.
A Machine learning approach can be especially useful in chronic diseases management where patho-physiological state of patients is steadily monitored in order to identify factors and anticipate the risky conditions.
Machine learning is usually applied to observational data, where the predictive variables are not under the control of the learner, as opposed to experimental data, where they are [158].
As the inference statistic approach also machine learning techniques are based on the probabilistic model theory [158] and there is a lot in common between the two disciplines, in terms of both the goals and techniques used.
Even though, there is a few significant differences of emphasis.
The statistical approach, in facts starts from a hypothesis, as instance the existence of a correlation between variables and checks the validity of that hypothesis through hypothesis testing.
In contrast, machine learning aims to use the data gathered from samples to come up with a description of the causes of the phenomenon [158].
The added value of machine learning techniques stand in the fact that automated techniques may be able to figure out meaningful patterns (or hypotheses) that may have been missed by the human observer[159].
In particular, machine learning techniques can be used when classical algorithmic solutions tent to be complex, there is lack of formal models, or the knowledge about the application domain is poorly defined [161].
This is the case of our study, where the acquired data refers not to a set of experiment but rather to clinical observations and no a priori models are known.

4.7.3. Basic Concepts of Machine learning

4.7.3.1. The learning problem

The key feature of machine learning systems is their ability to automatically learn programs from data.
In particular machine learning rise interest because it adapts the resolution strategies and algorithms to the features of the data.
This is basically done by the process of learning, by which given training data are expected to learn by an algorithm.
In general a machine learning algorithm is said to learn from experience E with respect to some class of tasks ***T*** and performance measure P, if its performance at tasks in[161].
This is the basic assumption of a machine learning problem, and the fundamental goal of machine learning is to generalize beyond the examples in the training set [161].
The task that machine learning addresses could be various, but in general it can be resumed in guessing a function f.
The hypothesis about the function to be learned is denoted by *h*.
Both f and h are functions of a vector-valued input $X = (x_1, x_2, \ldots, x_i, \ldots, x_n)$ which has n components.
The input vector is usually called as feature vector, input vector, pattern vector, sample, example, and instance.
The components, x_i, of the input vector are variously called features, attributes, input variables, and components.
The function *h* is though to be implemented by a device that has *X* as input and *h(X)* as output. The output may be a real number, in which case the process embodying the function, h, is called a *function estimator*, and the output is called an *output value* or *estimate*.

Alternatively, the output may be a categorical value, in which case the process embodying *h* is variously called a *classifier*, a *recognizer*, or a *categorizer*, and the output itself is called a label, a class, a category, or a decision.
An important special case is that of Boolean output values.
This is the case of for example of binary classification problem.
In its simplest form, the binary classification reduces to:

$$x \in X\,; y \in \pm 1 => p(y|x) \qquad 5.8$$

given a pattern x drawn from a domain X, estimate which value an associated binary random variable y ∈ {±1} will assume.
Binary classification problems fits very well in the modellization of diagnosis of a disease where the state of the patient are disease or no disease.[160].
A Boolean or binary predictor is also called *concept learning*, and the function is called a *concept.*
Both f and h themselves may be vector-valued. We assume a priori that the hypothesized function, h, is selected from a class of functions *H* called hypothesis space[163].
Sometimes we know that f also belongs to this class or to a subset of this class.
The function h is based on a training set, Ξ, of *m* input vector examples.

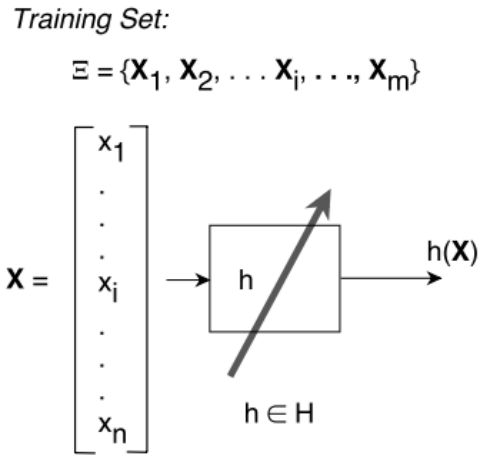

Figure 4.2: Machine Learning problem

There are two major types of learning processes.
In one, called *supervised learning*, where the values of *f* for the m samples in the training set, Ξ. are known.
In the other setting, termed *unsupervised learning*, we simply have a training set of vectors without function values for them. The problem in this case, typically, is to partition the training set into subsets, Ξ1, . . . , ΞR, in some appropriate way.
As it posed the problem of learning through machine learning has normally three different phases:

- **the training phase**, during which the model of learning is built using labelled data;
- **the testing phase**, during which the model is tested by measuring its classification accuracy on with held labelled data;
- **the deployment phase** during which the model is used to predict the class of unlabeled data.

The three phases are carried out in sequence.
Obviously different strategies and algorithms can be used to solve the learning problem. There are literally thousands available, and hundreds more are published each year [164]. But basically each one of them consist of a combination of just three components.

- *representation.* a classifier must be represented in some formal language that the computer can handle and belongs to a set of algorithms. This set coincides with the hypothesis space of the learner.
- *evaluation.* An evaluation function (also called objective function or scoring function) is needed to distinguish good classifiers from bad ones. The evaluation function used internally by the algorithm could be different from the external one used for optimization
- *optimization*, or a method to search among the classifiers in the language for the highest-scoring one. The choice of optimization technique is key to the efficiency of the learner, and also helps determine the classifier produced if the evaluation function has more than one optimum.

The different machine learning techniques or *learners* could vary on the representation component.
In the following paragraph the theoretical basis of the learners used in this work will be presented.

4.7.4. Learners theoretical basis

4.7.4.1. Random Forests

A random forest (RF) is a classifier consisting of a collection of tree-structured classifiers $\{h(x,\Theta_k), k = 1,...\}$ where the $\{ \Theta_k \}$ are independent identically distributed random vectors and each tree casts a unit vote for the most popular class at input x (Breinman, 2001)[166].
The RF base learner is typically based on the methodology of CART [167], Classification and Regression Trees (CART) is a classification method which uses historical data to construct so-called decision trees.
Decision trees classify instances by sorting them down a tree from the root to some leaf node, which provides the classification of the instance, splitting the learning sample into smaller and smaller parts [168].
Based on this idea, RF is defined as a generic principle of randomized ensembles of decision trees [169].
Recent work in computational biology has shown an increased use of random forest, owing to its unique advantages in dealing with small sample size, high-dimensional feature space, and complex data structures[169,170,171].
Furthermore RF can handle thousands of variables of different types with many missing values [165].
Considering a binary problem, each tree of the forest casts a unit vote, assigning each input (HD session in this case) to the most likely label class (1 or 0, i.e. IDH or not IDH respectively).
The prediction of the random forest is obtained by a majority vote over the predictions of the individual trees (Figure 4.4).

Figure 4.4: Example of random for forest breast cancer diagnosis and prognostic [169]

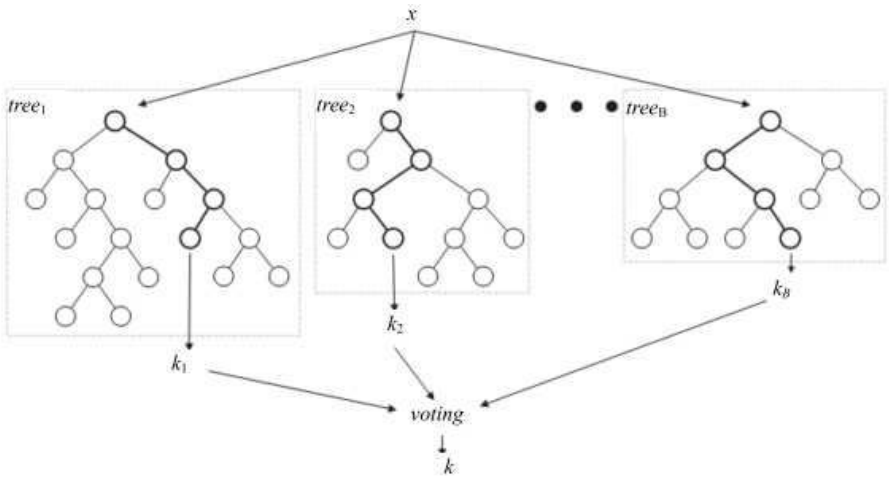

RF trees differs from CART as they are grown non-deterministically using a two-stage randomization procedure.
In RF, for each split on each bootstrap tree, the algorithm randomly samples a subset of the input variables to be used as candidates for the split.
Bootstrap methods take many repeated samples from the data with replacement, each time recording the predicted classification for each case.
In particular the random forest $Tb1B$ is built from each bootstrapped data, by recursively repeating the following steps for each terminal node of the tree since the minumun node size n_{min} is reached:

I. Select *m* variables at random from the *p* bootstapped
II. Pick the best variable/split-point among the m
III. Split the node into daughter node

So for the kth tree, a random vector Θ_k is generated, independent of the past random vectors Θ_k, Θ_{k-1} but with the same distribution; and a tree is grown using the training set and Θ_k, resulting in a classifier h(x, Θk) where x is an input vector.
This is the basis for *bagging* (short for "bootstrap aggregation"; an early resampling-based method. proposed by Breiman in 1996 [172], that aims to improve the classification by combining classification of randomly generated training sets leading to an improvement for unstable procedures, such as regression trees.
The purpose of this two-step randomization is to decorrelate trees so that the forest ensemble result with low variance [173].
When in facts, the inputs in the data set are highly correlated, this procedure addresses potential collinearity issues by giving each of the correlated predictors a chance to be used in different bootstrap trees. As decorrelation enhance accuracy , bootstrapping gives ongoing estimation of the generalization error of the combined ensemble of trees [173].
In general to define a random forest is necessary to include the follow main tuning parameters:.

- ***Number of Trees:***. the optimal number of trees in a random forest depends on the number of predictors: it needs to be at least one order of magnitude higher than the number of features in order exhaustively explore all the feature space during the forest building [174].
- ***Number of Predictors Sampled***: the number of predictors sampled at each split would seem to be a key tuning parameter that should affect how well random forests perform. Sampling 2-5 each time is often

adequate.

- ***Split criterion***: For each node of the tree it is required to define the criterion for the identification of the optimal observation separation rule and creation of the consecutive nodes (as in II.).

The estimation of error is then almost unbiased, but it has high variability, producing non-reliable estimates [175]. In particular the error of a forest of tree classifiers depends on the strength of individual trees and correlation between them. For each tree grown on a bootstrap sample, the error rate for observations left out of the bootstrap sample is called the "out-of-bag" error rate.
The *out-of-bag* (OOB) error is the average error for each z_i calculated using predictions from the trees that do not contain z_i in their respective bootstrap sample. The out-of-bag (OOB) error is also a measure is a method of measuring the prediction error of random forests[166,175].
The biggest disadvantage of random forests is that the analysis, which aggregates over the results of many bootstrap trees, does not produce a single, easily interpretable tree diagram.

4.7.4.2. Artificial neural networks

An Artificial Neural Network (ANN) is a learning algorithm that is inspired by the way of biological nervous systems, such as the brain, process information.
In simplified models of the brain, it consists of an input layer of neurons (or nodes, units),or one or two(or even three) hidden layers of neurons and a final layer of neurons and a final layer of output neurons[176].
Each neuron receives as input a weighted sum of the outputs of the neurons connected to its incoming edges.
Each connection is associated with a numeric number called *weigh.*
The output h_i of a neuron i is thus:

$$hi = \sigma(j = 1NVijxi + Tihid) \qquad 4.1$$

where σ() is called activation (or transfer) function, N the number of input neurons V_{ij} the weights, x_j inputs to the input neuron and $Tihid$ the threshold terms of the hidden neurons.
A neural network can be described as a directed graph whose nodes correspond to neurons and edges correspond to links between them (Figure 4.5).

Figure 4.5:Basic structure of a Neural Network[177]

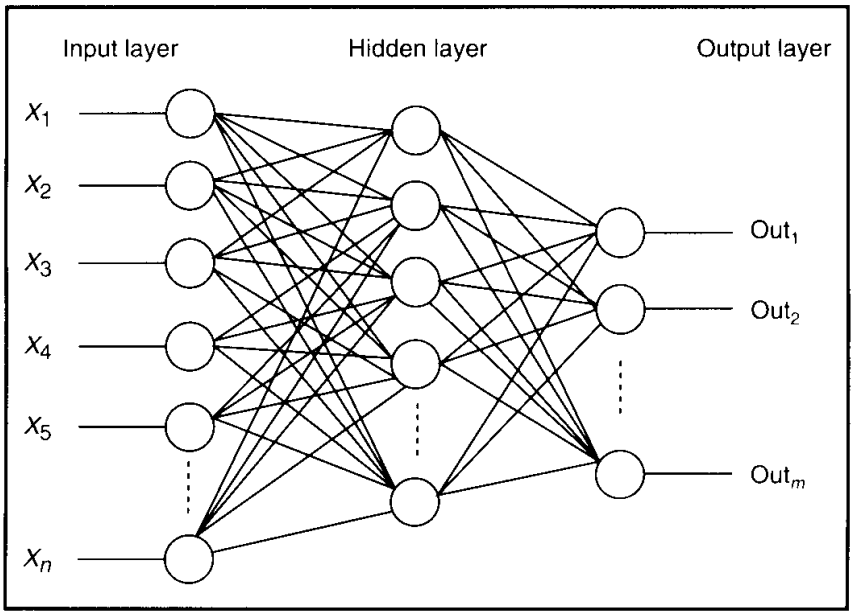

Based on the connection patterns and architecture, ANNs can be grouped into two categories:

- *Feed-forward networks*: in which graphs have no loop
- *Recurrent (or feedback) networks*, in which loops occur because of feedback connections

Neural Network can potentially reproduce any boolean function
Articial neural networks (ANNs) can be used as tools for prediction, classification, and decision support [178]. In medicine they have been applied successfully to several of pattern analysis and diagnostic problems[179]
Neural networks, provide good predictive accuracy in a wide variety of problem domains, but produce models that are notoriously difficult to understand.

Rosemblat perceptron

Rosenblatt's perceptron (Rosemblatt, 1988) [180] is the simplest form of ANN, which consists in a single neuron receiving an input vector (x_1, x_2, ...,x_n) and giving an output value back *f(x)*.
The input values correspond to the attributes, while the output is the prediction of the real target variable y. A weight w_j is assigned to each of the n input connections[180]:

$$w1x1 + wnxn - \theta = \boldsymbol{wx} - \theta \qquad 4.2$$

An activation function $g(\cdot)$ and a distortion constant θ are defined.
As it is the prediction for a new observation x
Given these elements, the prediction for a new observation x works as it follows:

$$fx = g(w1x1 + wnxn - \theta) = g(\boldsymbol{wx} - \theta) \qquad 4.3$$

The transfer function converts the linear combination of the inputs in a set composed by the target vales (v_1, v_2, …v_H).
The weight w_j and distortion θ can be established by iterative algorithms for each sample x_i. So, at each iteration the values w and are updated through recursive formulas based on the prediction error.
Rosenblatt's perceptrons can be combined to form a multi layered network capable to learn from complex processes.

Each node of the network works as a single Rosenblatt's perceptron.
These networks are composed by input nodes, hidden nodes and output nodes. For each observation the first ones receive the attributes values.
Usually a network has the same number of input nodes and attributes. Hidden nodes compute values operations and transformations hidden in the network. Every node could be linked to input nodes, output nodes or other hidden nodes. Output nodes give back a value which corresponds to the target value prediction.
The defined network is trained through a back-propagation algorithm, which is similar to the one illustrated for the Rosenblatt's perceptron.
The system begins with random weights at the connections between nodes.
Data sets with known outcome are entered at the input nodes (training data set). The ANN compares its own output value with the known outcome and calculates an error value. The error will change as the weights at the nodes change.
The ANN attempts to minimize the error by adjusting the weights according to the back-propagation algorithm. This process is repeated hundreds or thousands of times until a desired error level is achieved.
Artificial neural networks have several advantages over conventional statistical techniques, such as multiple regression analysis [181]. They are more flexible for the user and can solve non-linear problems, and the learning mechanism can fit both classification and esteem problems. Furthermore, attribute selection can be automatically handled: low coefficients values are assigned to redundant or not significant attributes. Main drawbacks are long training times and results that are difficult to interpret.

4.7.4.3. Support vector machines

Support Vector Machines are a learning tool originated in modern statistical learning theory.
SVMs understanding can start from this simple concept: a simple way to classify a set of points in a plan is to draw a line and call points lying on one side positive and on the other side negative. If the two sets are well separated, one would intuitively draw the separating line such that it is as far as possible away from the points in both sets (Figure 4.6).

Figure 4.6: Support Vector Machines basic concept[182]

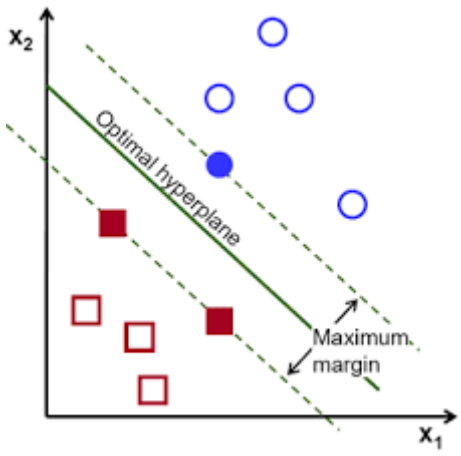

This intuitive choice captures the idea of *margin separation* [183].
Support vector machines (SVMs) realize this concept on a simple idea: map a *n*-dimensional input vector $\mathbf{x} \in R^n$ into a high dimensional (possibly infinite dimensional) feature space *H* by and construct an optimal separating hyperplane in this space. Different mappings construct different SVMs.
When the training data is separable, the optimal hyperplane is the one with the

maximal distance (in *H* space) between the hyperplane and the closest image $\phi(\mathbf{x}_i)$ of the vector $\mathbf{x}_i$ from the training data [184].

SVM problem for a Binary classification

SVM can be used for binary classification.

The resolution problem for SVM for a binary classification can be defined as follow.

Considering vector $x \in R^n$ as a pattern to be classified, and let scalar y denote its binary class label (i.e., $y \in \{1, 0\}$). In addition, let $\{(x_i, y_i) = 1, 2, ..., l\}$, denote a given set of training examples.

The problem is how to construct a classifier (i.e., a decision function), able to correctly classify an input pattern that is not necessarily from the training set. Linearly separable training patterns give the simplest case. That is, there exists a linear function of the form:

$$fx = i = 1l\lambda iyi\phi Tx1\phi Tx1 + b = fx = i = 1l\lambda iyiKxi, x + b \quad 4.4$$

Such that for each training example x_i, the function yields $f(x_i) \geq 0$ for $y_i = 1$, and $f(x_i) \leq 0$ for $y_i = 0$. w represents the hyperplane angular coefficients while b indicates its constant term.

In this way training examples from the two different classes are separated by the hyperplane solving the equation:

$$fx = i = 1l\lambda iyi\phi Tx1\phi Tx1 + b = fx = i = 1l\lambda iyiKxi, x + b \quad 4.5$$

For a given training set there may be infinite possible surfaces that divides the two classes setting to zero the empirical error on the training set.

The SVM classification is however based on finding the optimal hyperplane: the one that maximizes the separating margin between the two classes.

In other words, SVM finds the hyperplane that causes the largest separation margin between the decision function values belonging to the "borderline" examples from the two classes identified by two canonical hyperplane parallel to the separation surface itself.

This examples are called support vectors and they result the most important examples in the training set since they alone determine the classification rule. The separation margin can be expressed as:

$$\delta = 2|w| \text{ where } ||w|| = j \in N\omega j2 \quad 4.6$$

Mathematically, this hyperplane can be found by minimizing the following cost function:

$$Jx = 12wTw = 12w2 \quad 4.7$$

Subject to the constraints:

$$ywxi - b \geq 1 \qquad i \in M \quad 4.8$$

The objective function corresponds with the margin maximization, expressed as its reciprocal minimization, while the constraints force each x_i example to fall in the half-space corresponding to its y_i class.

This specific formulation may not be useful in practice since training data may not be completely separable by a hyperplane.

Slack variables, denoted as d_i, can be introduced to relax the separation bounds considering misclassification errors chance.

Accordingly, the cost function can be modified as follow, resulting in a more general optimization model:

$$Jw, b = 12w2 + Ci = lldi \quad 4.9$$

The updated constrains are:

$$yiwxi - b \geq 1 - di \qquad d_i \geq 0 \qquad 4.10$$

The objective function is now composed by two terms: the first one expresses the separation margin reciprocal while the second one quantifies the empirical error.
C is a user-specified, positive, regularization parameter that controls model generalization capacity and accuracy over training set.
This modified cost function constitutes the so-called structural risk (4.9).
The purpose of using model complexity to constrain the optimization of empirical risk is to avoid overfitting, a situation in which the decision boundary too well precisely corresponds to the training data thereby failing in perform well on future independent data sets.
In formulation of SVM learning is based on the principle of structural risk minimization.
Instead of minimizing an objective function based on the training samples (e.g. mean square error (MSE)), the SVM attempts to minimize a bound on the generalization error (i.e. the error made by the learning machine on test data not used during training).
For a given training set there may be infinite possible surfaces that divides the two classes setting to zero the empirical error on the training set.
The SVM classification is however based on finding the optimal hyperplane: the one that maximizes the separating margin between the two classes.
In other words, SVM finds the hyperplane that causes the largest separation margin between the decision function values belonging to the " examples" from the two classes identified by two canonical hyperplane parallel to the separation surface itself.
This examples are called support vectors and they result the most important examples in the training set since they alone determine the classification rule.
The separation margin can be expressed as:

$$fx = wTx + b = 0 \qquad 4.11$$

As a result, a SVM tends to perform well when applied to data outside the training set, finding an ideal equilibrium between empirical accuracy over the training samples and generalization capacity over new examples.
Indeed, it has been reported that SVM-based approaches are able to significantly outperform competing methods in many applications.
SVM achieves this advantage by focusing on the training examples that are most difficult to classify.

$$fx = wTx + b = 0 \qquad 4.12$$

These "borderline" training examples are called support vectors.
We could consider these support vectors as the most meaningful examples in the training set as they better represent the target classes characteristics.
Although SVM modeling gives returns black box model support vectors could play an essential role in classification rules interpretation.
Mathematically, this hyperplane can be found by minimizing the following cost function:

$$fx = wTx + b = 0 \qquad 4.13$$

to fall in the half-space corresponding to its y_i class.
This specific problem formulation may not be useful in practice since training data may not be completely separable by a hyperplane.
Slack variables, denoted as di, can be introduced to relax the separation bounds considering misclassification errors chance. Accordingly, the cost function can be modified as follow, resulting in a more general optimization model:

$$fx = wTx + b = 0 \quad 4.14$$

The updated constraints are:

$$yiwxi - b \geq 1 - di \quad 4.15$$

The objective function is now composed by two terms: the first one expresses by the separation margin reciprocal while the second one quantifies the empirical error. C is a user-specified, positive, regularization parameter that controls model generalization capacity and accuracy over training set. This modified cost function constitutes the so-called structural risk.
The purpose of using model complexity to constrain the optimization of empirical risk is to avoid overfitting, a situation in which the decision boundary too well precisely corresponds to the training data thereby failing in perform well on future independent data sets.
Linear separation surfaces result unsuitable in achieving a high accuracy classification in problems ruled by intrinsically non-linear regularity schemes.
The linear SVM can be extended to non-linear classifier by using a nonlinear operator φ(·) to map the input pattern x into a higher dimensional space H.
The operator φ(·) is a kernel k realization that project the non-linear pattern x from the attribute space into the feature space H where the optimal linear hyperplane can be determinate.
Because the SVM approach is data-driven and model-free, it may have important discriminative power for classification, especially in cases where sample sizes are small and a large number of variables are involved (high-dimensionality space)[185].

4.7.5. Overfitting

One of the main issues in supervised machine learning, from labelled training data, is model overfitting.
In machine learning, overfitting occurs when a learning model customizes itself too much to describe the relationship between training data and the labels. Specifically, overfitting occurs if the model or algorithm shows low bias but high variance [163]. If we consider a training set $t \in T^m$ and a class *y* and a classifier r, the "bias" of a solution f coincides with the approximation error defined as:

$$\varepsilon zf = 1mi = 1m(fxi - yi)2 \quad 4.16$$

and its "variance" with the sample error defined as is the mean error over the training sample:

$$\varepsilon fz = \varepsilon f(x) - \varepsilon(fz(x)) \quad 4.17$$

Figure 4.9 depict graphically an overfitting case for a parabolic predictor

Figure 4.9: Overfitting case for a parabolic predictor

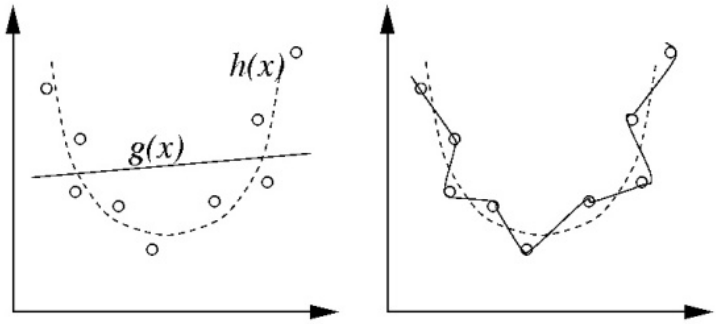

Overfitting tends to make the model very complex by having too many parameters. By doing this, it loses its generalization power, which leads to poor performance on new data. This leads to an identification attribute that will never correctly predict any examples outside the training set [165],
The most obvious consequence of overfitting is poor predictive performance on the validation dataset as the prediction model overreacts to minor fluctuations in the training data- To reduce overfitting in noisy situations, has been necessary to act on the training set for example operating cross-validation[164].

4.7.6. Performance Evaluation of Machine Learning Algorithms

Machine Learning algorithms can be evaluated on the basis of the confusion matrix and ROC curves[191]
Figure 4.9 depicts the structure of a confusion matrix: the columns reports the *Predicted Class* while in the rows are the *Actual Class*.
In the structure of the confusion matrix TN is the number of negative examples correctly classified (True Negatives), FP is the number of negative examples incorrectly classified as positive False Positives, FN is the number of positive examples incorrectly classified as negative (False Negatives) and TP is the number of positive examples correctly classified (True Positives).

Figure 4.10: Confusion Matrix

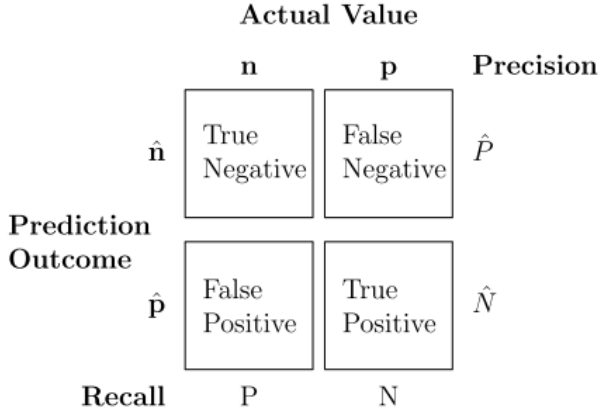

Confusion matrix can be used as basis to define performance evaluation for machine learning techniques.
A first performance evaluator based on confusion matrix is the predictive accuracy defined as:

$$Accuracy\ Acc = (TP + TN)(TP + FP + FN + TN) \quad 4.18$$

The Receiving Operation Characteristic (ROC) (Figure 4.10) [191] curve is a standard technique for summarizing classifier performance over a range of trade-off between TP and FP error rates.

Figure 4.11: ROC-Curve

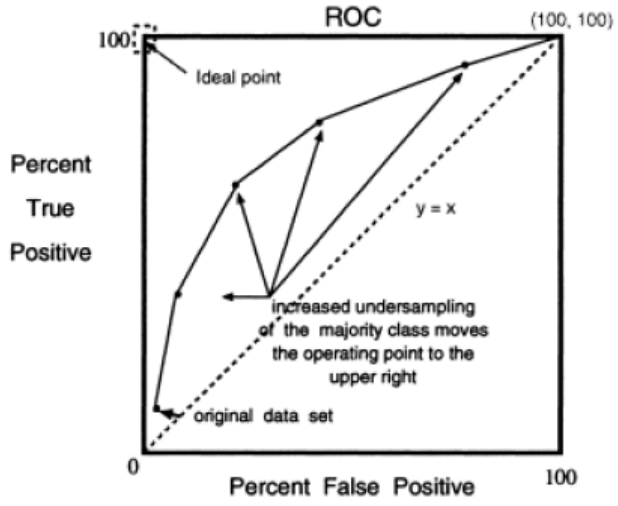

The ROC curve can furnish useful indicators to evaluate the classifier performances. ROC curves can be thought as representing the family of best decision boundaries for the relative costs of TO and FP.
The x-axis of the ROC curve represents the %FP, intended as:

$$\%FP = FP(TN + FP) \quad 4.19$$

The y-axis of the ROC is indeed the %TP:

$$\%TP = TP(TP + FN) \quad 4.20$$

As the point P(0,100) represents the scenario where all positive examples are correctly classified and no negative examples are misclassified as positive, and the line y=x , stand for the scenario of the randomly guessed class; the Area Under the Curve (AUC) can be considered an effective metric for the prediction accuracy obtained by ROC curve.
The AUC of a classifier measures the probability that the classifier will rank a randomly chosen positive instance higher than a randomly chosen negative instance [192].

Precision and Recall
The ROC curves are usually the most used method to evaluate results for the binary decision problems. However when with highly skewed and asymmetric dataset *precision, recall* and F-measure [193,194] can offer a better evaluation.
Precision and recall can been obtained by the ROC curve as:

$$precision = TP(TP + FP) \quad 4.21$$

$$recall = TP(TP + FN) \quad 4.22$$

Precision or Confidence denotes the proportion of Predicted Positive cases that are correctly identified.
Recall or Sensitivity is the proportion of real Positive cases that are correctly Predicted Positive.
Neither of these takes into account the number of True Negatives, that indeed are considered in the F-measure, defined as:

$$F - measure = 1 + \beta 2 \cdot recall \cdot precision\ (\beta 2 \cdot recall \cdot precision) \quad 4.23$$

The F-measure represents the trade-off among different values of TP, FP and FN. It is expressed as follows: F where β corresponds to the relative importance of precision respect recall and it is usually set to 1.

Chapter 5 – Materials and Methods

5.1 Introduction

The proposed work has been developed within the framework of the "DialysIS" Project. "DialysIS - Dialysis therapy between Italy and Switzerland" is an international project cofounded by Regione Lombardia and European Union, through the INTERREG operative cooperation program between the two countries (IT/CH 2007-2013).
The project involves two reseach units of Politecnico di Milano (the Life Support System Unit at the department of Chemistry, Materials and Materials Engineering.and the Department of Management), and 4 dialysis units between Italy and Switzerland, namely Ente Ospedaliero Cantonale di Lugano (EOC), Switzerland, S.C. Nefrologia e Dialisi dell'A.O. della Provincia di Lecco, Italy Servizio di Nefrologia e Dialisi dell'A.O. di Como, Italy and Servizio di Nefrologia e Dialisi dell'A.O. di Varese, Italy.
The main efforts of the project was the development of a common platform to share information and clinical protocols among the involved partners in order to enhance standardized personalization of the therapies and improve patient and clinician mobility.
The Dialysis project operates on this framework, wanting to spread care provision even beyond transnational borders. The project is addressed to chronic uremic patient needing hemodialysis treatment to replace kidney functionality.
In particular the project has pursuit the following main goals:

- To develop and validate a computational models able to describe patient specific response to the treatment,
- To implement an automatic control system based on pressure and biochemical signals.

To implement a Web platform, to share and allow the remote consultation of models and therapy protocols developed and applied during the study and also later.
To provide new protocols and instruments, allowing to personalize dialysis treatment.
The web platform has been developed with the aim to ensure a better territorial continuity to the patient care.
In the mean time, the web platform represents the tool allowing extracting data from a dedicated DataBase and using the numerical model features as described in Chap 4.5.
In the field of Dialysis treatments, the availability of different kind of therapies and the huge variability of therapy's approaches in different clinical centers increase the complexity of the problem.
The Dialysis project bases acts on the development of a common repository of patient data in order to share clinical data and protocols ensuring: a higher patient mobility as well the sharing of knowledge and clinical approaches among different clinical centers, operating on the same large catchment area.

5.2 Dialysis Data Acquisition

A basic point of the Dialysis project has been the collection of data from the different involved nephrology and dialysis units. DialysIS study was structured in three different phases.
Phase 1: acquisition of the complete set of data at Lecco and Lugano clinical centres.
Phase 2: acquisition of the complete set of data at Como and Varese clinical centres, acquisition of a small set of data (without

blood composition monitoring) at Lecco and Lugano clinical centres
Phase 3: acquisition of the reduced set of data all over the involved centres, together with the bedside evaluation of final analysis.

5.2.1. Patient enrollement

DialysIS database was compiled integrating treatment recorded data and patient specific parameters measures.
For each patient, clinical records were also registered in order to have a better definition of their medical case.:
The patients enrolled within the study were adult, undergoing dialysis therapy since at least 3 months, and wearing a artero-venous fistula used as vascular access (AVF) [195,116].
The 65% of them was male and 35% women.
he medium age of the population was 70,07±10,89 with a dialysis age (time lasting rom the first treatment) of 61,5±10,89 months. The 31% are affected by diabetic nephropathy and 90% shows heart disease.

5.2.2 Data collection protocol

Personal and anamnesis data have been recorded for each enrolled subject;.
Additional data as clinical prescription, haematochemical data, machine acquisition data, hematochemical data have been recorded during each treatment sessions.
A bio impedance test, to evaluate the hydration status has been performed at the beginning of the first session and at the end of the last one. The BNP level has been also evaluated at the start of the session.
During each session, adversary odds, infusion and food and beverage consumption have been noted.
Table 5.1, shows a synopsis of collected data.
Data have been clustered by type/source and sampling frequency/timing.
Together with patient data also suspicious or abnormal events during the treatments have been noted and registered in order to be part of useful information for the final platform.
These information should be exploited to underline abnormal behaviour of the subject.
At least 6 treatments session have been registered for each of the patient, and for 12 of them the number of registered session rises to 8.
Data have been acquired by the written consensus of the patients.
The complete dataset at present contains 808 dialysis sessions referred to 145 patients.

Table 5.1: Synopsis of collected data[196]

Type/Source	Sampling Freq./Timing	Name[Unit]
Personal	Once a time	Patient ID, Sex, Date of Birth, Height, Weight
Anamnesic	Once a time and at each variation in the drug therapy	Clinical History, Drug Therapies, Dialysis age
Dialysis Machine	1/min	Ultrafiltration Rate (UF) [ml/h], Ultrafiltration Volume [ml], Weight loss [Kg], Dialysis fluid flow[ml/min], Dialysis fluid Temperature [°C], Hematic Flow [ml/min], Packed Cell Volume [%], Blood Temperature [°C], Relative Blood Volume (RBV)[%],
	Every 15 min	Diastolyc pressure[mmHg], Sistolyc pressure [mmHg], Heart Beat [1/min]
Hematochemical	Start Treatment Every hour End Treatment *each session*	pH, pO2[mmHg], pCO2 [mmHg], Cumulative Blood Volume [ml], Hemoglobin blood conc.[g/l], Urea blood conc. [g/l], *Blood Ionic Concentration of:* Calcium Ion*[Ca^{2+}]* [mmol/l], Magnesium Ion *[Mg^{2+}]* [mmol/l], Clorum Ion *[Cl^-]* [ml], Sodium Ion *[Na+]* [mmol/l]), Glucose Concentration[mmol/l]
	Start Treatment End Treatment *each session*	Albumine blood conc.[g/l], Phosphorous ion blood conc.*[PO^{4-}]*[mmol/l], *dialysis fluid Fluid Concentration of:* Calcium Ion*[Ca^{2+}]*[mmol/l], Magnesium Ion *[Mg^{2+}]*[mmol/l], Clorum Ion *[Cl^-]*[ml],Sodium Ion*[Na+]*[mmol/l]
	Start Treatment End Treatment *only 1stsession*	Creatinine blood conc. [mmol/l], Beta-2 microglobuline blood conc.[ng/l],
Patient Hydration Status Data	Start 1st Treat. End of last Treat.	**B**NP [pg/mL] PTH [ng/L] B_2 [ng/L] Body Mass Index(BMI) [Kg/m^2], Over Idration Index (OH) [l], % Over Idration Index (OH) [%], Lean Tissue Index (LTI) [Kg/m^2], Fat Tissue Index (FTI) [Kg/m^2],

Other tests, such as PTH, β-2 microglobuline and creatinine blood levels have Been conducted both at the beginning and at the end of the monitored sessions and, if necessary, also after 1 or 2 months.
Clinical manifestation of hypotension or abnormal event has been required to be registered by the clinical staff.
The set of data has been designed in agreement with the clinicians in order to obtain a complete screening of the several etiological factors of IDH as describes in Chap 3.
The collection of data has followed a share protocol between the involved clinical centers in order to ensure patients with homogeneous and quality

treatments and to improve the quality of data analysis collected during the study.
Lecco Ethics Committee approved the latest version of the study description on 31-05-2013.
Following this approval was ratified by the Ethics Committees of the other three hospitals.

5.3 Data collection Strategy – the Dialysis Data Infrastructure and Dialysis Matlib

The main problem related to the collection of data coming from different clinical centres has been their storage within a common structure.
Even if a common acquisition protocol was established, data have been supplied by the clinical centres in different and highly heterogeneous formats.
Each centre was in fact equipped with different dialysis machine and each vendor promotes the use of different licensed software to manage the output clinical data.
This problem is very common dealing with clinical data and can be identified as an interoperability problem. The strategy here adopted to solve this specific problem is the use of a Federate DataBase System (FDBS) as described in Par.4.4.
One of the significant aspects of a FDBS is that a single component DBS can be autonomous in its local operations and at the same time participate in a federation.
The DB federation has been achieved through the implementation of the Dialysis Data Infrastructure (DDI), the common data repository for all the involved centres.
Figure 5.2 resumes the overall framework of the Dialysis Data Infrastructure and describes its interaction with the Dialysis Matlib.

Figure 5.1: Dialysis Data Infrastructure Framework and interaction with Dialysis MATlib

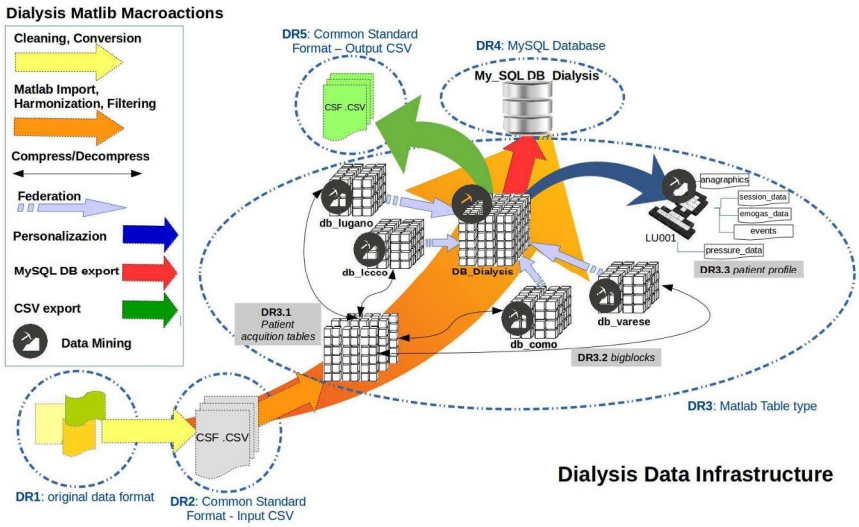

5.3.1. The Dialysis Data Infrastructure

The Dialysis Data Infrastructure has been designed to be a flexible tool both for the clinician and the researchers, supporting the sharing and the analysis of the clinical data recorded along the DialysIS project.
The DDI allows handling the data coming from each specific dialysis unit separately and in a customized way. Despite that customization, these data can

be gathered into a common repository, constituting a federation structure.
The DDI also allows extracting patient's specific data in order to perform personalized analysis.
As depicted in Figure 5.1, the DDI provides 5 levels of data representation (DR1, DR2 , DR3,DR4, DR5). The first two directly related to the primary data sources, coming from the clinics.
Level DR1 represents the raw data files as transmitted by the dialysis units.
These data are usually exported from proprietary software or even manually reported by the clinicians and are characterized by highly inhomogeneous formats.
The primary files of DR1 are stored and constantly uploaded on an online ftp repository, whose organization reflects the classification by centres, as in Figure 5.2.

Figure 5.2: ftp repository filesystem

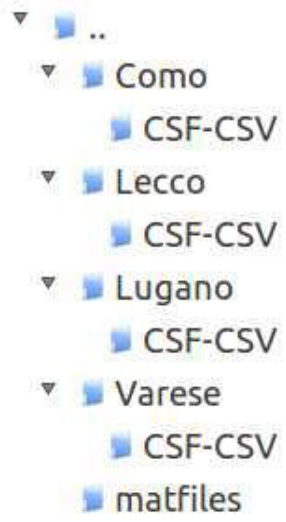

Each dialysis unit is associated to a unique centre's folder in the file system.
Each one of these folders contains also a CSF-CVS sub-folder, that's the repository for the Level DR2 data files. Level DR2 files are obtained by the conversion of original raw files into a Common Standard Format (CSF). CSF data are collected in tables, which will constitute a Common Database Schema (CDS) for the upper levels data structures.
In the CDS, each table groups information depending on the same acquisitions' source as described in Table 5.2.
The passage from DR1 to DR2 represents a first step of data interoperability.
In particular, interoperability is here achieved through the use of a common acquisition protocol among the different dialysis units, whose structure impact on the design choice for the CDS. Data at DR2 level are saved in the specific folder of the ftp-repository as CSF-CSV (Common Standard Format CSV) input file, that are .CSV files in row-column format with point-comma column separator. Each CSF-CSV corresponds to one of the tables listed in Table 5.2.

Table 5.2: CSF table schema

DR2 Table Name	Acquisition Source	Description
Anagrafica	HIS*, Clinical Records	Anagraphic/Anamnesic data
info_sedute	HIS, Clinical Records	Prescriptions on the treatment
dati_emogas_lab	Hemogas Analyzer, Hospital Laboratory	On-line hemato-chemical data
dati_pressori	Pressure Sleeve	Pressure Sleeve on-line acquisitions
dati_macchina	Dialysis Machine	Dialysis Machine on-line acquisitions
dati_bcm	Bioimpedenziometry	Patient hydration Status got by bio-impedentiometry
dati_dialisato	Clinical Records	Prescriptions on Dialisate Composition
dati_sacca	Dialisate bags datasheets	Dialisate bags initial composition
registro_eventi	Clinical Records	Sessions event register

Each table collects all the acquisitions referred to a specific patient.
In order to preserve the integrity of the DB internal references, tables are filled following some few basic principles:

- *each patient* is identified by a unique patientID composed by 5 alphanumeric characters: the first 2 are a couple of letters that identifies the clinical centre, the last 3 are digits representing a progressive number
- *each dialysis session*, for each patient is identified by a progressive number

The CSF-CSV files are named in a patient ID-oriented way as follow:

<nametable_patientID>.csv 5.1

The CSF-CSV input files represent a consistency layer for all the DDI.
All the further layers, in fact are based on the CSF-CSV.
For example, data in level DR3 are obtained by directly importing, filtering and harmonizing into Matlab® (Massachussets,US) the CSF-CSV (Figure 5.1).
In the Matlab® workspace *level DR3* data were then organized as table type variables (available since the R2013b version [136] of the software), used to store heterogeneous types of data, coming both from a text file or a spread sheet, in a uniform tabular format with rows and columns [136]
Table type variables has been also used to reproduce the structure of the CDS in the Matlab® environment.
In order to easily handle data analysis at different levels of aggregation, 3 different kind of DR3 representation has been implemented.
The first one is the DR3.1, containing data structured in *patient single tables.*
The *patient single table* follows the CDS structure and will allow iterative operations on the data related to a specific acquisition source at the patient's level.
Since they represent the more proximal import of the CSF-CSV input files into Matlab® workspace, the patient single tables inherit the same patientID-oriented organization and naming of level DR2.
As depicted in Figure 1, patient single tables can be gathered in huger structures by the compress Dialysis Matlib macro-action.
These huge structures are the DR3.2, also called *bigblocks*.
DR3.2 provides each single dialysis unit of a unique database obtained by the aggregation of single tables of each one of the patients treated in the same unit

(db_lecco, db_lugano, db_como, db_varese). The aggregation maintains the CDS, but at this level the patientID organization were loss.
Nevertheless the operation can be inverted by using the decompress Dialysis Matlib macro-action.
The DR3.2 data structures can be used for specific analysis, targeted to single clinical centres.
Moreover, the single dialysis unit databases can be federated into a main central data storage (DB_DialysIS), which collects all the acquired data. DB DialysIS can be used for general undifferentiated inquiries.
For high personalized purposes indeed, there is the DR3.3 data structure type, or *patient profile*, in which data are represented as compact patient data-struct, that contains all the tables of all the CSD in one Matlab® variable.
The patient ID identifies each 'patient data-struct', and each table will be accessible by the dot notation. DR3.3 format will facilitate personalization allowing an easy querying of patient specific data. All the data at level DR3 are saved in '.mat' files, stored in the common ftp repository in a proper folder.
The ultimate levels of data representation in the DDI are the DR4 and DR5, both obtained from the DB_Dialysis using dedicated export actions.
DB4 level stores data in the MySQL_DB_Dialysis, a MySQL® database, underpins a web platform, to be used as explained in the following paragraph.
The DB5 allows indeed having all the DB_Dialysis tables as .CSV output files in the common standard format with dot-point as column separator. The basic storage infrastructure used to gather data from the different clinical centres was based on a MySQL®DMBS System, leading to a flexible common schema.

5.3.2. *EER Schema of MySQL_DB_Dialysis*

Figure 5.3 reports the EER schema of the MySQL version of the DB_Dialysis

Figure 5.3: EER schema of the implemented database

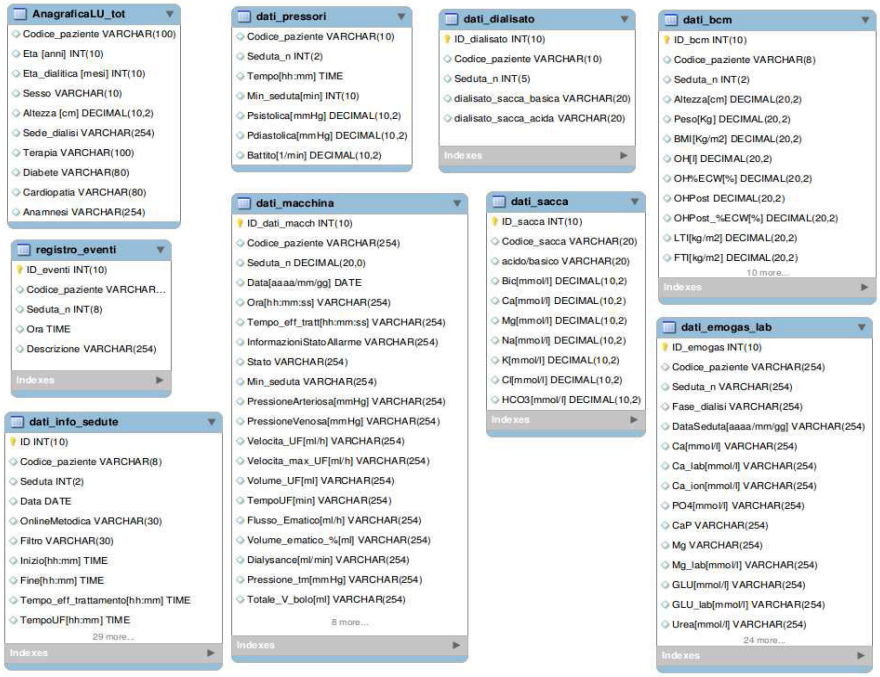

The EER schema translates the CSD format into a relational schema.
The schema design has been lead by some few basic principles, which are:

- **each patient** is identified by a unique ID of 5 alphanumeric characters: the first 2 were a couple of letters identifies the clinical center, the last 3 are digits representing a progressive number within the same center from 1 to 50 (Es. LU001 refers to the first enrolled patient in Ente Ospedaliero Cantonale di Lugano).
- **each dialysis session**, for each patient is identified by a increasing number,from 1 to n. Data are clustered by source/group of acquisition, so for example data coming from dialysis machine and hematochemical data are stored into two different relational tables.

As can be seen the diagram doesn't show relationships.
This choice is pretty unusual, with respect of the classical database structures, but has been done because the flexible structure has been realized only by a few number of essential association within variables distributed among tables.
Each clinical or personal clinical data is identified by a unique ID number and associated to a specific couple patient/session.
This allows to easy combine variables from tables sources in order to perform complex analyses.
The described structure has been conceived to meet the demand of a common sharing platform for the clinical data, taking into account the non-homogeneous formats of the different data sources.

5.3.3. *The Dialysis MATlib*

The Dialysis MATlib is a customized library, implemented in Matlab® code, to manage data in the framework of the Dialysis Data Infrastructure.
It acts on the raw data coming from the clinical units allowing converting, harmonizing and querying them in a versatile way in order to make them more interoperable. Dialysis MATlib follows the Extract, Transform, and Load (ETL) methodology logic.
The ETL methodology is frequently used in database operations, mainly in data

warehousing and refers to three simple processes [197]:

- **extract**, data from heterogeneous multiple data sources;
- **transform**, data into a proper storage format;
- **load,** the transformed data into a target database with a defined structure.

The DialysIS MATlib implements these processes exploiting the features of the relational tables and their conversion into the Matlab® table type variables.
The table data type indeed, allows to store variables that are either string or numbers in a unique rows and column-oriented structure.
Through a dot notation is therefore possible to easily access to table rows and column, making data manipulation more simple and direct.
Furthermore, the use of the vector and matrix transformations, typical of the Matlab® environment, allows an easier handling of data; errors correction, standardization and data format conversion can be massively performed using coding language instead of complex SQL queries.
Depending on their specific functionality, Dialysis MATlib functions have been divided into 8 groups, which correspond to the macro-actions on the DDI showed in Figure 5.1.
The description of the groups is reported in Table 5.2.
The Macro-actions of the DialysIS MATlib cover all the data workflow within the DDI: they practically act as an interoperability layer of the FDBS logic described in Figure 4.1.
More specifically, macro actions 0 and 1 build an interoperability layer.
Interoperability is here obtained directly by the Matlab® code that performs differentiated operations depending on the received input data.
The final outputs were tables in a standard format. Macro-actions 2 and 3 indeed act as federation layers. They coordinate the merging operations of dialysis units' databases into a common data repository, the DB_Dialysis.
An automatic data care process was performed by using an embedded architecture made by the interaction of the open source database management system (DBMS) LibreOffice Base, and ad-hoc developed Matlab® library (Dialysis Matlib) described in the following section.
The process performed data cleaning and harmonization procedures and the standardization of the export format.
On this way, it has been possible to guarantee the portability of storage data in a unique format, independently from the initial acquisition centre.

5.4 Data Analysis - Introduction

As discussed in Chapter 2.2 the hypotension onset in patients undergoing dialysis treatments can be due to several factors: related to the specific patient status (vascular and cardiac diseases, neuropathy, anemia, …), or to the treatment settings (sodium concentration, buffer composition, temperature of the dialysate, ultrafiltration rate, plasma refilling rate, type of membrane, type of nutrition and hydration, …).
Considering the patient's peculiar reaction to treatment, one of the open challenges is to quantify the risk of IDH onset, before the treatment start and then along the treatment.
Furthermore, having IDH events a multivariate origin, it is important to consider a wide set of clinical variables in order to find specific predictors.
The current work proposes two approaches of data analysis in order to predict IDH events (Figure 5.4)
The two approaches has been theoretically described in par. 4.4.
By them, the available data have been firstly analyzed by a classical inferential statistical approach in order to find out which variables from the available dataset would impact on the IDH onset.
This approach first analysis led to the definition of two clinical criterions to identify at the early stage of a dialysis session (start) the risk of IDH onset and to predict the IDH events along the session (intra-dialysis).

A second approach has been pursued ,considering the onset of IDH as a "black box" modelled phenomenon. As the scarse "a prori knowledge" of the etiology was available, a greater focus has been given on the prediction rather than the description.
For this reason, machine learning algorithms has been used, particularly random forest, artificial neural network and support vector machine has been tested.

Figure 5.4: Approaches to IDH Prediction

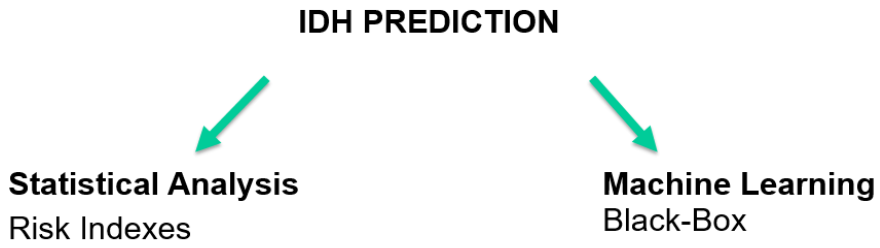

The performances of both the approaches has been evaluated on the available data, stored in the database, and pertaining to a total of 808 sessions, acquired by the different centers as follow:

- Lugano: 20 patients, 148 sessions;
- Lecco: 50 patients, 300 sessions;
- Como: 30 patients, 180 sessions;
- Varese: 30 patients, 180 sessions.

5.4.1. Dataset restrictions and pre-filtering

As described in Chap. 3 the causes of hypotension are multiple, the decrease in blood volume that occurs during hemodialysis is the main involved factor and different cardio-circulatory and hematochemical variables are involved in its manifestation.
During the treatment, the ultrafiltration at the dialysis filter level imply a fluid withdrawal from the vascular compartment, which is usually compensated by a fluid refill (plasma refilling phenomenon) from the interstitial to the vascular compartment. An impairment in these two flow rates, (at dialysis filter and capillary membrane level respectively) can imply a plasmatic volume depletion and consequently IDH onset.
This mechanism could lead both to impaired peripheral vasoconstriction, and autonomic dysfunction, that can be recognized in cardiac frequency and blood pressure abnormality [32].
In chronic hemodialysis patients, risk factors of hypotension include also shifts in extracellular volume, osmolarity, and electrolytes, dialysis-induced temperature changes, and altered vasoregulation [540].
On a clinical point of view, an accurate assessment of dry weight is crucial in all patients on dialysis and especially those patients prone to intradialytic hypotension [198].
This assumptions led to the selection of a subset of variables of interest all the variables registered in the DialysIS Database.
In particular the set has included: the main plasmatic ions concentration (i.e. calcium [Ca++], magnesium [Mg++], potassium [K+], sodium [Na+]), hematocrit as seen in [35,36], and complex parameters such as inter-session Weight Gain (WG) and MAP. Weight gain and MAP were calculated starting from the parameters available in the database as follow.

$$WG = Wend - Wstart \quad 5.2$$

where W_{end} stands for the patient weight at the end of the previous dialysis session, W_{start} represents the patient weight before the beginning of the current dialysis session, and the mean arterial pressure is calculated as:

$$MAP = 23SP - 13DP. \quad 5.3$$

where SP and DP stands for systolic and diastolic pressure, respectively.
These selected set of parameters aim to integrate various possible IDH triggers such as blood volume, ultrafiltration rate, heart rate and arterial stiffness[32].
In order to avoid
Since errors and outliers several times affect the collected data, a preliminary filter stage has been applied on the dataset in order to discard data corrupted or with values out of the physiological and the pathological ranges.
Table 5.3 resumes the range limits, taken from the literature [198,199], used to implement the preliminary filtering stage:

Table 5.3: Prefiltering limits

Parameter (UM)	Lower limit	Upper limit
Systolic Pressure (mmHg)	70	180
Diastolic Pressure (mmHg)	50	110
Weight Gain (Kg)	0	7
$[K^+]$ (mmol/l)	3.5	6.5
$[Mg^+]$ (mmol/l)	0.74	1.2
$[Ca^{2+}]$ (mmol/l)	0.8	1.3
$[Na^+]$ (mmol/l)	125	150

5.4.2. IDH Events identification – The IDH-D Criterion

The identification, on the recorded data, of the real IDH events within each session has been performed using an ad-hoc designed criterion, called IDH-D.
The criterion has been obtained from the ones proposes by Mancini et al. [32] and modified with a participatory revision with clinicians during the DialysIS Project in order to have a dependency only from the Systolic Arterial Pressure (SAP).
This criterion allow the identification of an IDH event if the one or more of the following conditions occurs:

D1: $SAP(t) < 75\% of SAP0$ with the concurrent presence of clinical symptoms

D2: $SAP(0) \geq 100mmHg \wedge SAP(t) \leq 90mmHg$

D3: $SAP(0) < 100mmHg \wedge SAP(t) \leq 90\% of SAP0$ with the concurrent presence of clinical symptoms or $SAP(0) < 100mmHg \wedge SAPt \leq 80\% of SAP(0)$ where SAP is the systolic arterial pressure evaluated at the beginning of the session (SAP(0)) and at the t time instant during the dialysis session (SAP(t)).

5.4.3. Pre-dialysis Statistical analysis

A first inquiry on the data was aimed on studying the influence of pre-dialysis conditions on the onset of IDH events during the treatment.
The analysis has been focused on the subset of data described in 5.5.3 considering the initial values of patient weight gain WG_0 (with respect to the end of the previous session), electrolytes concentration in blood $[Ca2+]_0$, $[Mg2+]_0$, $[Na+]_0$, $[K+]_0$, $[Cl-]_0$, $[Urea[mmol/l])]_0$, mean arterial pressure $[MAP]_0$.
As these values were referred to the state of the patient at the beginning of the treatment, they have been considered as representative of the pre-dialysis patient conditions.

5.4.3.1.Data Clustering

The available data referred to a heterogeneous population of patients, thus before applying inferential statistical methods and hypothesis testing, the data has been preliminary classified into groups.
Since the main goal of the analysis was the study of the influence of predialysis conditions on intra-treatment hypotension onset, one of the classification criteria was based on the automatic recognition of IDH events, as described in 5.5.4.

Figure 5.5: Data Clustering with two different dataset, dataset 1 HP/HR, Dataset 2 IDHy/IDHn

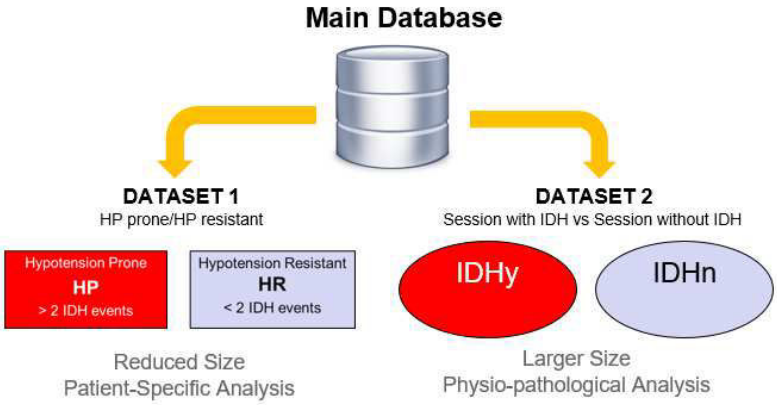

In particular 2 datasets has been created (Figure 5.5) following two classification By the first, the patient population has been split into 2 groups defined as Hypotension Prone (HP) patients, those who suffered of IDH in 2 or more sessions and Hypotention Resistant (HR) patients, whom showed at most 1 IDH episode.
Consequentially, the whole dataset of session as been splitted into the two groups : the group of sessions belonging to HP patients and the group of sessions of HR patients.
Figure 5.6, shows the classification algorithm for a typical patient.

Figure 5.6: Patient Classification Algorithm

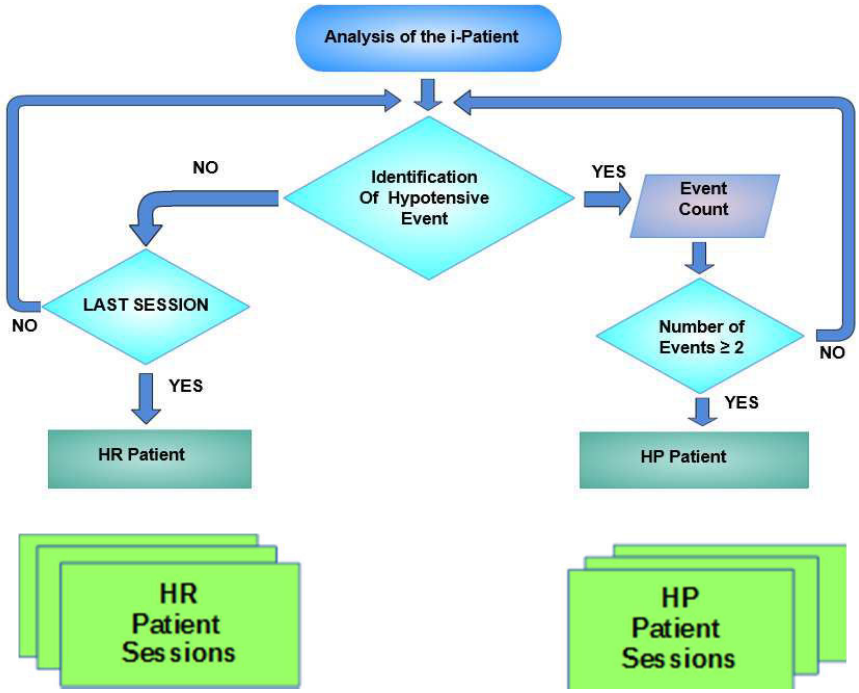

In the dataset 2, the single HD sessions were accounted, and the whole population of sessions was therefore divided in sessions characterized (IDH_y) or not (IDH_n) by the onset of IDH.
The rational behind the two datasets is following idea: Dataset 1 wanted to focus more on the analysis of the impact of patient specific variables on IDH, rather than on Dataset 2 the goal of the analysis was more on finding which variables strictly related could impact on IDH onset.

5.4.3.2, Inferential Statistical Analysis

For each variable of the dataset, distinct acquired series has been created for every group.
Identifying as <data> the generic variable, the series resulted in : $<data>_{HR}$ and $<data>_{HP}$ for the dataset 1 clustering and $<data>_{IDHy}$ and $<data>_{IDHn}$ for the dataset 2 clustering.
The main goal of this action was to verify the statistical difference of each <data> between the comparison groups.
The statistical difference was assumed by testing the hypothesis that mean and standard deviation of the series were different between the groups.
Depending on the Gaussian behavior, different test will be used to verify the hypothesis.
For the <data> series normality has been verified with two different approaches, and consequently two strategies has been pursued to check the statistical difference.
All the analysis has been conducted using Matlab® Statistical Toolbox [136].

Strategy 1: A Shapiro-Wilk normality test (SW), with a p-value<0,05 has been applied on the two series in order to verify normality [200].
The Shapiro-Wilk test, has been chosen because often used as normality test for small samples from a minimum of 3 to a maximum of 5000 units [201].
The strategy has been applied over each parameter only on *Dataset 1*.
Depending on the result of the Shapiro-Wilk normality test, parametric or non parametric tests to check the statistical difference was applied (Figure 5.6).

Figure 5.7: Data comparison algorithm between the two groups

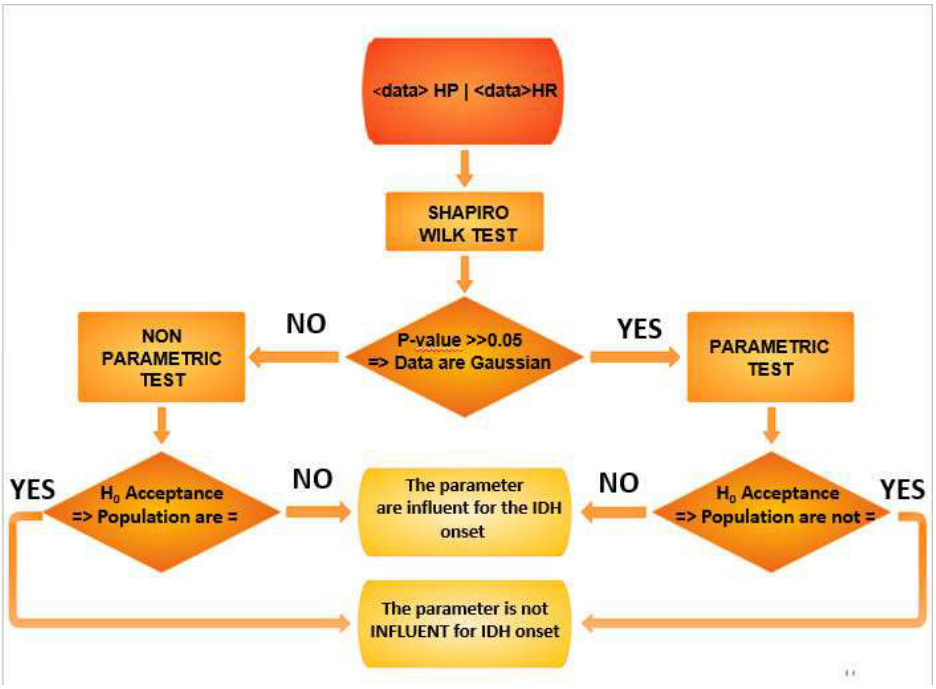

Table 5.4: resumes of the performed tests on the two groups of variables depending from the outcomes of the Shapiro-Wilk test**.**

	PARAMETRIC	NON PARAMETRIC
Mean comparison H_0 = population have the same mean value	t-test	Wilcoxon-Mann-Whithney
Variance comparison H_0 = population have the same variance	ANOVA One-way	Kruskal-Wallis

Strategy 2: a second strategy was based on the Kolmogorov-Smirnov (K-S) test to check the normality of the series. The Kolmogorov-Smirnov test is a non-parametric test to check normality on continuous one-dimensional probability distributions, which can be extended for the comparison of two independent samples. It measures a distance between the empirical distribution function of the sample and the cumulative distribution function of the reference distribution. Strategy 2 has been applied over each parameter on both Dataset 1 and 2.
K-S test results drive the choice for the following inference tests as suggested by Mustery and Bacarea 2010 and reported in Figure 5.8 [202].

Figure 5.8: Algorithm of inference test selection for data series[202]

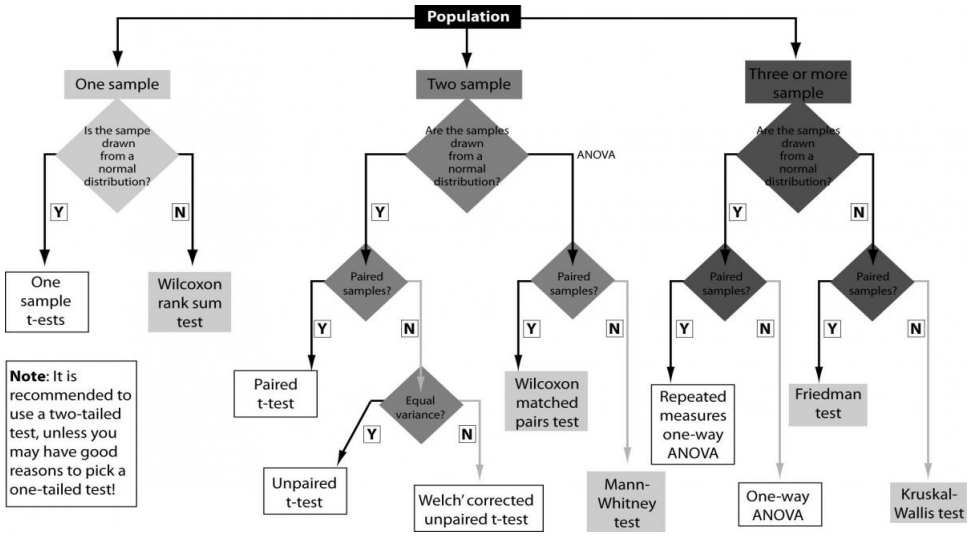

Since samples in Dataset 1 and 2 were not paired, one-way ANOVA and Kruskal-Wallis tests were performed [203]
If the population distribution was found to be normal one-way ANOVA test was applied, otherwise the Kruskal-Wallis test was used. Both these tests aim to highlight parameters that could be statistically different between the HP/HR groups in Dataset 1 and IDHy/IDHn populations in Dataset 2, respectively.

5.4.3.2. J index definition

The final goal of the statistical analysis was to develop a unique parameter for the offline prediction of IDH events, which should took into account the influence of predialysis conditions on hypotension onset.
This index, named J_i, to be evaluated at the beginning of each i session, has been defined as a weighted patient specific combination of the parameters that showed to be statistically different between the comparison groups, standing to the analysis described in 5.5.2.1 and Figure 5.5 ; these parameters were classified as influencing parameters IF (5.4) and would be the basic elements for the index composition.

$$Ji = c = 1NwcIF \qquad 5.4$$

The two strategies applied for the inference testing analysis lead to two version of the J_i-index called respectively J_{i1} and J_{i2} referring to *Strategy 1* and *Strategy 2*. The performences of the two versions of the index will be exposed and discussed in Cap.6 – Results.

5.4.3.3. Validation of the J-index

The performance of J_i in the prediction of IDH events onset during the sessions has been investigated during the validation phase.
Firstly, J_i index has been calculated for all the sessions of both the datasets, using 3 previous sessions for the longitudinal analysis in weight calculation. Parallel to the calculation of J_i, the presence of IDH events has been assessed using the IDH-D criterion.
Then the IDH onset risk identified by the J_i-index evaluation has been compared with the real presence of IDH events results from the IDH-D criterion.
The accuracy of the J index has been evaluated in terms of number of false positive and negative determined by the index with respect with IDH episodes

clinically recorded and automatically identified in the database according to the IDH_D criterion,

5.4.3.4. Centre dependent risk threshold assessment

The effects of the specific protocols adopted to manage hypotension in the different centers have been studied analyzing the distribution of the J_i values. Aim of this approach is to evaluate how to optimize the J_i index prediction ability, identifying algorithms to set a center-dependent risk threshold.
The average percentage of sessions characterized by IDH, based on literature data, is 25% [205]; we explore therefore the idea to use an alternative threshold set at the 75th percentile ($J_{th}=I_{75}$)) of the J_i values distribution, in each one of the involved centers. The 75th percentile would allows identifying as at risk of IDH the 25% of the sessions, characterized by higher J_i; the threshold value changes depending on the width of the J_i distribution; this approach should allow increasing the probability to effectively match an IDH episode, if pointed out by abnormal patient-specific values of the influencing parameters.
A second attempt has been done considering the percentage of sessions really characterized by IDH in each one of the centers (%IDH_c – retrospective evaluation on the enrolled patient, to have a wider set of data); the threshold has been than set to the 1- %IDH_c percentile ($J_{th}=I_{(1-\%IDHc)}$).
The sensitivity, specificity, TP, FP, TN, FN, PPV, NPV of the J_i index have been assessed using the new thresholds and the results have been compared with those obtained with $J_{th}=1$.
Intra-Dialysis Identifications and prediction of IDH onset.A second analysis, always based on a statistical approach, has been performed on the data recorded along the dialysis sessions.
For a preliminary exploratory inquiry, a dataset restricted only to the data of the session performed at the Ente Ospedaliero Cantonale di Lugano (EOC), Switzerland, S.C and Nefrologia e Dialisi dell'A.O. della Provincia di Lecco has been used.
The first study of the analysis has been the population composition assessment.
Then, the distribution of data referred to Systolic Arterial Pressure (SAP), Mean Arterial Pressure (MAP), Heart Rate (HR), blood concentration of the main electrolytes and pH was evaluated.
The final step of the analysis has been the design of a multiparameter criterion to identify hypotension during the treatment, by testing a set of single parameter criterion taken by literature.
Data during this phase has been further filtered through an embedded Matlab® function according to the guidelines of the Italian Society for Hypertension [205].
Specifically:

- SP, DP and Hearth Rate values has been filtered considering the following intervals
  - 50 mmHg<SP<300 mmHg
  - 40 mmHg<DP<150mmHg
  - SP<DP
  - 40 bpm<HR<150 bpm

1. Blood volume data acquired using Gambro Dialysis Machines (Città, stato), and exported from the Blood Volume Monitor (BVM) embedded into the machine has been processed by a 10 points Savitzky - Golay [208] smoothing filter (f= 21, k=8) to reduce noise while preserving frequency domain features of the original distribution.

5.4.4. Intra-treatment Statistical Analysis

A statistical study has been conducted on the dataset.
The following parameters have been considered:

- Systolic Arterial Pressure(SAP), analyzed on:
  - Intra-session trend
  - maximum intra-treatment variation peak (P_{Max}),
  - difference between star and end values of each session (SE)
  - difference between the maximum value and the minimum value of each treatment (Max-min);
- MAP and heart rate trend during the dialysis sessions;
- $[Ca^{2+}]$, $[Mg^{2+}]$, $[Na^{+}]$, $[K^{+}]$, $[Cl^{-}]$ and pH during the dialysis sessions.

The analysis has been performed on the whole analyzed population and among the population of patients within the same clinical centers.
A comparison between couples of categories has been done for each parameter, following the subsequent clustering:

A) By patient gender: men / woman
B) By clinical status: diabetic/non diabetic, insulin-dependent diabetic/ non-insulin-dependent diabetics, affected/not affected by cardiac diseases, hypertensive/non hypertensive;
C) By chronological age (C.A): 40 <C.A.< 70 years old/ C.A. >70 years old
D) By dialysis age (D.A):24 < D.A.<120 months/ D.A. > 120 months.

F test has been used to compare variances, T test (no equal variance or equal variance, depending on the F-test and ANOVA two way results has been used).
All the tests has been performed with a p-value of 0,05 and α=95%.
The results of the analysis have been reported in Chapter 6 – Results.

5.4.4.1. Design of multiparameter criterion to identify IDH during the treatment: effects of a single parameter variation

First of all, a literature research has been conducted on the existent studies
In particular three fitted criteria has been found and tested.
Two of them was based on pressure values constrains:

- **$SAP(0)_{140}$ criterion**: the systolic arterial pressure variation is linked to the onset of intra-dialysis hypotension.
  Mancini et al. has proposed a criterion of identification of IDH events based on the SAP variation with respect to its predialysis value [32]. The criterion is based on the initial value of SAP detection of BP set point for patients, or the pressure value at which the person usually begins to show discomfort:

  $SAP(0)_{140}$: 5.5

  - *If SAP(0)<140 mmHg*, the BP set point is equal to SAP(0)-30 mmHg
  - *If SAP(0)≥140 mmHg*, the BO set point is equal to 110 mmHg

  The $SAP(0)_{140}$ criterion has been implemented as a MATLAB® function in the MatLib and applied to the complete dataset.
  Its reliability has been tested comparing the prediction of $SAP(0)_{140}$ with the IDH events identified by the IDH-D criteria and compared to the clinical registers where symptoms / interventions / hypotension where reported by clinicians.
  The number of treatments identified by $SAP(0)_{140}$ application but not reported by IDH-D has been quantified as a parameter of reliability.

The predictive ability of the criterion has been also evaluated , applying concurrently the other criteria. (RBV_{13} and ΔK +).

- **MAP_{30} criterion** [208]: another method proposed in the literature for the detection of IDH, by Kinet et al. was based on the analysis of MAP value.

  This criterion associate a reduction of MAP greater or equal to 30 mmHg (5.5), with respect to its initial value to the risk of IDH onset [208].

$$MAP30: MAP(t) \leq MAP0 - 30\ mmHg \qquad 5.6$$

The criterion has been implemented on Matlab® as a function of the MatLIB, tested for each session , the detected episodes have been compared with the IDH-D criterion outputs.

A third criterion was based on the variation of RBV:

- **RBV_{13}** [63]**:** the loss of blood volume that occurs during the dialysis treatment is one of the main cause of IDH .The decrease of blood volume is associated with the ultrafiltration process.

If the UF rate is greater than the plasma refilling rate (PR), the blood volume may decrease implying hypovolemia. When the cardiovascular compensatory mechanisms, which physiologically contrasts hypovolemia, are compromised, hypotension may occur [63].

The literature indicates a 14% variation in blood volume as a critical threshold for RBV values. Here a 13% threshold has been considered so as to identify at the earlier stage the IDH onset, when due to volume depletion.

$$RBV13: RBVt \leq 13\%\ RBV(0) \qquad 5.7$$

The criterion has been implemented on Matlab® as a function of the MatLIB and tested for each session as $SAP(0)_{140}$ with a comparison of the IDH identified in the available data using IDH-D criterion.

Besides the ones, found in the literature, two additional IDH prediction criteria have been developed within the Dialysis Project.

The first one takes into account the hematic potassium concentration [K+] considered as a marker of arrhythmias. [87,63 106].

In collaboration with the clinicians involved in the project and analyzing the trend of potassium concentration on the first hour of treatment, the following criteria has been proposed:

ΔK^+ *criterion* : 5.8

1. $[K+]start > 5mmoll: KH1 + -Kstart+ \geq 20\% Kstart+;$
2. $3{,}5mmoll < [K+]iniziale < 5mmoll: KH1 + -Kstart+ \geq 10\% Kstart+;$
3. $[K+]start \leq 3{,}5mmoll;$

where $[K^+]_{start}$ is the initial value of potassium concentration, and $[K^+]_{H1}$ is the concentration of potassium at the first hour of treatment.

The initial value of potassium concentration defines the risk threshold for the concentration at first hour; this selective mechanisms results from the clinical practice: the assumption is that the higher is the initial potassium value, the highest is the tolerable variation.

It should also to be highlighted that a fall of the potassium concentration below 3.5 mmol / l is identified as hypokalemia [98,106].

The defined ΔK^+ criterion has been thus implemented as a Matlab® function and its performances in IDH identification compared with those of the other criteria.

Disrithtmia criterion:

Another criteria developed within the Dialysis project is related to the presence of IDH related dysrhythmias.
The analysis has been performed even if changes in the heart rate did not significantly differ between patients prone and resistant to IDH [209].
The HR series have been elaborated using an embedded MATLAB® function.
First of all, HR series has been preconditioned through three steps:

1. Value has been restricted within the physiological range (60-100 bpm);
2. The mean (HR) and the standard deviation $\sigma HRate$ of the values registered for all the session of each patient has been calculated;
3. For each individual a patient-dependent range has been defined as ($HR \pm \sigma HR$): the aim was to consider the specific patient response to dialysis treatment;
4. Each HRate series has been filtered within the patient specific range.

A further criterion proposed to identify the risk of hypotension along the dialysis sessions, was:

$$dim20: HRatet \leq 20\% HRate(0) \quad 5.7$$

Any decrease of 20% in heart rate compared to the initial heart rate value HR_0 (both decrease or increase) could result in a risk of hypotension.
The dim20 criterion has been further tested in combination with the previously exposed criteria.

5.4.4.2. Design of multiparametric criteria predict IDH along the HD

After the evaluation of the performance of indicators based on the observation of single parameters, also a composite criteria, based on the simoultaneous monitoring of multiple parameters have been defined and tested.
IDH risk can be associated to the following conditions:

Multiparametric Criteria*:* 5.8

1. If SAP(0) ≥140mmHg, SAP(t)≤110mmHg and in the mean time were registered a:
   - decrease of RBV≥13% and decrease of HR≥20%
   - warning $3{,}5mmoll < [K+]iniziale < 5mmoll: KH1 + -Kstart+ \geq 10\% Kstart +$ and $dim20: HRatet \leq 20\% HRate(0)$

2. If 115 ≤SAP(0)≤ 140 mmHg and SAP(t) decrease > 23% and in the mean time were registered a:
   - decrease of RBV≥13% and decrease of HR_{ate} ≥20%
   - warning $3{,}5mmoll < [K+]iniziale < 5mmoll: KH1 + -Kstart+ \geq 10\% Kstart +$ and $dim20: HRt \leq 20\% HR0$

3. If SAP(0) ≤ 115 mmHg, for ΔSAP(0)≥16% of the value at starting session.

All over thesubcriteria, pressure variations has been considered with a tolerance of 2 mmHg.
The multiparameter criterion has been implemented as a MATLAB® function.
The prediction performances of this criterion has been tested, comparing the obtained results with the real IDH occurrence based on IDH_D criterion.

5.5 Machine Learning Analysis Approach

5.5.1. Introduction

Beside the classical statistical analysis a machine learning data mining approach has been applied on the available dataset
In particular the machine learning approach has been tested to predict IDH event from pre-dialysis conditions and considering the IDH prediction as a binary classification problem as:

$$x \in X ; y \in \{IDH, noIDH\} \Rightarrow p(y|X) \quad 5.9$$

.
where the domain of y was IDH, noIDH and X the set of parameters belonging to the Dialysis-DB assumed to be influent on IDH onset.
According to literature analysis and our operative requirements three different algorithm has been explored for the prediction of IDH event: Random Forest, Artificial Neural Networks and Support Vector Machines, that have been intensively described in Par 4.4.3.

5.5.2. Algorithm implementation

5.5.2.1. Preprocessing

A particularly important problem to work properly with machine learning techniques is working effectively with large data sets.
Literature suggests that the predictive power of the classifiers is largely dependent on the quality and size of the training sample [210].
In particular several experiments have the tested evidenced that the variance of the classifier prediction can be expected to decrease as the cardinality of training set increase [211].
For this reason Dataset 2 has been considered the best candidate dataset in order to test and validate machine learning algorithms.
Respect to the version used for the inferential statistical analysis, the dataset has been widened with further attributes, all of them referred to the pre-dialysis condition considered as the value of the series at t_0.
Definitely the complete set of attributes considered has been as in Table 5.4 :

Table 5.4: Attributes of the revised Dataset 2

Main plasmatic concentrations	Calcium[Ca++]
	potassium [K+]
	magnesium[Mg++],
	Sodium[Na+]
Additionary plasmatic concentration	Clorine concentration[Cl-]
	Phosphates concentration
Urea Concentration	[Urea]
Hematocrit	Ht
Sex	Sex
Weight Gain	WG
IDH during session	IDH_y

As data were coming from clinical routine registrations, it is accounted that part

of them can be corrupted or affected by missing values.
For this reason, even if a primary filter was performed by the Dialysis-Matlib functions a further pre-condition process has been done before the learning process in order to decrease the dataset avoiding variability, and grant machine learning models to be at the best possible performance [212].
Different strategies has been evaluated in order to obtain the desired result:

- only examples with less than 10% missing values, for each attribute, were kept.
- Hematocrit were then removed since a large measures amount (more than 30% over the total) was missing from the available database
- Given the high variability in urea and phosphates concentration in blood values due to chronic kidney disease they were not filtered.

The finally dataset consisted of 653 record, but one of the main problems regarded the presence of imbalanced dataset: less than 15% of the sessions belonged to the positive class of IDH (IDHy).

5.5.2.2. Dataset Balancing

The final obtained dataset resulted imbalanced: less than 15% of total example belonged to the positive class (IDHy).
A dataset is imbalanced if the classification categories are not equally represented [212].
Class imbalance is a problem for machine learning algorithms.
Classifiers generally perform poorly on imbalanced datasets because they are designed to generalize from sample data and output the simplest hypothesis that best fits the data, based on the principle of Occam's razor [213,214].
Thus with imbalanced data, in a the simplest hypothesis is often the one that classifies almost all instances as negative[214].
Moreover, opposite to other machine learning applications, the medical diagnostic problem does not end once the model classifies new instances. That is, if the instance is classified as sick, or positive, (i.e. the most important class) the generated knowledge should be able to provide the medical staff with a novel point of view about the given problem [215].
For these reasons different strategies have to be applied in order to maximize the minority class classification accuracy, since, in binary classification problems, the majority class accuracy is guaranteed by default.
There are normally to ways to address class imbalance: one is to assign distinct costs to training samples and try to reduce the misclassification costs [216]
The other indeed, acts on re-sampling the original dataset, either by over-sampling the minority class and/or under-sampling the majority class [218].
Two different oversampling techniques for the minority class and a related majority class downsampling have been combined, generating five different datasets from the starting one.
The chosen oversampling techniques were: Bootstrap Resampling[218] and Synthetic Minority Oversampling Technique[216].
While Bootstrap Resampling consists in a simple random sampling with replacement, in SMOTE the minority class is oversampled by creating synthetic samples.
Extra training data are obtained performing specific operations on real data. In particular in our case, examples have been generated by operating in feature space, rather than in data space, as the minority class was defined by the target variable.
Oversampling was performed by taking each minority class sample and introducing synthetic examples along the line segments joining any/all of the k minority class nearest neighbors [k-class]. Depending on the amount of over-sampling required, neighbors from the k nearest neighbors were randomly chosen.

The two different balancing techniques for the minority class have been combined with a related majority class down-sampling. The goal was to maximize the minority class classification accuracy, since, in binary classification problems, the majority class accuracy is guaranteed by default [220].
For the SMOTE synthetic sample generation k=5 nearest neighbours have been considered.
Five different datasets have been generated from the starting one:

- *Dataset A*: 500% minority class SMOTING and no majority class downsampling, resulting in 1118 examples;
- *Dataset B*: 300% minority class SMOTING and relative majority class random dowmsampling, resulting in 745 examples;
- *Dataset C*: 100% minority class SMOTING and relative majority class random dowmsampling, resulting in 366 examples;
- *Dataset D*: 100% minority class Bootstraping and relative majority class random dowmsampling, resulting in 373 examples;
- *Dataset E*: 50% minority class SMOTING and relative majority class random dowmsampling, resulting in 280 examples

The availability of five synthetic datasets allowed investigating the classifier performance on different oversampling and down sampling combinations.

5.5.2.3. Rapid Miner Implementation

The whole algorithm implementations followed a common path in terms of attribute selection, model validation and evaluation.
All the implementation has been pursued using the following schema Figure 5.9:

Figure 5.9: Algorithm implementation schema []

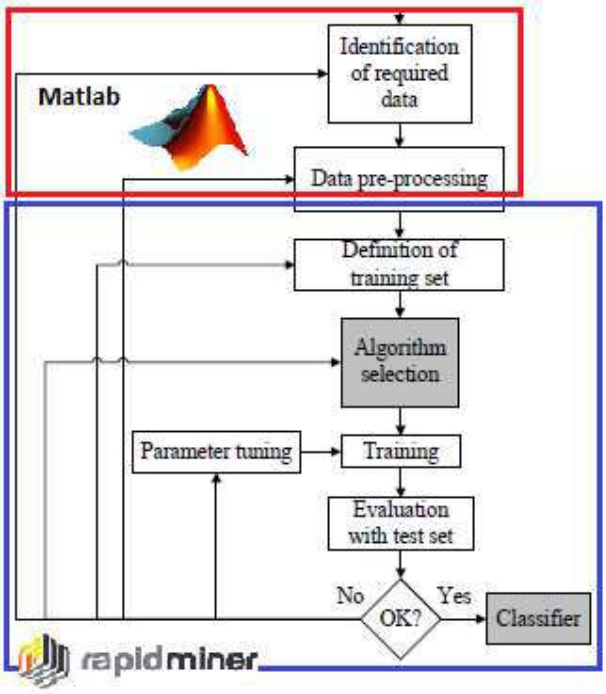

All data have been token from the Dialysis-DB through Matlab® and transferred to RapidMiner® Studio by a .CSV sheet to implement Machine Learning algorithms.
RapidMiner® Studio (company, city, state) is a software platform that provides an integrated environment for machine learning, data mining, text mining, predictive analytics and business analytics [221].

RapidMiner® allows to threat operations on data, as a blockchain allowing to manage complex operation in a simple way and has been chosen as the best solution to implement the machine learning algorithms on the present study.
In the RapidMiner® studio environment, IDH events has been set as the target variable in the learning process while all the other attributes were specifically treated by each proposed classification algorithm.
Random Forest, Artificial Neural Network and Support Vector Machine were trained and tested on each one of the dataset A, B, C, D and E.

5.5.3.4. Overfitting avoidance strategy

In order to avoid the overfitting a two step strategy has been adopted: the classifier has been first trained and tested through k-fold Cross Validation (CV) on the 90% of the entire dataset.
The advantage of k-Fold Cross validation is that all the features in the dataset are eventually used for both training and testing
In K-fold cross-validation (CV), we split the sample into K disjoint subsets D_h (h = 1, 2, . . . , K) of (approximately) equal size.
The model is trained K times, each time leaving out one of the subsets from the training, but using only the omitted subset to compute the prediction error[221].
n K-fold cross-validation (CV), we split the sample into K disjoint subsets $t_{h.}$.
Considering t_h(h = 1, 2, . . . , K) is the training set obtained by removing the h_{-th} subset $D_{ħ}$ and let m = n/K (n multiple of K) be the number of units in each subset.
the k-CV-estimator is defined as the average error on the K analysis committed by the classifiers *A(-)* in the corresponding partitions t_h.
The k-cv prediction error estimator on the k-CV partition P on the total set of data S_n defined as follows [222]:

$$\varepsilon Sn,,P = 1Kh = 1K1mj\epsilon th\, L(yj, fxj) \qquad 5.10$$

If K equals the training sample size n, the strategy is known as ‘‘Leave-One-Out’’ cross-validation (LOO) [222].
A k-cv prediction error estimator is an unbiased estimator of the prediction error ε on data sets of n—n/k size [223,224], but it is biased for ε on data sets of size n because only a subset of the instances with size n-n/k is used for training.
The main problem with K-fold CV is that the training-sets t_1, c_2, . . . , t_K are not independent samples, i.e. they have(n−2m) cases in common, and also the test sets t_h come from the same data [226]. This implies that the variance of ε can be very large, as no unbiased estimation of σ2(ε) is possible.
As the variance of ε depends on the partition [221,224] as the estimation of ε,is important to define the right partition for the dataset.
Many studies shows that K-fold CV shows lower variability than LOO[223] and that a reliable estimate of ε can be obtained with K = 10 for n > 100[225].
In this work a stratified 10-fold CV is used: k=10 is an adequate compromise between training sets overlap and prediction error variance while the stratified sampling allows to have folds containing approximately the same proportions of labels as the original dataset [226,221]. Even if the use of CV should provide an "overfitting free" model evaluation the resulting model has been tested again on the remaining 10% of the dataset, in order to provide further generalization capability.

5.5.3.5. Random Forest implementation

A 10-fold CV has been used, with k=10 as an adequate compromise between training sets overlap and prediction error variance while stratified sampling allowed to have folds containing approximately the same proportions.
Thus for the implementation of the random forest 3 main tuning parameters has been set:

- **number of trees:** as RF does not over fit or require a huge computational effort, tree number were set to 250, rounding up the result of this simple algorithm: attributes number needs to be at least one order of magnitude higher than the number of features, in order to exhaustively explore all the feature space during the forest building.
- **bagging:** the bagging of tree has been set standing that for each tree growth log(n)+1 attributes were selected among the n available
- **split Criterion**: Gini Impurity Index was used to split the nodes; it is a measure of the feature impurity with respect to output classes

The feature with the highest Gini Index was chosen as split in that node. It is defined as:

$$Giniq = 1 - h = 1Hpk \qquad 5.11$$

where q is the considered node and p_h, h_2 H[1; 2; :::;H], is the relative frequency of target class value for the observations included in q;

- **Voting Strategy:** confidence voting selects the class that has the highest accumulated confidence.

The RF algorithm has been implemented through the software RapidMiner.
Figure 5.10 shows the block-chain of the process.
The first blocks represents the process of reading the data from the CSV files, the block “Split Data” indeed will split the database into basic elements.

Figure 5.10: Implementation of the RF process through RapidMiner software

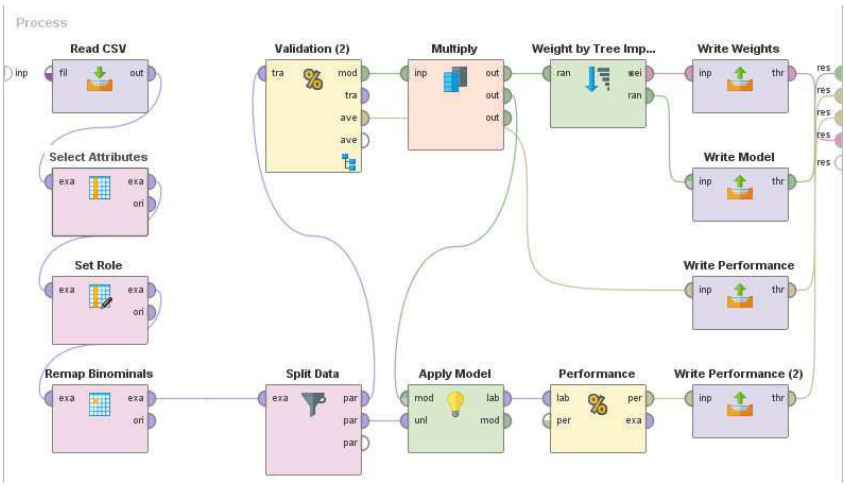

5.5.3.6. Implementation of Artificial Neural Network Machine

The implementation of the Artificial Neural Network algorithm required some additional pre-processing operations.
In particular the missing values were replaced from the average values.
Sex attribute, initially set as nominal, has been converted to numerical for the network creation.
For the IDH prediction the choice has been done for the feedforward networks in which the underlying graph does not contain cycles[227,174].
As binary attribute it has been mapped as a 0,1 variable.
The following parameters has been set:

- **Attributes Normalization**: the ANN algorithm uses an usual sigmoid function as the activation function. The contribution of an input will heavily depend on its variability relative to other inputs.
  It becomes essential to rescale the inputs so that their variability reflects their importance. For lack of better prior information, it is common to standardize each attribute to the same range on the same standard deviation. The attribute value range has then been scaled to -1 and +1.
- **Training cycles:** in back-propagation the output values are compared with the correct answer to compute the value of some predefined error-function. The contribution of an input will heavily depend on its variability.The error is then feedback through the network. Using this information the process is repeated 500 times or less if the training error gets below to 105
- **Learning Rate**: determines how much the weights are changed at each step, it affects the speed at which the ANN arrives at the minimum solution determines how much the weights are changed at each step. It affects the speed at which the ANN arrives at the minimum solution. If it is too high, the system will either oscillate about the true solution, or it will diverge completely. If the step-size is too low, the system will take a long time to converge on the final solution. It has been set to 0.2.

Figure 5.11: Implementation of the ANN process through RapidMiner software

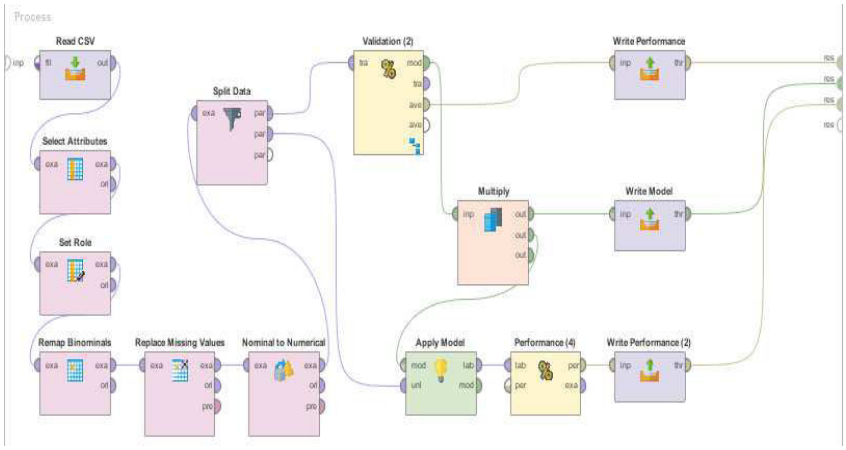

5.5.3.7. Implementation of the Support Vector Machine

SVMs are widely used in computational biology due to their high accuracy, their ability to deal with high-dimensional and large datasets, and their flexibility in modeling diverse sources of data [228,229].
SVM are particularly fitted for classification problems and in the recent years they have been used for several applications like handwritten digit recognition, object recognition, speaker identification, face detection in images, and text categorization.
For these reason, they have been chosen to address the binary classification problem of IDH identifications.
As for the ANN implementation also Support Vector Machine required the Sex attribute conversion from nominal to Boolean and the residual missing value replacement, the same strategy has been implemented as in the case of ANN [229].
Before the application of SVM a scaling procedure has been applied.

Figure 5.12: Implementation of the SVM process through RapidMiner software

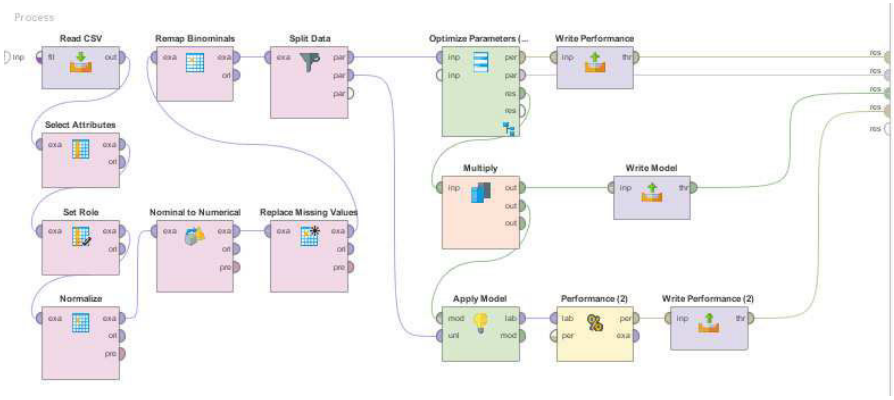

The SVM learner has been implemented thanks to the LibSVM tool.
The LibSVM was still available in the RapidMiner environment, and has been used to perform through aa normalization of all the attributes through the z trasformation. The outputs has been used to train the SVM.
The statistical normalization converted the data into a normal distribution with mean=0 and variance=1.
The used formula for the statistical normalization has been:

$$z = (x - \mu)s \qquad 5.11$$

where X is the attribute values vector, u the mean of attribute values and s its standard deviation. The SVM has been implemented using an RBF Kernel [229], to address non linearities between labels and attributes, without an high employment of setting parameters.
In particular the used set of setting parameters has been:

- **γ gamma** defines the influence of a single training example. It can be seen as the inverse of the influence radius of the samples selected by the model as support vectors. Technically large **γ** leads to high bias and low variance models while low **γ** defines models characterized by low bias and high variance
- **C** is the parameters that, in soft margin cost function, controls the influence of each individual support vector.

It trades of training examples misclassification against the decision surface simplicity. A low C makes the decision surface smooth, while a high C aims at classifying all training examples correctly by giving the model freedom to select

Best suiting and C values have to be determined. A grid-search strategy, in addition to ten-fold CV, has been applied: various pairs of (γ, C) have been tried and the one with the best CV accuracy is chosen. The optimization gave back different parameters for each dataset:

- λ=0.3474 and C=1.5849 for Dataset A;
- λ =0.1672 and C=1.5849 for Dataset B;
- λ =0.0805 and C=7.9433 for Dataset C;
- λ =0.7219 and C=1.5849 for Dataset D;
- λ =0.7219 and C=1.5849 for Dataset E.

5.5.3. Algorithm Performance Evaluation

All the proposed algorithms performance were evaluated starting from confusion matrix analysis as explained in Chap 4.4.
In particular for each classifier and for each dataset AOC, Accuracy, precision, recall and F-measure have been evaluated.

5.5.4. Algorithm Performance Comparison

All the tested machine learning algorithms have been developed over the same training sets, exploring different datasets in order to test different balancing techniques.
The performances of the different machine learning algorithms, and the different balancing techniques has been compared on the basis of AOC, Accuracy, precision, recall and F-measure.

Chapter 6 – Results

6.1 Inferential Statistics Approach

6.1.2 Pre-dialysis period analysis

The final goal of the statistical analysis was the development of a multifactorial index for the offline prediction of the IDH events risk. The index, named J, has been defined as a weighted sum of the parameters that showed to be statistically different, between the considered groups, as described in 5.4. The index want give the clinician a risk highlights already in the early phase of the treatment.
The different strategies applied for the inference analysis lead to different versions of the J-index, respectively named J_1 and J_2 with reference to the applied Strategy 1 and 2.
The prediction ability of both the J index' versions has been evaluated in terms of accuracy and precision.

6.1.1.1. Results from Strategy 1

Figure 6.1.A and B graphically shows the results of the inferential statistical comparison

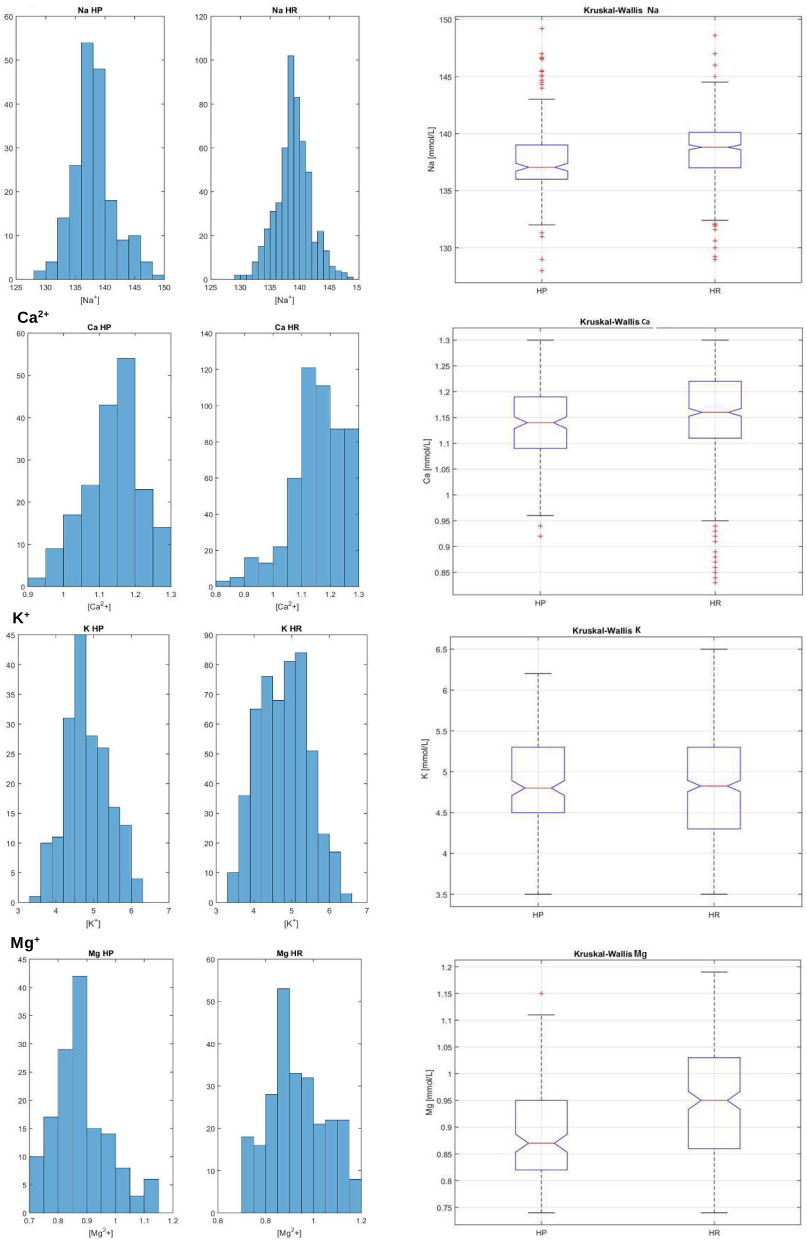

Figure 6.1.A: Box plot Comparison of Ionic Concentrations

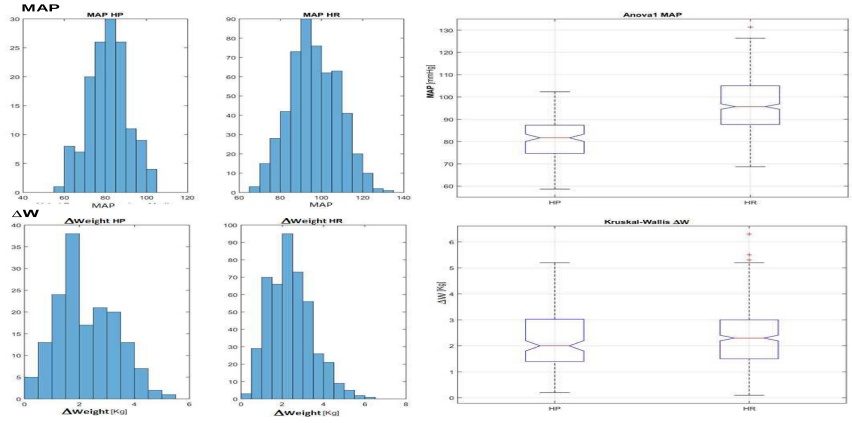

Figure 6.1.B: Box plot Comparison of MAP and ΔW

The figure shows as the initial values of initial potassium concentration $[K^+]_0$, systolic (SBP) and diastolic (DBP) blood pressures, mean arterial pressure (MAP) and interdialysis (from the end of the previous session) weight gain (ΔW) result statistically different between the HP and HR patients.
Specifically, in HP patients ΔW and the $[K^+]_0$, were significantly higher and blood pressure (SBP, DBP, MAP) significantly lower, if compared to those of the HR patients ($p<0.01$).
Based on these results, the first version of the J index was defined as follow:

$$J_{1i} = \frac{\alpha}{\overline{K}} \cdot K_i^+ + \frac{\beta}{\overline{\Delta W}} \cdot \Delta W_i + \frac{\gamma \cdot \overline{MAP}}{MAP_i} + hp_{ii} \qquad 6.1$$

where $\overline{K}$, $\overline{\Delta W}$ and $\overline{MAP}$ are respectively the cumulative mean values for the potassium concentration, the weight gain and the mean arterial pressure of the patient at the beginning of the previously monitored sessions; K_i, ΔW_i, MAP_i are the same parameters, evaluated at the beginning of the current session and hp_i is the hypotension proneness of each patient, evaluated taking into account the number of IDH detected during the last three previously monitored session [195].
α, β γ are the coefficients allowing to weight the influences of each equation term on the onset of hypotensive events during the current session: these coefficients could be dynamically adjourned based on the longitudinal analysis of $[K^+]$, SAP, DAP, and ΔW.

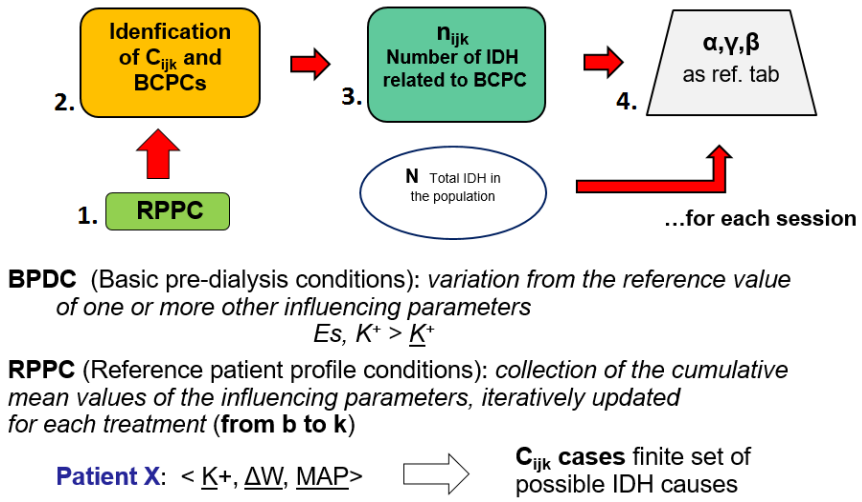

Figure 6.2: J_1 index weight definition 1.RPPC calculation 2.Identification of the Cijk and BCPC on the basis of the RPPC, 3. Count of the n_{ijk} cases, 4. Definition of the Weight Coefficients on the basis of the C_{ijk} cases,and n_{ijk}

Figure 6.2. resumes the calibration process designed to weight coefficients.
The process starts by considering the Reference Patient Profile Condition (RPPC), defined as the collection of the cumulative mean values of the influencing parameters, iteratively updates for each treatment starting from b to the k-1 treatment, where b is the number of the available treatments for the longitudinal analysis and k is the total amount of the monitored sessions for each patient.
RPPC has been evaluated respectively for b equal to 3 and 5 sessions.
The RPPC are the references for Basic Pre-Dialysis Conditions (BPDC).
In particular, any variation of an influencing parameter from the RPPC defines a basic pre-dialysis conditions (BPCD), that traduces a potential risk of hypotension related to a variation from a patient-specific physiological condition.
The combination of the various possible BPCD represents the framework of the Cijk cases, a finite set of possible IDH causes that could lead to IDH at the treatment start.
The Cijk determine the values of the weight coefficients on the basis of number of previous hypotensive events related to the specific BPCDs (nijk) and the number of hypotensive events (N) registered on the whole population, as reported in Table 6.1[195].
Based on the approach on the definition of the index, J_1 index values higher than 1 point out IDH risk on the incoming session.

Table 6.1: Collection of possible IDH causes (Cijk cases),

Occurring BDPC	C_{ijk}	n_{ijk}	α,β,γ
None	C_{000}	n_{000}	$\begin{cases}\alpha=\frac{n_{000}}{N}\\ \beta=\frac{n_{000}}{N}\\ \gamma=\frac{n_{000}}{N}\end{cases}$
$BDPC_1$: $K_t^+ \geq \overline{K}^+$	C_{100}	n_{100}	$\begin{cases}\alpha=\frac{n_{100}}{N}\\ \beta=0\\ \gamma=0\end{cases}$
$BDPC_2$: $\Delta W_t \geq \overline{\Delta W}$	C_{020}	n_{020}	$\begin{cases}\alpha=0\\ \beta=\frac{n_{020}}{N}\\ \gamma=0\end{cases}$
$BDPC_3$: $MAP_t \leq \overline{MAP}$	C_{003}	n_{003}	$\begin{cases}\alpha=0\\ \beta=0\\ \gamma=\frac{n_{003}}{N}\end{cases}$
$BDPC_1$&$BDPC_2$: $K_t^+ \geq \overline{K}^+$ $\Delta W_t \geq \overline{\Delta W}$	C_{120}	n_{120}	$\begin{cases}\alpha+\beta=\frac{n_{120}}{N}\\ \frac{\alpha}{\beta}=\frac{n_{100}}{n_{020}}\\ \gamma=0\end{cases}$
$BDPC_1$ & $BDPC_3$: $K_t^+ \geq \overline{K}^+$ $MAP_t \leq \overline{MAP}$	C_{103}	n_{103}	$\begin{cases}\alpha+\gamma=\frac{n_{100}}{N}\\ \frac{\alpha}{\gamma}=\frac{n_{100}}{n_{030}}\\ \beta=0\end{cases}$
$BDPC_2$ & $BDPC_3$: $\Delta W_t \geq \overline{\Delta W}$ $MAP_t \leq \overline{MAP}$	C_{103}	n_{103}	$\begin{cases}\beta+\gamma=\frac{n_{023}}{N}\\ \frac{\beta}{\gamma}=\frac{n_{020}}{n_{003}}\\ \alpha=0\end{cases}$
$BDPC_1$ & $BDPC_2$ & $BDPC_3$: $K_t^+ \geq \overline{K}^+$ $\Delta W_t \geq \overline{\Delta W}$ $MAP_t \leq \overline{MAP}$	C_{123}	n_{123}	$\begin{cases}\alpha+\beta+\gamma=\frac{n_{123}}{N}\\ \frac{\alpha}{\beta}=\frac{n_{100}}{n_{020}}\\ \frac{\beta}{\gamma}=\frac{n_{020}}{n_{003}}\end{cases}$

6.1.1.1. J_1 index evaluation

The prevalence of IDH, evaluated on the data available for each center, results to be 37.3% for Lugano, 9.4% for Como and Varese and 8% for Lecco.
Table 6.2, section a. shows the results of the calculation of Ji on each involved center, when the threshold of J (J_{th}) is set equal to 1.
The table reports the values of sensitivity, specificity, true and false positives and negatives, PPV, NPV, % of predicted IDH, determined comparing Ji outputs in terms of IDH risk and real IDH occurrence.
J_i allows to predict real IDH events in almost the 77% of the cases. The data acquired in Lugano and Lecco Dialysis Units were the ones statistically analyzed

to identify the influent parameters (84 and 82% of the IDH events respectively predicted); the data acquired at Como and Varese Dialysis Units were instead used to verify the applicability of the index in different centers, that is confirmed by the satisfying performances of J_i in both the two new sets of data (63 and 68% of IDH events respectively predicted).

Table 6.2: Ji index performances in terms of sensitivity (Sens.), specificity (Spec.), true and false positive and negatives, Positive Predicted Values (PPV) and Negative Predicted Values (NPV), when: a. Jth =1; b. Jth= I75; c. Jth= I(1-%IDHc). were used**.**

a. J_{th} = 1	**Sens.**	**Spec**	**TP**	**TN**	**FP**	**FN**	**PPV**	**NPV**	**IDH***
Lugano,CH	0.84	0.52	16	33	30	3	34.8	52.3	16/19 (84%)
Lecco, I	0.82	0.84	9	107	20	2	31.0	84.3	9/11 (82%)
Como, I	0.63	0.77	5	56	17	3	22.7	76.7	5/8 (63%)
Varese, I	0.78	0.78	7	56	16	2	30.4	77.7	7/9 (78%)
b. $J_{th}=I_{75}$	**Sens.**	**Spec**	**TP**	**TN**	**FP**	**FN**	**PPV**	**NPV**	**IDH***
Lugano,	0.53	0.84	10	53	10	9	50.0	84.1	10/19 (53%)
Lecco, I	0.82	0.80	9	102	25	2	26.5	80.3	9/11 (82%)
Como, I	0.63	0.79	5	58	15	3	25.0	79.5	5/8 (63%)
Varese, I	0.78	0.82	7	59	13	2	35.0	81.9	7/9 (78%)
c. $J_{th}=I_{1-\%IDHc}$	**Sens.**	**Spec.**	**TP**	**TN**	**FP**	**FN**	**PPV**	**NPV**	**IDH***
Lugano,	0.89	0.52	17	24	39	2	30.4	38.1	17/19 (89%)
Lecco, I	0.82	0.91	9	115	12	2	42.9	90.6	9/11 (82%)
Como, I	0.78	0.78	4	58	15	4	21.1	79.5	4/8 (50%)
Varese, I	0.78	0.88	7	63	9	2	43.8	87.5	7/9 (78%)

6.1.1.3. Center dependent risk threshold assessment

Figure 6.2 shows the distribution of J_i values in each one of the involved dialysis centers: the J_i values of each monitored session are represented with blank circles, star-shaped symbols are superimposed to the blank circle, when the corresponding session is characterized by IDH. The prediction threshold J_{th}=1 is shown by a continuous line; $J_{th}=I_{75}$ as a dashed line; $J_{th}=I_{(1-\%IDHc)}$. as a dash-dotted line. The number of star-filled points over each threshold corresponds to the TP cases, the ones below to the FNs. The ability of J_i to highlight IDH risk in terms of sensitivity, specificity, TP, TN, FP and FN, when the new thresholds

were used, is summarized in Table 6.2, section b. and c.
The use of $J_{th}=I_{75}$ decreases the FPs in 3 centers out of 4, but does not improve either sensitivity or specificity. The TP and the sensitivity in Lugano results even worsened.
The use of $J_{th}=I_{(1-\%IDHc)}$ brings to improved or stable sensitivity, and allows improving specificity in 3 out of the 4 centers, with stable values in the other one. Average PPV and NPV slightly increase with the new thresholds, with no statistically significant differences[232].

Figure 6.3: J_i values distribution for Regional Hospital of Lugano, Switzerland (A); Dialysis Unit, A. Manzoni Hospital Lecco, Italy (B); Sant'Anna Hospital, Como, Italy (C) and Circolo Hospital and Macchi Foundation, Varese, Italy (D). The prediction threshold initially set at 1 is drawn as a continuous line. The dash-dotted line represents the 1- $\%IDH_c$ quartile ($J_{th}= I_{(1-\%IDHc)}$ the dashed line represents the 75th percentile for each J_i distribution (J_{th}=q(75)).

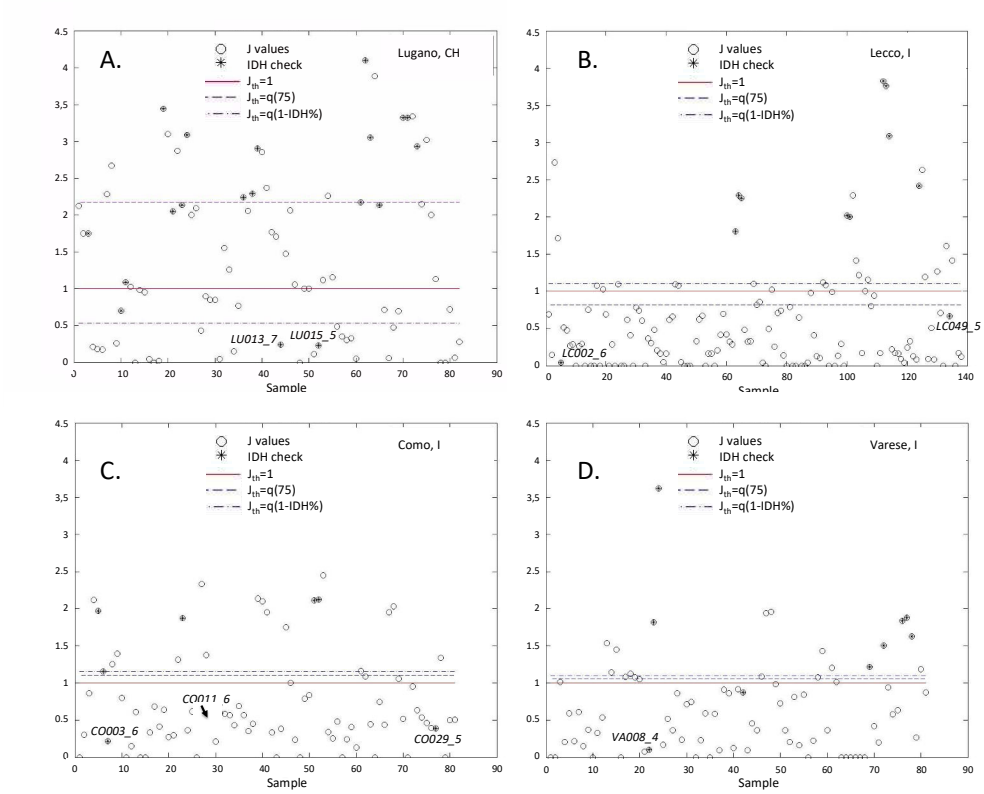

6.1.1.2 Results from strategy 2

As exposed in the previous chapter, in the Strategy 2 Kolmogorov-Smirnov and Kruskal-Wallis, statistical tests were performed over the attributes for both Dataset 1 and 2.
Kolmogorov-Smirnov and Kruskal-Wallis results are here displayed together with the relative p-values and the consequent binary classification depending on the null hypothesis acceptance or refusal.
The result is set to 0 if the null hypothesis cannot be rejected at the 5% significance level, 1 if the null hypothesis can be rejected at the 5% significance level.
In particular:

- K-S Null Hypothesis: a random sample X could behave as standard normal distribution;
- K-W Null Hypothesis: independent samples from two or more groups come from distributions with equal medians.

It follows that the samples of parameters characterized by the result 0 in

Kolmogorov-Smirnov come from normal distributions while the ones characterized by the result 1 do not come from normal distributions.
In the same way the 0 value as result of the Kruskal-Wallis test identifies those parameters which are not statistical significant in describing the considered dataset; while 1 highlights instead those parameters which have a relevant role in describing the dataset.

Dataset 1

The population of the first dataset is divided in Hypotension Prone and Hypotension Resistant patients on the basis of IDH-D criterion described in §5.4.2.
Tab.6.3 A and Tab.6.3 B displays the Kolmogorov-Smirnov test results for both Hypotension Prone and Hypotension Resistant patients: all attributes are characterized by very small, or even null, p-values, in both Hypotension Resistant and Prone populations, implying that all the attribute samples do not come from normal distribution.
After the normality check, Kruskal-Wallis test for statistical significance were then performed.
Its results are reported in Tab.6.3 C.

Table 6.3: Result of statistical test on Dataset 1
A) K-S results for Hypotension Resistant (HP) patients data
B) K-S results for Hypotension Prone (HR) patients data
C) K-W results: HP vs HR

A.

	p-value	**Result**
$[K^+]$	0	1
$[Na^+]$	0	1
$[Ca^{++}]$	9.1518×10^{-308}	1
$[Mg^{++}]$	5.0082×10^{-215}	1
Ht	0	1
ΔW	3.3000×10^{-258}	1
MAP	0	1

B.

	p-value	**Result**
$[K^+]$	0	1
$[Na^+]$	0	1
$[Ca^{++}]$	4.6083×10^{-68}	1
$[Mg^{++}]$	1.2867×10^{-247}	1
Ht	5.6914×10^{-106}	1
ΔW	1.7855×10^{-83}	1
MAP	5.2830×10^{-258}	1

C.

	p-value	**Result**
$[K^+]$	0.9567	0
$[Na^+]$	2.0035×10^{-14}	1
$[Ca^{++}]$	0.0496	1
$[Mg^{++}]$	$1.9728\times10-9$	1
Ht	0.1402	0
ΔW	0.2369	0
MAP	1.3665×10^{-45}	1

The analysis showed that Sodium, Calcium, Magnesium concentrations and the Mean Arterial Pressure significantly differs between the two groups.

Dataset 2

In the second dataset each single dialysis session is considered as a sample; the Sessions characterized by at least an IDH Event (IDH_{-y}) were compared with the Sessions without IDH Events (IDH_{-n}).

The statistical analysis on the Dataset 2 is then aimed to highlight the parameters that results more physiologically relevant during an IDH event.

The Kolmogorov-Smirnov test results are presented in Tab.6.2 A and Tab.6.2 B. Also in Dataset 2, in both the considered populations, each attribute is characterized by a very small p-value: the considered attributes samples do not come from normal distribution.

The Kruskal-Wallis test for statistical significance was then performed; its results are reported in Tab.6.2 C.

The most statistically significant parameters in describing IDH events seem to be the Sodium and Magnesium concentrations and the Mean Arterial Pressure (MAP).

.

Table 6.4: Result of statistical test on Dataset 2
C) K-S results for Hypotension Resistant IDH-y sessions data
D) K-S results for Hypotension Prone IDH-n sessions data
C) K-W results: IDH-y vs IDH-n

A.

	p-value	Result
$[K^+]$	2.3104×10^{-46}	1
$[Na^+]$	5.3369×10^{-49}	1
$[Ca^{++}]$	6.3977×10^{-38}	1
$[Mg^{++}]$	8.3988×10^{-25}	1
Ht	1.1745×10^{-58}	1
ΔW	2.0590×10^{-52}	1
MAP	2.4225×10^{96}	1

B.

	p-value	Result
$[K^+]$	7.4118×10^{-306}	1
$[Na^+]$	1.2894×10^{-308}	1
$[Ca^{++}]$	9.5423×10^{-159}	1
$[Mg^{++}]$	1.1427×10^{-127}	1
Ht	3.9794×10^{-202}	1
ΔW	0	1
MAP	0	1

C.

	p-value	Result
$[K^+]$	0.3902	0
$[Na^+]$	0.0055	1
$[Ca^{++}]$	0.7840	0
$[Mg^{++}]$	1.7960×10^{-7}	1
Ht	0.1402	0
ΔW	0.2369	0
MAP	1.3665×10^{-45}	1

J_2 definition

Based on the Strategy 2 results, a new version of the J index, called J_2, has been implemented.
The new index has been designed taking into consideration that the pre-treatment evaluation of J_1 index into the everyday clinical practice highlights some potentially critical behaviors as a difficult threshold setting due to index linearity and an *hp* weight with regard to threshold assessment.
J_2 is defined as a sigmoid representing the actual patient conditions as shifted, depending on patient IDH history. The new index has been then defined as:

$$J_{2i} = \frac{1}{1+\alpha e^{-\beta}} + hp_n \qquad J_{2i} \in [0,1] \tag{6.2}$$

where β is the independent variable, α controls sigmoid steepness and hp determines the shift.

The index can be viewed as a risk scale, where 1 stands for maximum IDH risk.
α is the Weight Gain Parameter and expresses the role of inter-sessions weight gain and, indirectly, of intra-session blood volume removal. It is defined as:

$$\alpha = \frac{t_{dial}}{240}\frac{\overline{\Delta W}}{\Delta W_0} \qquad 6.3$$

where t_{dial} is the treatment duration in minutes (i.e. a standard treatment is assumed to 240 minutes), $\overline{\Delta W}$ and ΔW_0 are the patient mean and current weight gain, respectively. A higher weight gain or a short treatment time implies a higher ultrafiltration rate and therefore an higher IDH risk. This implies, on its time, a lower α value, driven by to a sigmoid shaping.
β is the Blood Pressure Parameter, defined as:

$$\beta = a\frac{\overline{MAP}}{MAP_0} + b \qquad 6.4$$

a regulates index sensitivity, *b* is randomly chosen to include β in the interval [0, 10] while $\overline{MAP}$ and MAP_0 are the averaged and current mean arterial pressures, respectively.
The β coefficient imply that lower pre-session MAP values lead to higher IDH risk: this condition determines a β increase, and a higher J_2 value in the IDH risk scale.
The Hypotension Proneness Parameter is named hp_i and quantifies the patient-specific proneness to incur in hypotension during the treatment.
This parameter is expressed as the number of IDH-free sessions between the current and the *i-th* ones.

$$hp_i = \sum e^{-\sqrt{t_i}} \qquad 6.5$$

The negative exponential dependence from the time codifies that an hypothetic i-th IDH event can occur decrease with a inversely proportional relationship to the time t during the session.

Results of J_2 version testing

J_2 ability in the discrimination of IDH_{-y} sessions, with respect to the IDH_{-n} ones has been investigated. The index has been analyzed as one of the other parameters characterizing Dataset 2, following the Strategy 2 algorithm exposed in 5.4.2.
A Kolmogorov-Smirnov test has been then primarily applied, to test the eventual normality of the distribution, followed by a Kruskal-Wallis test to effectively evaluate the discriminant power of J on IDH_{-y} and IDH_{-n} sessions (Table 6.5).
The Kolmogorov-Smirnov test highlighted, as displayed in Tab. 6.3-A, that the J_2 index sample do not come from a normal distribution. The Kruskal-Wallis test determined indeed the statistical relevance of the J_2 index, as can be seen from Tab. 6.5-B.
The box-plot related to the tests are displayed in the Appendix A.

Table 6.5: Result of statistical test on J_2
A. Kolmogorov-Smirnov results, J_2 index
B. Kruskal-Wallis results, J_2 IDH_{-y} vs J_2 IDH_{-n}

A.

	p-value	**Result**
J_2 IDH_{-y}	2.9500×10^{-27}	1
J_2 IDH_{-n}	1.1040×10^{-109}	1

B.

	p-value	**Result**
$J_{2\ IDH\text{-}y\ /IDH\text{-}n}$	1.6482×10^{-5}	1

6.2. Intra-Dialysis Identifications and prediction of IDH onset.

Here are presented the results obtained studying what happen during the dialysis.
In particular in paragraph 6.2.1 the results on population analysis will be presented.
Paragraph 6.2.2 reports the results of the IDH criteria evaluation.

6.2.1 Population composition assessment

The population composition assessment has shown that among the 20 patients recruited from the EOC center was 20: 7 females (35%) and 13 males (65%). On 20 patients 7 was affected by diabetes mellitus and 5 of them were insulin-dependent; 17 patients have a more or less severe heart disease (85%), as many arterial hypertension.
On a deeper analysis 7 patients were affected by diabetes, have heart disease and arterial hypertension (35%); 8 were both cardiac and hypertensive (40%); 2 subjects had a heart disease but no diabetes or hypertension (10%) and as many suffer from high blood pressure but not diabetes or heart disease (10%).
The age range was 42-90 years, with a mean age of 70 years; the range of dialysis age, intended as the time passed from the first treatment was 3-77 months, with an average of 49 months. All subjects underwent on HDF therapy.
The number of patients recruited at the Dialisi dell'A.O. della Provincia di Lecco Patients were 50, and in particular 26 females (52%) and 24 males (48%).
Individuals affected by diabetes mellitus type 2 were 16 on 50 (32%): 8 of them insulin-dependent. 30 of the treated patients suffered of less severe heart disease (60%), 40 arterial hypertension (80%).
More precisely: 10 patients were both diabetics, that cardiac and hypertensive (20%); 4 were affected by diabetes and a heart disease (8%); 15 suffered of cardiac distress and hypertension (30%); 2 patients were diabetic but not hypertensive (4%); 5 subjects were hit by heart disease with no diabetes or hypertension (10%); 10 patients were hypertensive but not affected by heart-disease or diabetes (20%).
The age range is 48-88 years, with a mean age of 71.3 years; the range of dialysis age is 4-422 months, the average age is 70.22 months. Most of the subjects, namely 76%, was under SDH therapy (38 patients), while 12 underwent on HDF therapy (24%).

6.2.2 Intra-treatment Statistical Analysis – Relevant Results

The analysis has outlined statistical differences between the clusters on the selected set of parameter.
In particular with reference to:

- Systolic Arterial Pressure (SAP):
  - *Intratreatment trend*: SAP is statistically different between the cluster of diabetic and non diabetics of EOC Lugano and between the HDF and HD patient of Lecco
  - *maximum intratreatment variation peak (PMax):* no statistical differences has been observed between the analyzed clusters,
  - *intratradialysis variation (start to end) of each session (SE):* there were not statistical differences among the observed values and there aren't correlation between the values
  - *the difference between the maximum and the minimum values of each treatment (Max-min):* there aren't statistically significant differences between the clusters
- MAP and HR:
  - *Intratreatment trend:* SAP is statistically different between diabetic and non diabetics of EOC Lugano and between the HDF and HD patient of Lecco
  - [Ca2+]: there aren't statistically significant differences between the clusters
  - [Mg2+] and pH: cardiac patients denotes a significant statistical difference among control group and cardiac patients

6.2.3 Single parameters criteria

Here are reported and commented the results of the single criteria evaluation regarding the IDH criteria evaluation and the multicriteria evaluation
The complete results are listed in Appendix B.

6.2.3.1 SAP(0)140 criterion

Table B.1 show the result of the of the application of the $SAP(0)_{140}$ criterion $SAP(0)_{140}$ in EOC Lugano and to the A.O. Lecco.
The results shows the number of session identified by the $SAP(0)_{140}$ in the conditions SAP(0)<140, SAP(0) ≥140 and in the whole $SAP(0)_{140}$ form.
Table B.1.A particularly reports the application of the criteria on session recorded at the EOC Lugano; $SAP(0)_{140}$ identified IDH onsets when the BP set point has been reached on 65/150 sessions (43,33).
More in deep, the 66,15 % of them, that correspond to 43/150 sessions (14,67%) has a SAP(0) < 140, indeed the remaining 33,85 (22/150) shows SAP(0) ≥140 mmHg.
Generally the number of session with SAP(0)≥140 are 38/150 (25,33%)., thus those with lower initial pressure are 112/150 (74,67%).
Figure 6.3 graphically resumes the outcomes of the application of the criteria on the dataset:

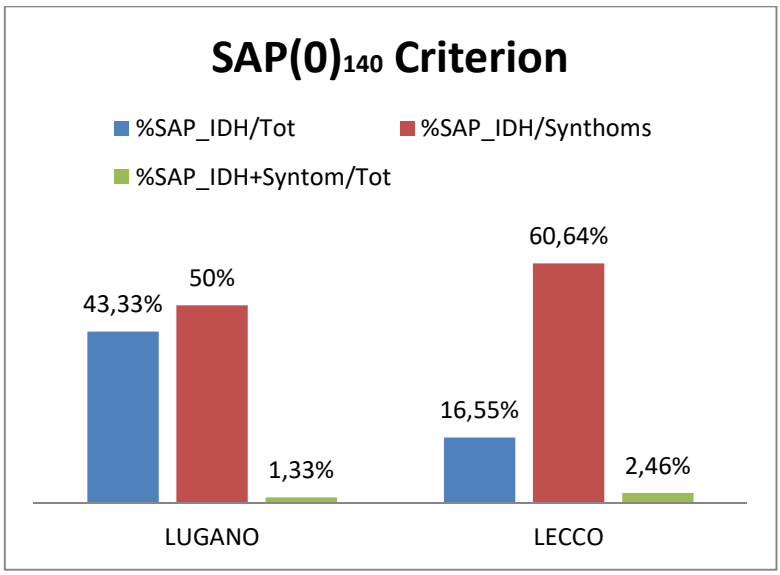

Figure 6.4: Result of the application of $SAP(0)_{140}$ Criterion

In order assess the reliability of the $SAP(0)_{140}$ criterion, the percentage of true positive (TP), false positive (FP), true negative(TN), false negatives (FN) and the assessment of Specificity and Sensibility, PPV and NPV with respect to the classification performed by IDH-D has been done.
Table 6.6 reports the results of the analysis:

Table 6.6: Results from the comparison between $SAP(0)_{140}$ A and IDH-D criterion.

SAP 0<140	**%Sensitivity**	**%Specificity**	**PPV**	**NPV**	**TP**	**%TP**	**FN**	**TN**	**FP**
EOC Lugano	48,89	83,33	51,2	82	22	48,9	23	105	21
A.O. Lecco	55,00	96,20	55	96,2	11	55	9	228	9
Total	50,77	91,74	52,4	91,2	33	50,8	32	333	30
SAP 0≥140	**%Sensitivity**	**%Specificity**	**PPV**	**NPV**	**TP**	**%TP**	**FN**	**TN**	**FP**
EOC Lugano	17,78	88,24	36,4	73,9	8	17,8	37	105	14
A.O. Lecco	25,93	91,70	25,9	91,7	7	25,9	20	221	20
Total	20,83	90,56	30,6	85,1	15	20,8	57	326	34
SAP 0_140	**%Sensitivity**	**%Specificity**	**PPV**	**NPV**	**TP**	**%TP**	**FN**	**TN**	**FP**
EOC Lugano	66,7	83,3	58,8	87,5	30	66,7	15	105	21
A.O. Lecco	62,07	88,31	38,3	95,2	18	62,1	11	219	29
Total	64,86	86,63	49	92,6	48	64,9	26	324	50

The criteria show an high specificity and high NPV value for both the data in EOC Lugano and A.O. Lecco, as can be shown in Figure 6.4 that reports the comparison of PPV and NPV values in the two centers.

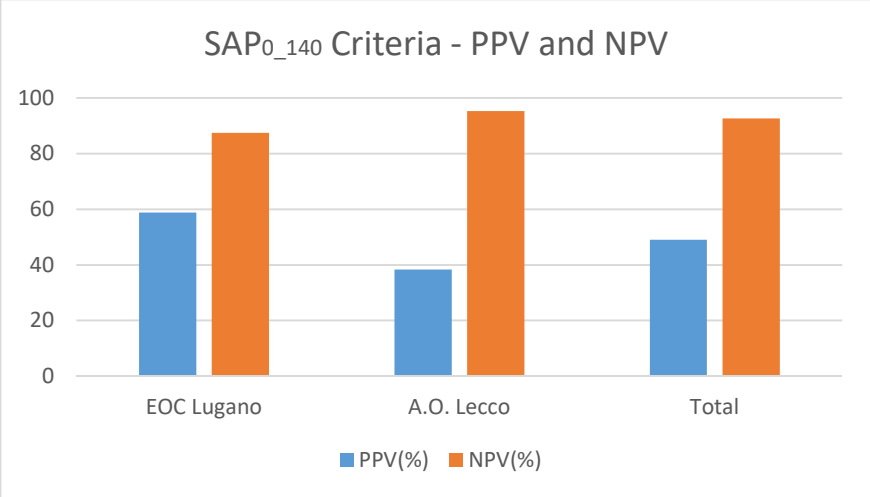

Figure 6.5: Results from the comparison between MAP_{30} and IDH-D criterion.

6.2.3.2 MAP_{30} Criterion

Table B.2 reports the result of the application of the MAP_{30} criterion applied on both EOC Lugano and to the A.O. Lecco datasets.
With respect to the EOC Lugano dataset, the MAP criterion has been able to identify as IDH affected 16/150 sessions (10,67%) in 8/20 patients (40%).
Only 1 on 4 of these sessions have been reported on the clinical records (25%).
The application of the criteria on the dataset of A.O. Lecco has shown that the criterion can to identify as IDH affected 28/284 session (9,86%) in 16/48 patients (33,34%).
No session reported on the clinical records has been correctly classified by the MAP_{30} criterion.
Figure 6.5 graphically resumes the outcomes of the application of the criteria on the dataset:

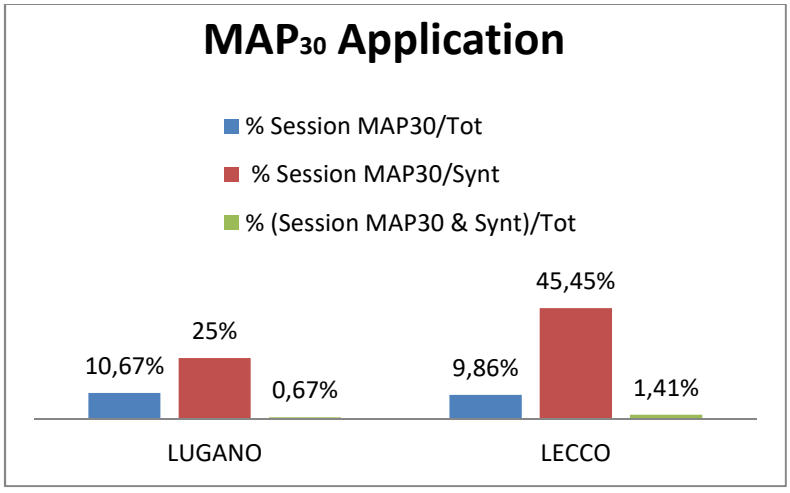

Figure 6.6: Results from the comparison between MAP_{30} and IDH-D criterion.

In order assess the reliability of the SAP(0)140 criterion, the percentage of true positive (TP), false positive (FP), true negative(TN), false negatives (FN) and the assessment of Specificity and Sensibility, PPV and NPV with respect to the classification performed by IDH-D has been done.
Table 6.7 shows the results of the comparison
Particularly:

- with reference to the results for the EOC Lugano; 6 sessions have been classified as IDH affected using MAP_{30} out of the total of 16 classified by the IDH-D criterion (37.50%), (true positive)
- with reference to the results of the A.O. of Lecco the RBV_{13} is able to

recognize 9 sessions out of the total of 28 (32.14%), (true positive), indeed 19 sessions out of 28 results as false positives (67.86%).

Table 6.7: Results from the comparison between MAP_{30} and IDH-D criterion.

MAP 30	%Sensitivity	%Specificity	PPV	NPV	TP	%TP	FN	TN	FP
EOC Lugano	37,5	86,45	22,2	93,1	6	37,5	10	134	21
A.O. Lecco	31,03	88,31	23,7	91,6	9	31	20	219	29
Total	33,33	87,59	23,1	92,2	15	33,33	30	353	50

Figure 6.6 that reports the comparison of PPV and NPV values in the two centers.
It can be seen that the criteria shows an high specificity and high NPV value for both the data in EOC Lugano and A.O. Lecco.

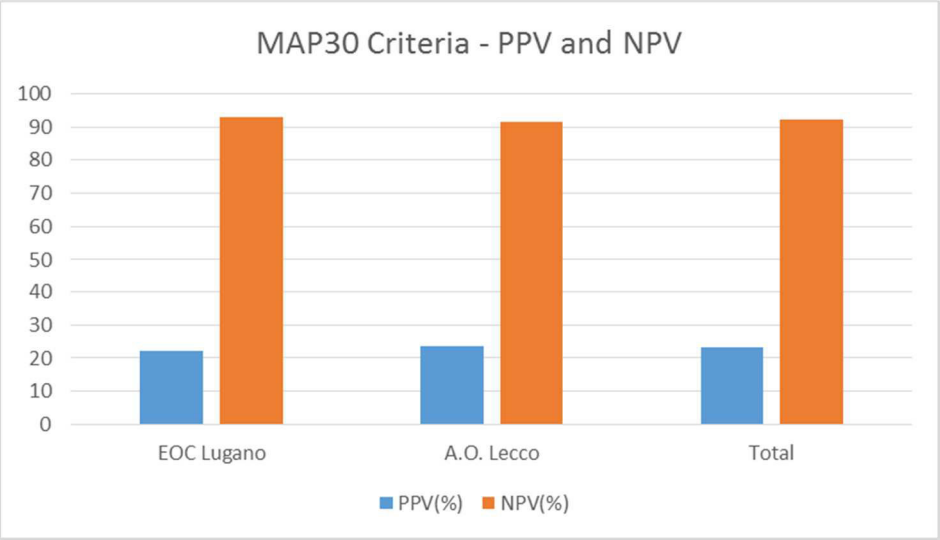

Figure 6.7: MAP30 PPV- NPV comparison

6.2.3.3 RBV_{13} criterion

Table B.3 reports the result of the application of the MAP_{30} criterion applied on both EOC Lugano and to the A.O. Lecco datasets.
The application of the RBV criteron lead to the following results:
on EOC Lugano dataset:

- the criterion is able to identify 46/140 IDH session (33,45%)
- the comparison with the clinical records shows that the criterion detects 1/ 4 sessions (25%) reported

on A.O. Lecco dataset:

- the criterion is able to detect 92/275 sessions (32,62%) in 50/50 patients (100%)
- the comparison with the clinical records shows that the criterion is able to identify 5/9 where the data on RBV was available (55,56%) in 3/5 patient (60%).

Figure 6.7 graphically depicts the obtained results:

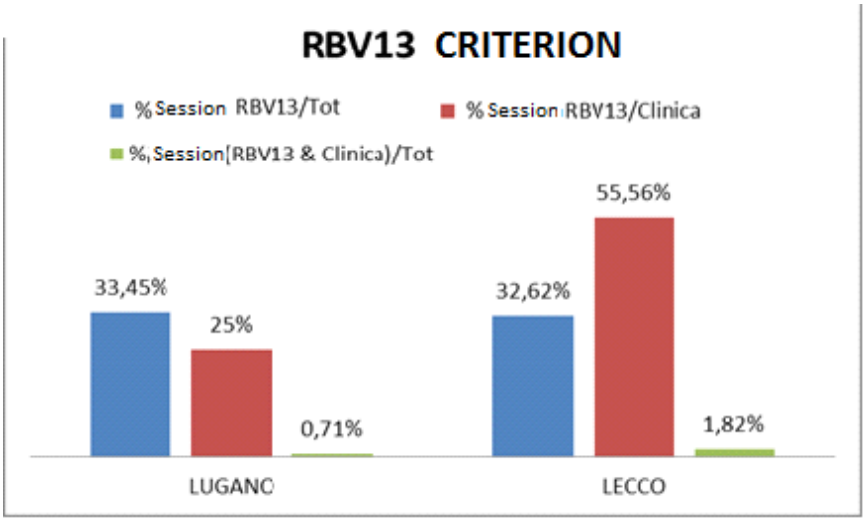

Figure 6.8: Results from RBV_{13} Criterion.

In order assess the reliability of the RBV_{13} criterion, the percentage of true positive (TP), false positive (FP) true negative(TN), false negatives (FN) and the assessment of Specificity and Sensibility, PPV and NPV with respect to the classification performed by IDH-D has been done. The results are reported in Table 6.8:

Table 6.8: Results from the comparison between RBV_{13} and IDH-D criterion

RBV 13	%Sensitivity	%Specificity	PPV	NPV	TP	%TP	FN	TN	FP
EOC Lugano	43,5	78,33	43,5	78,3	20	0,43	26	94	26
A.O. Lecco	15,22	70,11	15,2	70,1	14	0,15	78	183	78
Total	24,64	72,70	24,6	72,7	34	0,25	104	277	104

Figure 6.8 that reports the comparison of PPV and NPV values in the two centers.

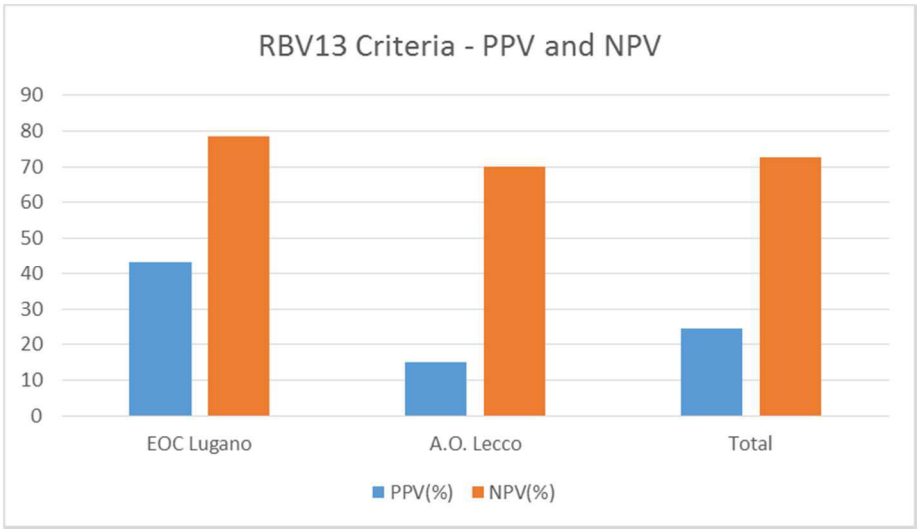

Figure 6.9: RBV13 comparison between PPV and NPV

6.2.3.4 ΔK^+ criterion

Table B.4 reports the result of the application of the MAP_{30} criterion on both EOC Lugano and to the A.O. Lecco datasets.
Its application lead to the following results:

- on EOC Lugano dataset:
  - *dK1* is able to identify 20/150(13,34%) session with dangerous variations of blood potassium concentration
  - *dK2* is able to identify 65/150(43,34%) session with dangerous variations of blood potassium concentration
  - *dK3* is able to identify 80/150(53,34%) session with dangerous variations of blood potassium concentration
  - totally the ΔK^+ is able to identify 112/150 (74,67%) session with dangerous variations of blood potassium concentration
  - the comparison with the clinical records, shows that the criteria is able to identify 4/4 sessions reported.
- on A.O. Lecco dataset:
  - *dK1* is able to identify 43/296(14,53%) session with dangerous variations of blood potassium concentration *dK2* is able to identify 117/296 (39,53%) session with dangerous variations of blood potassium concentration
  - *dK3* is able to identify 88/296 (29,73%) session with dangerous variations of blood potassium concentration
  - totally the ΔK^+ is able to identify 169/296 (57,09%) session with dangerous variations of blood potassium
  - the comparison with the clinical records, shows that the criteria is able to identify 3/11 (27,27%) sessions reported.

Figure 6.10 reports graphically the results of the application of ΔK^+ criterion on the dataset.

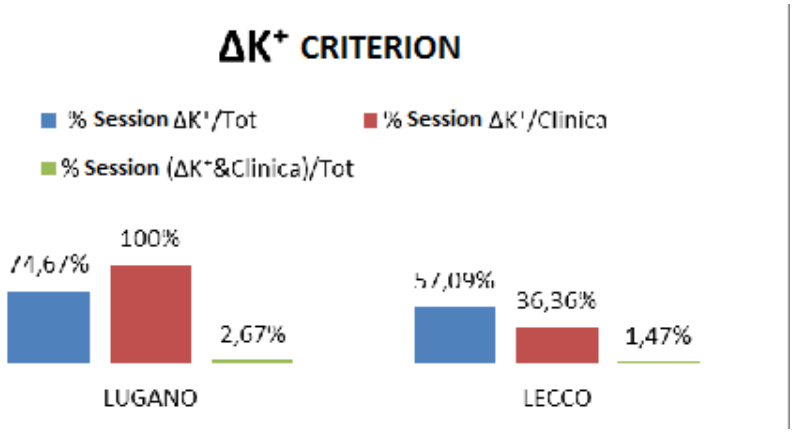

Figure 6.10: Results of the application of the ΔK^+ criterion

In order assess the reliability of the ΔK^+ criterion, the percentage of true positive (TP), false positive (FP), true negative(TN), false negatives (FN) and the assessment of Specificity and Sensibility, PPV and NPV with respect to the classification performed by IDH-D has been done. The results are reported in Table 6.9:

Table 6.9: Results from the comparison between **ΔK^+** and IDH-D criterion

ΔK+	Sensitivity	Specificity	PPV	NPV	TP	%TP	FN	TN	FP
EOC Lugano	54,4	56,4516129	68,9	78,3	31	68,9	26	94	81
A.O. Lecco	44,83	63,1205674	44,8	70,1	13	44,8	78	183	156
Total	59,46	61,08	59,5	72,7	44	20,8	104	277	237

Table 6.9 shows that:

- *with reference to the results for the EOC Lugano dataset;* 31 sessions have been detected as IDH affected using the complete ΔK^+ criterion on the total of 45 classified by the IDH-D criterion (68,89%)
- *with reference to the results of the A.O. of Lecco dataset*; the ΔK^+ criterion is able to recognize 13 sessions on the total of 29 (44,83%) that have been classified as IDH affected by the IDH-D criterion.

Figure 6.11 that reports graphically the comparison between PPV and NPV values in the two centers.

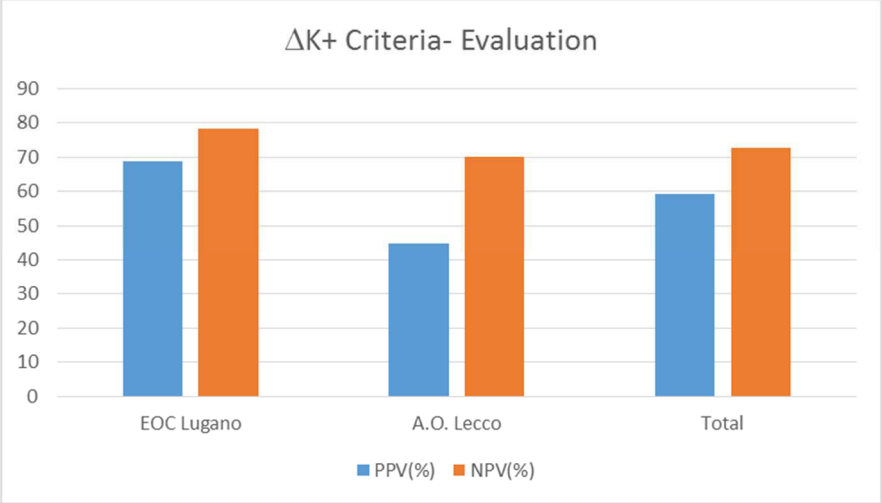

Figure 6.11: ΔK^+ comparison between PPV and NPV

.

6.2.3.5 Dysrhythmia criterion

Table B.5 reports the result of the application of the MAP_{30} criterion on both EOC Lugano and to the A.O. Lecco datasets.
The results shows that:

- on EOC Lugano dataset:
  - the criteria is able to identify 88/150 session classified as IDH by IDH-D (58,67%)
  - the comparison with the clinical records shows that the criterion detects 1/ 4 sessions (25%) reported
- on A.O. Lecco dataset:
  - the criterion is able to detect 92/275 sessions classified as IDH by IDH-D (32,62%).
  - the comparison with the clinical records shows that the criterion is able to identify 5/9 sessions (25%) reported

The criteria has been also tested considering both the variation on diminishing and increase of the 20% of cardiac rhythm and in particular:

- on EOC Lugano dataset
  for $HRate(t) \leq 20\%\ HRate(0)$
  - the criterion is able to identify 62/150 session (41,34%)
  - the comparison with the clinical records shows that the criterion detects 1/ 4 sessions (25%) reported

for HRate(t) ≥ 20% HRate(0)

- the criterion is able to identify 26/150 session classified as IDH by IDH-D (54,17%)

on A.O Lecco dataset

for HRate(t) ≤ 20% HRate(0)

- the criterion is able to identify 63/284 session classified as IDH by IDH-D (21,18%)

for HRate(t) ≥ 20% HRate(0)

- the criterion is able to identify 64/284 session classified as IDH by IDH-D (22,53%)

In order assess the reliability of the dysrithmia criterion, the percentage of true positive (TP), false positive (FP), true negative(TN), false negatives (FN) and the assessment of Specificity and Sensibility, PPV and NPV with respect to the classification performed by IDH-D has been done.
The results are reported in Table 6.10:

Table 6.10: Results from the comparison between dysrithimia and IDH-D criteria

Dysrhythmia	**Sensitivity**	**Specificity**	**PPV**	**NPV**	**TP**	**%TP**	**FN**	**TN**	**FP**
EOC Lugano	41,9	56,4516129	57,8	72,3	26	68,9	36	94	81
A.O. Lecco	65,52	63,1205674	65,5	80,3	19	44,8	45	183	156
Total	60,81	61,08	60,8	72,7	45	20,8	104	277	237

Figure 6.12 reports graphically the comparison between PPV and NPV values in the two centers and in total.

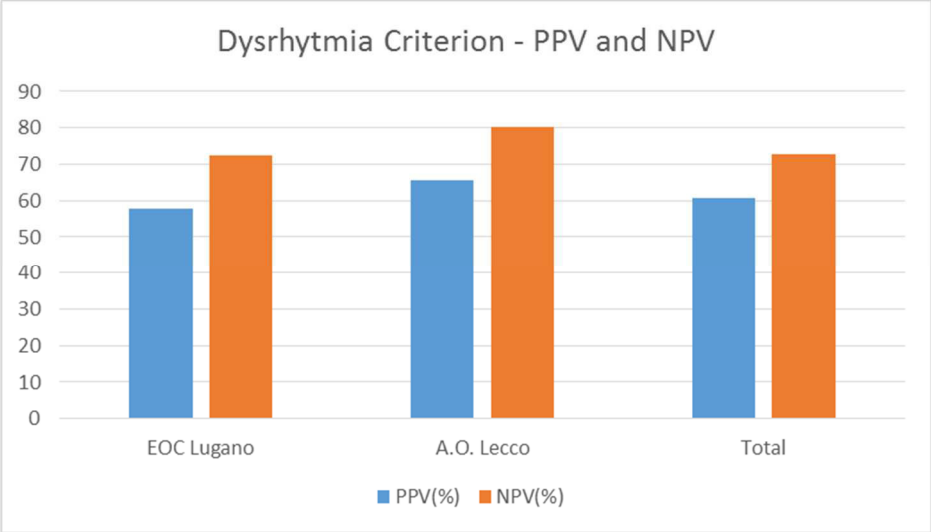

Figure 6.12: Dysrhytmia criterion comparison between PPV and NPV

6.2.4 Comparison between the criteria performances and cross application

The performances of the single criteria in term of IDH detected and false positives, have been compared. with the detection of IDH by the IDH-D criteria. The results are shown in Table 6.11.

Table 6.11: Comparison between the criterions

Predictive Criteria	%IDH Identified	%Sensitivity	%FALSE_positives
SAP$_o$140	66,22%	64,86%	57,14%
MAP30	20,27%	33,33%	65,90%
RBV13	49,27%	24,64%	75,36%
DIM20	60,81%	60,81%	64%
ΔK$^+$	59,46%	59,46%	84,34%

The comparison shows that the number of identified IDH stands around 50-66% on the application of all the single criteria and signaled false positive are between 57%-74%.
The criteria has been also tested in their cross application.
Table 6.12 and 6.13 resumes synthetically the results of the cross application of the criteria:

Table 6.12: Comparison between the criterions – true positives

	SAP$_o$140	RBV13	DIM20	ΔK$^+$
SAP$_o$140				
RBV13				
DIM20				
ΔK$^+$				

45-70% 44%-30% 29-20%

Table 6.13: Comparison between the criterions – false negatives

	SAP$_o$140	RBV13	DIM20	ΔK$^+$
SAP$_o$140				
RBV13				
DIM20				
ΔK$^+$				

45-60% 61-80% 81-90%

The combination of two criteria lead to lower identification of IDH events and to higher false negatives percentages.
This results lead to the definition of a multiparametric criteria.

6.2.5. The multiparametric criteria

The multiparametric criterion as defined in 5.8 has been applied on the two datasets: the result of the application are reported in
Table B.6.
Particularly the results shows that:

- on EOC Lugano dataset:
  mc1:
    - the criteria has been able to identify 10 sessions with IDH; 8 of them correspond to the IDH-D classification (80%) and 2 are false positives (20%)

  mc2:
    - the criteria has been able to identify 22 sessions with IDH; 16 correspond to the IDH-D classification (72,72%) and 6 are false positives (27,27%)

  mc3
    - the criteria has been able to identify 20 sessions with IDH; 17 correspond to the IDH-D classification (85%) and 3 are false positives (15%)

  the whole criteria
    - the criteria has been able to identify 52 sessions with IDH; 41 correspond to the IDH-D classification (78,85%) and 11 are false positives (21,15%).
- on A.O. Lecco dataset
  mc1:
    - the criteria has been able to identify 11 sessions with IDH; 7 of them correspond to the IDH-D classification (63,64%) and 4 are false positives (36,36%);

  mc2:
    - the criteria has been able to identify 14 sessions with IDH; 10 correspond to the IDH-D classification (71,43%) and 4 are false positives (28,57%)

  mc3
    - the criteria has been able to identify 13 sessions with IDH; 19 correspond to the IDH-D classification (76,93%) and 3 are false positives (23,07%).

  the whole criteria
    - the criteria has been able to identify 27 sessions with IDH; 41 correspond to the IDH-D classification (71,05%) and 11 are false positives (28,95%).

Totally the multiparametric criteria has been able to identify the 98.55% of sessions with hypotension as defined by IDH-D and with a percentage of 24.24% of false positives.

Table 6.14: Comparison between the criterions – true positives

Multiparam	Sensitivity	Specificity	PPV	NPV	TP (SA	%TP	FN	TN	FN
EOC Lugano	39,5	90,5172414	37,8	78,3	17	91,1	26	94	11
A.O. Lecco	44,83	63,1205674	44,8	70,1	13	44,8	78	183	156
Total	40,54	69,02	40,5	72,7	30	44,8	104	277	167

Figure 6.14 reports graphically the comparison between PPV and NPV values in the two centers and in total.

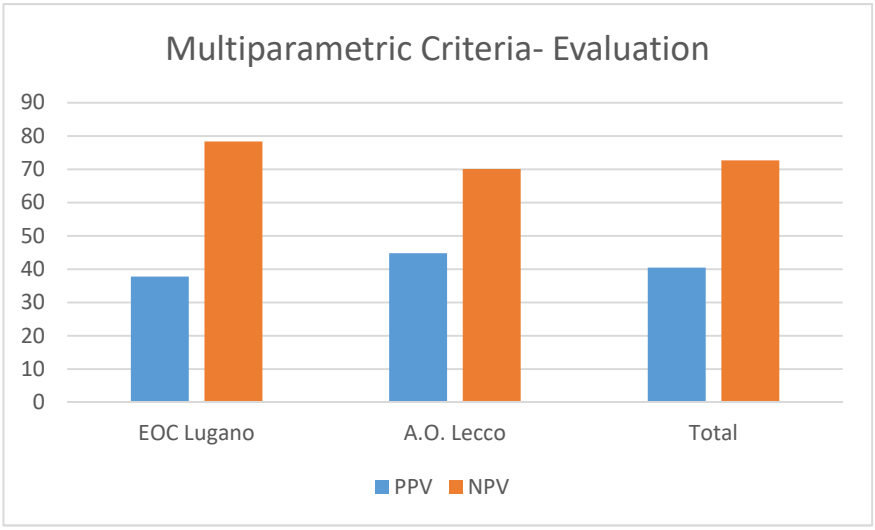

Figure 6.13: Multiparametric criterion-comparison between PPV and NPV

6.3 Machine Learning Approach

All the three different machine learning techniques (Random Forest, Artificial Neural Network and Support Vector Machine) were implemented over five different datasets (A, B, C, D, E), each of which was divided in a Validation (90% of the total) and in an Independent Testing (the remaining 10%) subsets in order to have an additional indicator for eventual model overfitting.
Recalling the five datasets:

- *Dataset A:* 500% minority class SMOTING and no majority class downsampling, resulting in 1118 examples; (higher samples, minority class SMOTING)
- *Dataset B*: 300% minority class SMOTING and relative majority class random downsampling, resulting in 745 examples;
- *Dataset C*: 100% minority class SMOTING and relative majority class random dowmsampling, resulting in 366 examples;
- *Dataset D:* 100% minority class Bootstraping and relative majority class random downsampling, resulting in 373 examples;
- *Dataset E*: 50% minority class SMOTING and relative majority class random downsampling, resulting in 280 examples

The main evaluation parameters are here reported in Table 6.13 and 6.14.
The complete Confusion Matrices and ROC Curves are listed in the Appendix "A2 Machine Learning".
Each model, in the implementation, validation and independent testing phases has been evaluated by the following parameters:

- **Overall Accuracy:** quantifies how well a model correctly identifies a condition. It is defined as the portion of true results among the total number of examined cases;
- **Precision:** is the fraction of retrieved instances that are considered relevant instances. In the following tables the precision values refer to the prediction target class: IDH events;
- **Recall:** is the fraction of relevant instances that are true positives. In the following tables the recall values refer to the prediction target class: IDH events;
- **AUC:** is defined as the area underlying the ROC curve. It can be considered as equal to the probability that the classifier will rank a randomly chosen positive instance higher than a randomly chosen negative one
- **f-measure:** considers both precision and recall to compute a more general score.

6.3.1. Random Forest Evaluation

Random Forest performance is summarized in Table 6.15.
The best overall accuracy is achieved by the models developed over Dataset D and E, but these models appear to suffer of faint overfitting: particularly for Dataset E, the independent test highlights that all parameters, excluded the AUC, overrun the variability interval determined by the model validation.
This could be attributed to the Dataset D and E small size.
Dataset C model results unsatisfactory under every aspect: low accuracy, precision, recall, AUC and f-measure are combined with high variability intervals.
When the model is validated over the Datasets A and B; high values of the performance parameters were achieved, with acceptable variability intervals. In general the model has higher recall values rather than prediction for all the datasets. This means that the model is reliable on identifying true positive conditions.
In general all the obtained models are characterized by large variability intervals (e.g. from ±3.52% to ±8.22% for accuracy and from ±3.11% to ±9.09% for f-measure), underling a strong correlation between the composition of the training sets and the model performances.

Table 6.15: Result of evaluation of Random Forest Algorithm

		ACC	**PRC**	**RCL**	**AUC**	**f-measure**
A	Val.	77.31±4.08%	73.21%	85.89%	0.833±0.029	79.01±3.77%
	Ind.	81.25%	76.06%	93.10%	0.871	83.72%
B	Val.	76.42±3.52%	71.32%	84.69%	0.844±0.042	77.42±3.11%
	Ind.	77.03%	73.33%	86.84%	0.807	79.52%
C	Val.	70.21±6.09%	67.76%	67.76%	0.818±0.081	66.95±9.09%
	Ind.	86.11%	88.89%	84.21%	0.913	86.49%
D	Val.	81.52±6.75%	77.98%	83.97%	0.913±0.048	80.70±7.41%
	Ind.	78.38%	75.00%	83.33%	0.924	78.95%
E	Val.	84.05±8.22%	81.54%	86.89%	0.923±0.064	84.01±8.35%
	Ind.	75.00%	60.00%	90.00%	0.878	72.49%

6.3.2. Artificial Neural Network

The results obtained evaluating the Artificial Neural Network approach are summarized in Table 6.16.
The best overall accuracy is achieved when the model is trained over Dataset D and E, even if the variability intervals of accuracy, may suggest a marked dependence from the training sets.
The results obtained during the independent testing over the Dataset D outperform those reached on the validation set, confirming this supposition.
Furthermore, the model trained over Dataset C is characterized by a low accuracy (73.86%) and a high variability interval (±7.07%), highlighting how reduced datasets combined with the considered machine learning technique strongly strengthen the relationship between training set and model performances. The model obtained from Dataset A perform well both in terms of overall accuracy and class recall keeping narrow variability intervals. Class recall results acceptable for all the trained models since, as explained in the previous chapter, a high sensitivity test has been considered as a fundamental requirement during the implementation phase.
Also for ANN, SMOTING technique for dataset balancing appears to grant most performant IDH predictions.
Best results are obtained with no minority class downsampling.
In general ANN has higher precision values rather than recall : the model is more powerful in identifying positive instances of IDH from the retrieved entries.

Table 6.16: Result of evaluation of Artificial Neural Network Algorithm

		ACC	PRC	RCL	AUC	f-measure
A	Val.	80.69±3.57%	78.23%	84.80%	0.869±0.041	81.41±3.13%
	Ind.	84.82	90.20%	79.31%	0.898	84.40%
B	Val.	78.36±3.61%	75.36%	81.25%	0.858±0.024	78.14±3.92%
	Ind.	77.03%	75.61%	81.58%	0.846	78.48%
C	Val.	73.86±7.05%	70.89%	73.68%	0.829±0.060	72.30±7.23%
	Ind.	77.78%	86.67%	68.42%	0.882	76.47%
D	Val.	81.17±4.39%	85.09%	87.82%	0.896±0.061	86.38±4.63%
	Ind.	91.89%	89.47%	94.44%	0.921	91.89%
E	Val.	85.62±5.15%	82.58%	89.34%	0.874±0.045	85.54±5.64%
	Ind.	82.14%	72.73%	80.00%	0.856	76.19%

6.3.3 Support Vector Machine

The Support Vector Machine models performances are summarized in Tab.6.17. The best results, in terms of overall accuracy, Area Under Curve and f- measure, are achieved when using the models developed over Dataset D and E. These performances, as obtained on Random Forest and Artificial Neural Network analysis, are characterized by large variability intervals, specifically with regard to the f-measure parameter.
Both the models show class precision higher than class recall, achieving even the 100% in the independent testing phase.
The model trained over Dataset C has the lowest performances among the considered datasets, remarking lack of predictive power. Furthermore, the independent test accuracy (75%) falls outside the variability interval identified during the validation phase (85.09%±8.01%), showing the possibility of model overfitting. Dataset B performances are acceptable for each evaluation parameter. Dataset A reached high performances characterized by narrow variability intervals (e.g. accuracy = 88.26% ± 2.80%) revealing a high independence from training set composition.
Both the models obtained from Dataset B and A are characterized by class recall higher than class precision highlighting the high sensitivity of the considered models.

Table 6.17: Result of evaluation of Support Vector Machine Algorithm

		ACC	**PRC**	**RCL**	**AUC**	**f-measure**
A	Val.	80.69±3.57%	78.23%	84.80%	0.869±0.041	81.41±3.13%
	Ind.	84.82	90.20%	79.31%	0.898	84.40%
B	Val.	78.36±3.61%	75.36%	81.25%	0.858±0.024	78.14±3.92%
	Ind.	77.03%	75.61%	81.58%	0.846	78.48%
C	Val.	73.86±7.05%	70.89%	73.68%	0.829±0.060	72.30±7.23%
	Ind.	77.78%	86.67%	68.42%	0.882	76.47%
D	Val.	81.17±4.39%	85.09%	87.82%	0.896±0.061	86.38±4.63%
	Ind.	91.89%	89.47%	94.44%	0.921	91.89%
E	Val.	85.62±5.15%	82.58%	89.34%	0.874±0.045	85.54±5.64%
	Ind.	82.14%	72.73%	80.00%	0.856	76.19%

6.3.4 Algorithm Performance Comparison

Tables 6.18-6.22 reports the comparison of the performances among machine learning algorithms and the different balancing techniques.
The results, show that the best overall results were achieved by models trained over Dataset D and E(e.g. overall accuracy for SVM model: 92.50% ± 5.02% and 92.93% ± 4.38%, respectively).
These datasets are the ones obtained through minority class oversampling with replacement and majority class down sampling.
This procedure re-turned small datasets, leading to minority class information redundancy and majority class information loss.
On the other hand, models trained and validated over the datasets obtained through SMOTE are generally less performing, but their results, characterized by tighter variability ranges, and can be considered as has having higher generalization error.
Particularly Dataset A (Table 6.18), the one obtained through high minority class SMOTE and no majority class down sampling, has the best performance and smallest variability intervals (e.g. SVM model overall accuracy: 88.26% ± 2.80%).

Table 6.18: Dataset **A**, performance comparison

		ACC	PRC	RCL	AUC
RF	*Val.*	$77.31\% \pm 4.08\%$	73.21%	85.89%	0.833 ± 0.029
	Ind.	81.25%	76.06%	93.10%	0.871
ANN	*Val.*	$80.69\% \pm 3.57\%$	78.23%	84.80%	0.869 ± 0.041
	Ind.	84.82%	90.20%	79.31%	0.898
SVM	*Val.*	$88.26\% \pm 2.80\%$	78.23%	89.90%	0.948 ± 0.020
	Ind.	91.96%	87.93%	96.23%	0.965

Table 6.19: Dataset **B**, performance comparison

		ACC	PRC	RCL	AUC
RF	*Val.*	$76.42\% \pm 3.52\%$	71.32%	84.69%	0.844 ± 0.042
	Ind.	77.03%	73.33%	86.84%	0.807
ANN	*Val.*	$78.36\% \pm 3.61\%$	75.36%	81.25%	0.858 ± 0.024
	Ind.	77.03%	75.61%	81.58%	0.846
SVM	*Val.*	$85.97\% \pm 4.96\%$	82.10%	90.31%	0.921 ± 0.039
	Ind.	86.49%	85.00%	89.47%	0.937

Table 6.20: Dataset C, performance comparison

		ACC	PRC	RCL	AUC
RF	*Val.*	$70.21\% \pm 6.09\%$	67.76%	67.76%	0.818 ± 0.081
	Ind.	86.11%	88.89%	84.21%	0.913
ANN	*Val.*	$73.86\% \pm 7.05\%$	70.89%	73.68%	0.829 ± 0.060
	Ind.	77.78%	86.67%	68.42%	0.882
SVM	*Val.*	$85.09\% \pm 8.01\%$	84.31%	83.77%	0.901 ± 0.073
	Ind.	75.00%	71.22%	76.47%	0.836

Table 6.21: Dataset D, performance comparison

		ACC	PRC	RCL	AUC
RF	*Val.*	$81.52\% \pm 6.75\%$	77.98%	83.97%	0.913 ± 0.048
	Ind.	78.38%	75.00%	83.33%	0.924
ANN	*Val.*	$81.17\% \pm 4.39\%$	85.09%	87.82%	0.896 ± 0.061
	Ind.	91.89%	89.47%	94.44%	0.921
SVM	*Val.*	$92.54\% \pm 5.02\%$	95.71%	87.58%	0.967 ± 0.044
	Ind.	91.89%	100.00%	85.71%	0.958

Table 6.22: Dataset E, performance comparison

		ACC	PRC	RCL	AUC
RF	*Val.*	$84.05\% \pm 8.22\%$	81.54%	86.89%	0.923 ± 0.064
	Ind.	75.00%	60.00%	90.00%	0.878
ANN	*Val.*	$85.62\% \pm 5.15\%$	82.58%	89.34%	0.874 ± 0.045
	Ind.	82.14%	72.73%	80.00%	0.856
SVM	*Val.*	$92.03\% \pm 4.38\%$	95.41%	87.39%	0.974 ± 0.033
	Ind.	89.29%	100.00%	76.92%	0.867

Chapter 7 – Discussion

7.1 Introduction

The performed analyses has produced different outcomes, in particular:

- Dialysis Database
- Dialysis Matlib
- J_1 and J_2 index for pre-dialysis IDH detection
- A multiparametric criterion for the intra-dialysis IDH detection
- Machine Learning Algorithms

Those outcomes will be discussed in the further paragraphs.

7.2 Dialysis Data Infrastructure and Dialysis Matlib

The DDI and the Dialysis MATlib constitute a versatile tool to manage the clinical data of the Dialysis Project.
The combination of these two elements has been used to overcome the hard data interoperability problems persisting among the data collections of the involved dialysis units. Currently, the whole system can perform 4 levels of interoperability by the definition of Wang et al. [143].
Starting from the practical interoperability given by the diffuse internet connection, the presence of a common data format provides syntactic and semantic interoperability. The DDI and DDR platform ensures several levels of interoperability, from syntactical to practical.
Practical interoperability has been particularly important in the Dialysis Project. Since the study involved different clinical units, it was central to give a tool capable to share analyses, mining and data management functionalities among heterogeneous users in different clinical centers [**Error! Reference source not found.**].
A key element in the implementation of practical interoperability has been the definition of the possible macro-actions on the different datapools [116].
The macroactions can be considered as the concrete implementation the interoperability and the federation layers described in Figure 1. They are performed by functions that have been coded in Matlab®.
All the interoperability architecture has been designed on the basis of the federated approach, allowing a multiple hierarchies structure based on the DR levels.
It can be argued that the idea of multiple hierarches is not new in the dialysis field and other approaches are more common in literature. These approaches are mainly based on ontologies and controlled dictionaries [149].
In this sense, the federated approach used for the construction of the DDI, appears quite unusual and seems to lack of portability.
Nevertheless, the implementation of the DDI through the federated database approach as allowed to exploit the potentials of Matlab®.
Once the data are translated into workspace variables, they are available to be treated as heterogeneous data in a vector-matrix logic.
Furthermore they are available to be elaborated by Matlab® toolboxes.
Currently, Matlab® is providing several toolboxes for large dataset management and exploratory analysis [136] like the Machine Learning, the Database and the SVM Toolboox.
As the Dialysis MATlib provides a standardized input workflow, the DDI can be widened any moment with new data.
Therefore these data could be treated in Matlab® by “MapReduce” and “memmap” functions [230]. These functions are suitable for analyzing large datasets that cannot fit computer's memory. Moreover, MapReduce can connect to the well-known big-data platform Hadoop [230]. So the use of MATLAB®

as main developing environment presented several advantages.

7.3 Pre-dialysis Period

7.3.1. Comments on Analysis - Strategy 1

The statistical analysis of the clinical dataset allowed to define J_1 (6.1) as predictive index of hypotension during the dialysis treatment.
J_1 resulted a multifactorial index, based on the weighted combination of the pre-dialysis values of potassium concentration [K+], MAP, and weight gain (ΔW) taking into account also the proneness of the specific patient to IDH.
These parameters results useful for their physiological and statistical relevance and their can be easily retrieved during daily clinical practice in dialysis units.
J_1 has been calculated at the beginning of each session, through non-invasive measurements.
It's structure givesthe clinician useful information on the probability of IDH onset during the specific treatment, that can be tuned and personalized to avoid IDH onset.
Furthermore, J_1 offers a personalized IDH risk assessment.
The weight coefficients are indeed adjourned based on the longitudinal analysis of the influencing parameters.
As described in Par 6.1.1. the weight coefficient calibration is based on the cumulative mean, of the influencing parameter for the individual patient (RPPC), in a set of reference patient profile conditions that defines the normality of predialysis condition of each patient (BPDC).
This means that the J_1 prediction depends both by the clinical history of the patient and his conditions at start of the treatment.
The influence of each influencing parameter on the J_1 index prediction is weighed in a different way according to the characteristics of each patient and to his proneness to hypotension.
On this assumptions, J_1 thus results as weighted combination of the pre-dialysis parameter values designed to be patient-depend and coherent to the multifactorial nature of the IDH onset.

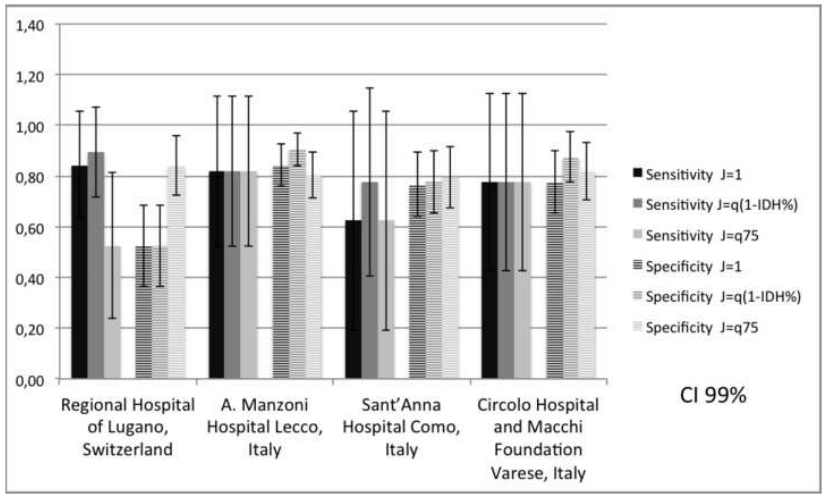

Figure 7.1: Ji sensitivity and specificity for the different centres and thresholds. Error bars represent the Confidence Interval at 99% (CI 99%)[231].

J_1 has been assessed in its prediction abilities with different center depended thresholds J_{th}.
The results showed that J1, when J_{th}=1, allows identifying, since the early stage of the sessions, the 77% of IDHs.
Figure 7.1 shows that J_1 sensitivity and specificity result always around 70- 80%,

independently from the inter-center variability.
In the literature, screening tests characterized by similar performances were accepted for pathologies, like IDH, whose prevalence is under 30% (18-20).
The use of a unique threshold (J_{th}=1) does not lead to the same performances in the different centers[232].
This dependency can be statistically explained by the existence of a relationship among the prediction of a clinical test and the prevalence of the investigated pathology (here IDH) [233-235]. The different prevalence can be on its turn explained either by the not homogeneous patient characteristics or by the different protocols used to manage IDH in the different centers.
Standing the absence of alternative reliable methods (gold standard) to evaluate the risk of IDH onset since the early stage of the HD treatment, the proposed index, based on easily measurable data, could be useful as a first screening for the clinician and the nurses that could benefit by the in-advance knowledge of the session-specific patient risk to develop IDH.
A limit to the J_1 use is that its calculation require data relative to at least 3 previous sessions to identify the patient-specific weights of the index, thus implying the availability of a relevant database in the center. This limit could be overcome with the automation of the data recording process and the integration of data acquired from different devices, as the ongoing healthcare digital transformation encourages [196].
Furthermore J_1 it presents a difficult threshold setting due to index linearity; and an unbalanced hp weight that do not considers the evolution of the risk during the treatment.
The linearity does not facilitate the possibility to add other influencing factors for an increased phenomena description
.

7.3.2. Comments on Analysis - Strategy 2

Statistical tests were run over the two different datasets making possible to analyze the IDH distributions from two different perspectives: Dataset 1 allowed to consider the risk of IDH related to the patients proneness while Dataset 2 focus more on the physiological events connected to the single HD session.
The preliminary Kolmogorov-Smirnov (K-S) normality tests highlighted the non-normality distributions for all attributes, in both datasets.
Different pathologies and relative drugs use and dosage may have played a crucial role on these results.
The Kruskal-Wallis and ANOVA tests to assess the statistical differences between the groups returned quite similar results: in both datasets Sodium and Magnesium Concentration and Mean Arterial Pressure resulted statistically different between the two groups.
On Dataset 1 also Calcium showed to be statistically different, pointing out how the patient characterization could have different statistical dynamics with respect to the physiological description of IDH events.
Analysing the complete results of the statistical analysis it can be pointed out that higher electrolytes concentrations and lower MAP, could characterize the Hypotension Prone and No IDH Events populations(Fig. A.1-A.4, A.7, A.8-A.11, A.14).
Particullarly, the analysis has permitted to propose a new index J2 (6.2) as an evolution of J1, based on the weighted combination of the pre-dialysis values of Mean Arterial Pressure and Inter- sessions Weight Gain and the treatment duration.
J_2 mathematical function consists in a sigmoid representing the present patient conditions shifted depending on patient IDH history: β is the independent variable, α controls sigmoid steepness and hp determines the shift.
The new version of the index J_2 tries to overcome the limits of J_1.
Firstly as it comes from the analysis of both Dataset 1 and 2, it considers both inter- and intra-patients variability.
Compared to J_1, J2 index can be viewed as a continuous risk scale, where 1

stands for maximum IDH risk, instead of a discrete prediction.
Furthermore it modulates the hypotension proneness by the time t_{dial} of the treatment, considering that the risk of IDH can decreases by the time during the session.
Due to non linear formulation (6.2) it also allows to add futher parameters to the prediction.
However, as can be seen in Attachment A Fig. A.15, even if J_2 is able to discriminate between the HP and HR patients, the risk scale results quite short: most values are included in the interval 0.75−0.85 for both populations.

7.4 Intradialysis-dialysis Period

7.4.1 Population composition assessment

The intra-treatment Statistical Analysis highlighted that the collected pressure data belongs to different populations for each of the performed clustering, with the exception of patients with different therapies (HDF vs HD), referring to the data pool in the center of Lecco.

This result can be explained considering the high variability of the parameter within the treatments and between the subjects do to the highly-dependent patient response to the treatment, related to the specific conditions at the beginning session of the subject and his clinical picture - as well as to possible measurement errors.

The intradialysis variations of pressure (difference between initial and final values, between the maximum and minimum values), and in particular the maximum (maximum pressure variation) are less disperse and more comparable.

Considering the MAP trends indeed, difference between diabetic and non-diabetics patients of EOC Lugano and between the HDF and HD patient of Lecco have been registered. However this is not possible to uniquely identify comparable categories and trends among the two centers.

Similar conclusions can be reached regarding heart rate trends.

For systolic pressure, MAP and heart rate it is not possible to identify significantly comparable categories. It then outlines a highly heterogeneous picture, that lead to consider an inter-treatment variation rather then a trend as a representative parameter of the session.

The statistical study of the concentration values in the blood of the main electrolyte and the pH during the dialysis treatment, has not led to determine specific differences within the clusters, as the data are part of the same population.

This can be attributed to significant intra- and inter-subject variability of these parameters, to the specific clinical condition of the patient at the beginning of the session (different for each treatment even for the same patient), and to the specific treatment conditions due to the different dialysis fluid composition used by the centers.

Furthermore, the causes variations of the analyzed parameters; the variation of a single electrolyte has repercussions on others, thus resulting in an extremely complex system.

In conclusion it was not possible to define clinical categories of patients for whom the analyzed parameters (pressure, heart rate, electrolytes, pH) have similar trends. The pool of patients is therefore to be considered heterogeneous. It is preferable to also analyze and compare variations of the parameters instead of their intradialytic trend.

7.4.1 Intra-treatment IDH risk identification

Standing to Table 6.11, the application of the tested predictive criteria shows low overall percentages of IDH identified ($SAP(0)_{\_140}$: 66,22% ; MAP_{30}: 20,27%; RBV_{13}: 49,27%; dim20: 60,81% ; ΔK^+ : 59,46%) and sensitivity ($SAP(0)_{\_140}$; MAP_{30}: 33,33%;; RBV_{13}: 24,64%; dim20: 60,81% ; ΔK^+: 59,46%), accompanied with high percentages of false positives($SAP(0)_{\_140}$: 57,14%; MAP_{30}:65,90%;; dim20: 60.81%; RBV13: 75.36%; ΔK^+: 84.34%).

It can ben therefore concluded that the single criteria do not have a sufficient predictive efficacy.

Even the simultaneous application of two criteria do not detect a sufficient number of sessions with hypotension as defined by IDH-D (Table 6.12 and 6.13) even with a percentage of false positives below the 30%.

This result has highlighted the need of a multiparameter criterion (Par. 5.5.3.4.) for the IDH risk assessment during the dialysis treatment.

In particular the multiparameter criterion, collects in a unique set of conditions that physiological parameters (systolic blood pressure, change in RBV, variation in the [K^+] and Heart Rate), associated to the mayor determinants that contributes to the IDH risk [198,233].

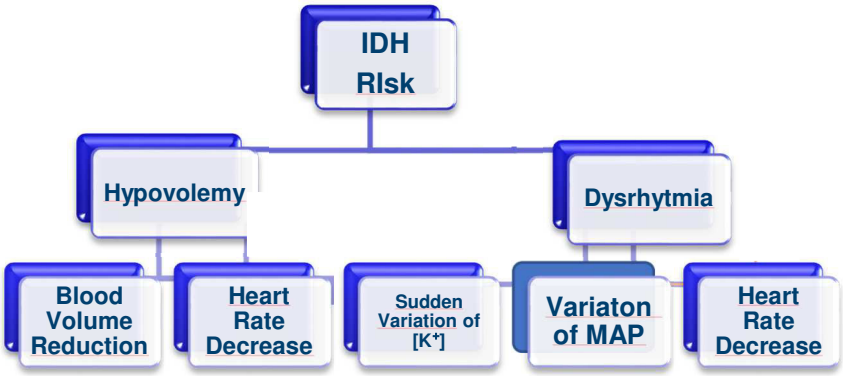

Figure 7.1: Decomposition of the IDH risk in two mayor determinants and associated physiological variables

As indeed described in Par 2.3, hypotension is strictly related to an altered and pathological cardiovascular response to the decreased circulating volume induced by ultrafiltration.
Furthermore, the variable used in the composition of the multiparameter criteria, can be considered as "sensor variables" [88] of one of more of the three controls acts exposed in Par 2.3.
As instance, the variation of RBV can be associated to the venous return in the cardiac cavity, the variation of HR indeed describes the effects of the increased hearth rate due to the increase in the cardiac output.
The multivariate criterion has been structured to reflect the physiological framework of causes to predict the IDH risk.
The first risk assessment is performed: comparing the value of the Systolic Arterial Pressure at time t of the session with the initial value of SAP through the $SAP(0)_{140}$ criterion
SAP has been the eligible measure for the IDH management in several studies [32].
Considering this criterion it can be observed that for $SAP(0)\geq 140$, at the beginning of the session, the application of the $SAP(0)_{140}$ conditions has been able to detect all the session classified as IDH by IDH-D (cfr Table X:X appendix C).
For $SAP(0)\leq 140$, indeed the criteria has not been able to match all the IDH standing to the IDH-D definition and an high number of false positives has been detected.
The $SAP(0)_{140}$ criterion, is thus selected for the session with $SAP(0)\geq 140$ when systolic starting pressure is greater or equal to 140 mmHg.
A decrease over a threshold of $SAP(t) \leq 110$mmHg has been also considered as risky for the onsets of hypotension.
In the complementary case $SAP(0) \leq 140$ two strategies have been implemented.
For $115 \leq SAP(0) \leq 140$ mmHg, the risk of IDH is identified with a variation of 23% of the value of SAP(0)
For $SAP(0)\geq 115$ mmHg the risk of IDH is identified with a variation of 16% of the value of SAP(0)

The mere evaluation of the pressure drops from the initial value is not sufficient to detect hypotensive episodes without obtaining a high number of false positives.
Thus, the multiparametric criteria provides the aggregation of other criteria to the $SAP(0)_{140}$
Particularly a second level of risk assessment has been added considering RBV_{13} criterion and a decrease of HR equal to 20% with respect to HR(0).
Those conditions describe a typical state of hypovolemia with insufficient compensation by cardiovascular system (hypovolemic hypotension)[198,113].
Alternatively the multiparametric criteria evaluates the combination of pressure variation together with the conditions expressed by the ΔK^+ criterion and the decrease greater or equal to 20% of HR.
Potassium unbalances and heart rhythm variation may in fact cause hypotension and arrhythmia[98], in particular hypokalemia might affect the release of norepinephrine or otherwise impair autonomic reflexes.
These conditions are associated to both the cases of SAP(0) greater than or equal to 140 mmgH and $115 \leq SAP(0) \leq 140$ mmHg.
For $SAP(0) \geq 115$ mmHg the evaluation of pressure is considered sufficient to a risk of IDH onset.
The multiparameter criterion thus defined has been able to identify the 98.55% of sessions with hypotension as defined by IDH-D and with a percentage of 24.24% of the reported false positives.
This assumptions shows how the application of a multiple combined criteria, rather than a single criterion lead to better performances in terms of reliability of the IDH prediction.
However percentage of false positives, i.e. alarms that the system would produce on the basis of patient information, set at the beginning of session, it's anyway high
One possible interpretation of these results could be due to the fact that session that shows the predialysis conditions, leading to hypotension, but finally the compensatory mechanisms occurs in order to avoid the onset of hypotension.
Furthermore clinical intervention by the nurses could occur during the session and vanish the progression through an hypotensive state.

.

7.5 Machine Learning Approach

A general overview of the results shows that SVM models outperform the RF and ANN ones in all the five cases.
This consideration highlights, how SVM kernel non-linearity, used for SVM modelling perfectly adapts to the prediction problem complexity, and provides reliable results almost regardless from the size or composition of training data[236].
Particularly the best overall accuracy has been obtained by SVM on Dataset D and E(e.g. overall accuracy for SVM model: 92.50% ± 5.02% and 92.93% ± 4.38%, respectively): these datasets have been rebalanced through minority class oversampling with replacement and majority class down sampling[231].
A further analysis highlights that, although all the considered parameters remain quite similar, ANN models reach better performance when developed over the bigger datasets (i.e. Dataset A Tab. 5 , Dataset B Tab. 6 , Dataset C Tab. 7), while RF models are able to guarantee much higher AUC values when trained over smaller sized datasets (i.e. Dataset D Tab. 8 , Dataset E Tab. 9).
This could be ascribed to the Random Forest capability of growing efficiently even on less numerous training sets. On the other hand, a high data availability seems to benefit the backpropagation algorithm used in Artificial Neural Network training.
A gold standard for the proposed applications in nephrology is hardly identifiable. Generally, given the high variety of studied pathologies and diseases, the performance of such models is highly variable.
Referring particularly to IDH prevention, without focusing on a data mining approach, few relevant studies, principally based on real-time PPG and ECG signals, were found [68],[237][238]but they refer to the identification of IDH onset during the therapy.
Trying to qualitatively compare the performances of the machine learning approach with those of the intra-dialysis PPG and ECG-based predictors, the here proposed predictor seems to be characterized by higher, and more generalizable, overall accuracy and AUC values.
Specifically, in Sandberg et al. [239] have been achieved 0.93 (95% confidence interval 0.61-1.00) and 0.71 (95% confidence interval 0.56-0.80) AUC values for acute symptomatic and symptomatic IDH prediction respectively, while in [Sandberg et al. 2013] were reached 100% sensitivity and 93% specificity in predicting acute symptomatic IDH, and 71% sensitivity and 50% specificity in predicting symptomatic IDH.
Furthermore, the machine learning predictor shows higher accuracy even if compared with J-index. J allows in fact identifying at the beginning of the session the 77% of the IDH events, even if asymptomatic, as considered by the IDH-D Dialysis Criteria. Averaged sensitivity and specificity were respectively 77% and 73%, lower than those here obtained by the best performance of SVM on Dataset and in general by the overall performances through machine learning algorithms.
Compared to the J-index analysis, it can be considered that the Machine Learning estimation has been performed only over Dataset 2: this implies that the intra-subject variability should be underestimated on the prediction done by machine learning , and thus that the performances of the J index and the Machine Learning algorithms could not be compared and that naturally Machine Learning algorithms brings to better performances.
However, the intra-subject variability could be considered as part the single example variability (that is referred to the single session on Dataset 2), and thus stands in the features space. It does affect not affect indeed the true error related to the prediction.
As boot the techniques – J index and address the prediction – address the same binary classification problem (IDH, noIDH), considering the same feature space (the influencing factors for each session), their performances can be compared.

It has also to be taken into consideration that PPG and ECG data are not available in the actual clinical practice and that their use will imply nurses extra-work, a barrier to the routinely use of the proposed strategies, while the predictive strategies proposed in this work are based over easy-access and non-invasive measures, determining a more effective IDH offline prediction tool for both patients comfort and clinical usefulness.
The applied algorithm could achieve better performance through further parameters optimizations: more computational costing procedures (e.g. evolutionary or quadratic optimization)[240] may lead to better parameter values choices. For SMOTE balanced dataset, where artificial data are produced , better perfomances can be obtained returning of the learner in presence of new set of data: as Snoeck et el suggest, a possible solution could be the use of Bayesian algorithms[241].

Chapter 8 – Conclusions

Intradialysis Hypotension is the most common adverse complication during hemodialysis.
Its early prediction and prevention represent an important target for the development of optimized and personalized clinical protocols that allow to preserve the patient's medical condition on dialysis over time.
In clinical practice, they are often only recognized once manifested.
The multifactorial nature of IDH events onset requires the use of a multivariate approach to deal with.
Furthermore, where the IDH does not determine the occurrence of recognizable symptoms in the patient, they cannot be identified.
Currently there is a lack of clinical predictive instruments that could allow clinicians to preventively manage the IDH onset.
Thus, the current study has been focused on finding innovative clinical predictors of IDH events at the intra-dialysis and the pre-dialysis phase, bythe analysis and collection of a great amount of data.
All the analysis have been executed within the Dialysis Project (Dialysis therapy between Italy and Switzerland), a multicentric study addressed defining protocols and standards to improve the dialysis therapies in the more efficacious and personalized way possible.
The DialysIS Project, has involved 4 clinical centers between Lombardy and Switzerland that has provided clinical data of patient on HD and HDF treatment.
All the data acquired has been stored, into a multilevel common data storage system that as allowed to share clinical data among the project partners overcoming the routinely problem of data interoperability among dialysis facilities[116].
The common platform has been built using a Federated Database System (FDBS) approach [145] by the implementation of the Dialysis Data Infrastructure (DDI), a unique multilevel standardized data structure supported by a Matlab® library, and the Dialysis MATlib (DM) a MATLAB-based mining library (Dialysis MATlib) that was able to convert, harmonize and query the raw data coming from the clinical units [1961] by an ETL logic.
The development of a common platform for data gathering was a necessary step to make possible, in a simple way and with appropriate statistical significance, the analysis of a large amount of data in order find out IDH predictors from the available data.
Furthermore the multilevel DR structure has allowed the possibility to perform further analysis both at center and patient scale.
Definitively, the collected data, referred to 818 session performed by 150 patients and constitute the basis to develop the predictors of hypotensions.
The predictors particularly have been developed by the data analysis performed Using two approaches, a classical inferential statistical one and a machine learning strategy.
The conducted inferential statistical analysis, highlighted the recruited patients pool present an high heterogeneity and it has been difficult to identify specific comparable trends between the parameters are and clinical categories.
During the statistical analysis a new definition of hypotension has been used.
The definition was based on the elaboration of a set of criteria extracted from a literature study, that has been modified by a confrontation with the clinicians involved in the project.
This indeed reflected the wide heterogeneity and the high peculiar patient-response, even considering the possible and frequent errors of measurement during the acquisition phases.

Considering both, the intra-dialysis and the pre-dialysis phase, the statistical analysis, it is possible to highlight that the MAP (Mean Arterial Pressure), the Weight Gain and the concentration of electrolytes in blood (mainly Potassium) influence the onset of hypotension.
These results can be hypothesized to be conduced to a physiological interpretation.
As hypotensionmain occurs when compensatory mechanisms for hypovolemia are overwhelmed by excessive fluid removal: each one of of this "influencing factor" can be considered as a "sensor variable" of one or more cardiovascular control mechanism (c.f.r Par. 2.3) that intervene or faults during the dialysis ultrafiltration.
On this assumption, and considering the multifactorial nature of IDH, multivariate criteria has been defined for both the intra-dialysis and predialysis phase.
Particularly, the definition of the J indexes (J_1 and J_2) for the pre-dialysis phase and the multiparameter criterion for the intradialysis phase has been the main outcomes of the inferential statistical analysis
J is a multifactorial index, that can be calculated at the beginning of each session, through non-invasive measurements and gives the clinician useful information on the probability of IDH onset during the specific treatment.
This is a really important feature of the developed index in order to provide a personalization and an improvement of the dialysis therapy.
The index has been proposed in two versions.
The average sensitivity and specificity of the prediction are respectively 77 % and 73% when $J_{1th}=1$[195].
This value can be improved but its set a good start in order to provide clinical indicator of the IDH onset even better performance for the index could be obtained.
Possible future improvements that will grant a better forecasting accuracy of the J index should include the automatic update of the registration information on the pre-dialysis patient.
In this way the system will take into account also the intra-subject variability of the influencing parameters over the time due to the changes of subject conditions at the beginning of the session.
Other improvement could lie in considering higher sampling frequencies for the HR, and more sample taken at the beginning of the treatment.
In this case the sample taken at the start session might be particularly affected by the patient intra-variability, while repeated measurement in a few minutes could lead to have a less disperse evaluation of the patient status.
Considering the statistical analysis on the intra-dialysis period, a multiparameter criteria has been developed.
The multiparameter criteria, address the problem with a similar approach of the J indexes. It led to the identification of almost all the sessions with hypotension (as defined by IDH D) (98,55%), indicating an acceptable rate of false positives (24,24%).
Besides the inferential statistical analysis, a machine learning approach to IDH prediction has been investigated to assess the risk of IDH in the predialysis phase, testing three different learners algorithms have been compared: Random Forest, Artificial Neural Network and Support Vector Machine.
The tested algorithms showed high prediction performances in terms of accuracy and precision, even higher if compared with the J index prediction.
Among the tested algorithm, Support Vector Machine resulted the overall best one.
During the dialysis treatment, the changes in concentration of intracellular and extracellular electrolytes may increase susceptibility to arrhythmias.
It can be concluded the as the nature of IDH is multivariate, and the datasets showed a great variability, machine learning algorithms offers valuable tool

capable to predict IDH onset, even high data variability and cardinality.
Despite the limits highlighted in the previous section, the comparison with similar studies [237] allow to consider the machine learning, a valuable data oriented tool for IDH dialysis prediction.
In conclusion the J index. The multivariate criteria and machine learning algorithms provides the clinicians useful instruments for a better management and prediction of hypotension onset during dialysis treatment.

References

2. Hall E. J., Guyton and Hall textbook of medical physiology. Philadelphia, : Saunders Elsevier, 2011.
3. Baldissera F., Porro C.A. Fisiologia e biofisica medica, terza edizione, Poletto editore, 2005
4. Bronzino J.D.. The Biomedical Engineering Handbook, chapter 130: Artificial Kidney. CRC Press, 1999.
5. Boulpaep, E. L., Boron, W. F., Caplan, M. J., Cantley, L., Igarashi, P., Aronson, P. S., & Moczydlowski, E. G. (2009). Medical Physiology a Cellular and Molecular Approach. *Signal Transduct*, *48*, 27.
6. Costantino M.L. , Dispense del corso Sistemi di supporto alla vita. Politecnico di Milano, AA 2013-2014.
7. Netter, F. H. (2015). *Netter Atlante di anatomia umana*. Edra Masson.
8. Gerich, J. E. (2010). Role of the kidney in normal glucose homeostasis and in the hyperglycaemia of diabetes mellitus: therapeutic implications. *Diabetic Medicine*, *27*(2), 136-142.
9. Birn, H., & Christensen, E. I. (2006). Renal albumin absorption in physiology and pathology. *Kidney international*, *69*(3), 440-449.
10. Carlsen, O., & Nathan, E. (1987). Renal fraction of cardiac output cleared of radioactive indicator in 123iodine-hippuran gamma camera renography. Clinical Physiology and Functional Imaging, 7(2), 165-171.
11. Shih, C. J., Chao, P. W., Ou, S. M., & Chen, Y. T. (2017). Long-Term Risk of Cardiovascular Events in Patients With Chronic Kidney Disease Who Have Survived Sepsis: A Nationwide Cohort Study. *Journal of the American Heart Association*, *6*(2), e004613.
12. Dirks J, Remuzzi G, Horton S, et al. Diseases of the Kidney and the Urinary System. In: Jamison DT, Breman JG, Measham AR, et al., editors. Disease Control Priorities in Developing Countries. 2nd edition. Washington (DC): The International Bank for Reconstruction and Development / The World Bank; 2006. Chapter 36.
13. Gutch, C. F., & Stoner, M. H. (1980). *Review of Hemodialysis for Nurses and Dialysis Personnel* (Vol. 80, No. 11, p. 2102). LWW.
14. Lote, C. J., & Lote, C. J. (1994). *Principles of renal physiology*. London: Chapman & Hall.
15. Saltzman, W. M. (2009). *Biomedical engineering: bridging medicine and technology*. Cambridge University Press.
16. Thomas, R., Kanso, A., & Sedor, J. R. (2008). Chronic kidney disease and its complications. *Primary care: Clinics in office practice*, *35*(2), 329-344.
17. O'Connor, N. R., & Corcoran, A. M. (2012). End-stage renal disease: symptom management and advance care planning. *American family physician*, *85*(7).
18. Davenport, A. (2009, May). Can advances in hemodialysis machine technology prevent intradialytic hypotension?. In *Seminars in dialysis* (Vol. 22, No. 3, pp. 231-236). Blackwell Publishing Ltd.

19. Tong, A., Budde, K., Gill, J., Josephson, M. A., Marson, L., Pruett, T. L. & Wong, G. (2016). Standardized outcomes in nephrology-transplantation: a global initiative to develop a core outcome set for trials in kidney transplantation. *Transplantation Direct*, *2*(6).
20. Elmoazzen, H. Y., Elliott, J. A., & McGann, L. E. (2009). Osmotic transport across cell membranes in nondilute solutions: a new nondilute solute transport equation. *Biophysical journal*, *96*(7), 2559-2571.
21. Report SIN-RIDT 2010, anno 2008, 51°Congresso della Società italiana di Nefrologia
22. Hoenich, N. A. (2008). Membranes and filters for haemodiafiltration. In *Hemodiafiltration* (Vol. 158, pp. 57-67). Karger Publishers.
23. Martello, M., & Di Luca, M. (2012). Acetate Free Biofiltration. *G. Ital. Nefrol*, *29*(S55), s62-s71.
24. Thomas, R., Kanso, A., & Sedor, J. R. (2008). Chronic kidney disease and its complications. *Primary care: Clinics in office practice*, *35*(2), 329-344.
25. Ledebo, I., & Blankestijn, P. J. (2010). Haemodiafiltration—optimal efficiency and safety. *NDT plus*, *3*(1), 8-16.
26. Levey, A. S., Coresh, J., Balk, E., Kausz, A. T., Levin, A., Steffes, M. W.& Eknoyan, G. (2003). National Kidney Foundation practice guidelines for chronic kidney disease: evaluation, classification, and stratification. *Annals of internal medicine*, *139*(2), 137-147.
27. Basile, C. (2001). Should relative blood volume changes be routinely measured during the dialysis session?. *Nephrology Dialysis Transplantation*, *16*(1), 10-12.
28. Palmer, B. F., & Henrich, W. L. (2008). Recent advances in the prevention and management of intradialytic hypotension. *Journal of the American Society of Nephrology*, *19*(1), 8-11.
29. Schreiber MJ Jr. Clinical dilemmas in dialysis: managing the hypotensive patient. Setting the stage. Am J Kidney Dis 2001;. 38: S1–S10.
30. Shimizu, K., Kurosawa, T., & Sanjo, T. (2008). Effect of hyperosmolality on vasopressin secretion in intradialytic hypotension: a mechanistic study. *American Journal of Kidney Diseases*, *52*(2), 294-304.
31. Charra, B., Chazot, C., & Laurent, G. U. Y. (1999). Hypertension/hypotension in dialysis. *Kidney international*, *55*(3), 1128-1130.
32. Mancini, E., Mambelli, E., Irpinia, M., Gabrielli, D., Cascone, C., Conte, F., & Dal Canton, A. (2007). Prevention of dialysis hypotension episodes using fuzzy logic control system. *Nephrology dialysis transplantation*, *22*(5), 1420-1427.
33. Bayya, A., Rubinger, D., Linton, D. M., & Sviri, S. (2011). Evaluation of intradialytic hypotension using impedance cardiography. *International urology and nephrology*, *43*(3), 855-864.
34. Hoenich N., Katopodis K. (2002) Clinical characterization of a new polymeric membrane for use in renal replacement therapy. Biomaterials; vol 23, pp 3853–3858.
35. Shoji, T., Tsubakihara, Y., Fujii, M., & Imai, E. (2004). Hemodialysis-associated hypotension as an independent risk factor for two-year mortality in hemodialysis patients. *Kidney international*, *66*(3), 1212-1220.
36. Tislér, A., Akócsi, K., Borbás, B., Fazakas, L., Ferenczi, S., Görögh, S., & Tóth, E. (2003). The effect of frequent or occasional dialysis-associated hypotension on survival of patients on maintenance haemodialysis. *Nephrology Dialysis Transplantation*, *18*(12), 2601-2605.

37. Schreiber, M. J. (2001). Clinical case-based approach to understanding intradialytic hypotension. *American journal of kidney diseases*, *38*(4), S37-S47.
38. Donauer, J. (2004, September). Hemodialysis-Induced Hypotension: Impact of Technologic Advances. In *Seminars in dialysis* (Vol. 17, No. 5, pp. 333-335). Blackwell Science Inc.
39. Ahlstrom, C., Johansson, A., Uhlin, F., Länne, T., & Ask, P. (2005). Noninvasive investigation of blood pressure changes using the pulse wave transit time: a novel approach in the monitoring of hemodialysis patients. *Journal of Artificial Organs*, *8*(3), 192-197.
40. Nitzan, M., Babchenko, A., Khanokh, B., & Landau, D. (1998). The variability of the photoplethysmographic signal-a potential method for the evaluation of the autonomic nervous system. *Physiological measurement*, *19*(1), 93.
41. Beige, J., Sone, J., Sharma, A. M., Rudwaleit, M., Offermann, G., Distler, A., & Preuschof, L. (2000). Computational analysis of blood volume curves and risk of intradialytic morbid events in hemodialysis. *Kidney international*, *58*(4), 1805-1809.
42. Laude, D., Elghozi, J. L., Girard, A., Bellard, E., Bouhaddi, M., Castiglioni, P.,& Janssen, B. (2004). Comparison of various techniques used to estimate spontaneous baroreflex sensitivity (the EuroBaVar study). *American Journal of Physiology-Regulatory, Integrative and Comparative Physiology*, *286*(1), R226-R231.
43. Casagrande G. (2007) "Hydro - Electrolytic Hydro-Electrolytic Equilibrium and Cardiac Mechanics Alterations in Hemodialysis Patients."
44. Rubinger, D., Backenroth, R., & Sapoznikov, D. (2013, May). Sympathetic nervous system function and dysfunction in chronic hemodialysis patients. In Seminars in dialysis (Vol. 26, No. 3, pp. 333-343).
45. Sulowicz, W., & Radziszewski, A. (2006). Pathogenesis and treatment of dialysis hypotension. Kidney International, 70, S36-S39.
46. Raja, R. M., & Po, C. L. (1994). Plasma Refilling During Hemodialysis with Decreasing Ultrafiltration: Influence of Dialysate Sodium. *ASAIO journal*, *40*(3), M423-M425.
47. Mark, a L. (1983). The Bezold-Jarisch reflex revisited: clinical implications of inhibitory reflexes originating in the heart. *Journal of the American College of Cardiology*, *1*(1), 90–102.
48. Dasselaar, J. J., Huisman, R. M., de Jong, P. E., & Franssen, C. F. (2005). Measurement of relative blood volume changes during haemodialysis: merits and limitations. Nephrology Dialysis Transplantation, 20(10), 2043-2049.
49. Teng, J., Tian, J., Lv, W. L., Zhang, X. Y., Zou, J. Z., Fang, Y., ... & Ding, X. Q. (2015). Inappropriately elevated endothelin-1 plays a role in the pathogenesis of intradialytic hypertension. Hemodialysis International, 19(2), 279-286.
50. Bradshaw W., (2011). Intradialytic hypotension and blood volume and blood temperature monitoring, *Nephrology,* no. 16, pp. 13-18,
51. Leung, K. C., Quinn, R. R., Ravani, P., & MacRae, J. M. (2014). Ultrafiltration biofeedback guided by blood volume monitoring to reduce intradialytic hypotensive episodes in hemodialysis: study protocol for a randomized controlled trial. Trials, 15, 483. [48--27]
52. Santoro, A., Mancini, E., Paolini, F., Cavicchioli, G., Bosetto, A., & Zucchelli, P. (1998). Blood volume regulation during hemodialysis. American journal of kidney diseases, 32(5), 739-748.
53. Stiller, S., Bonnie-Schorn, E., Grassmann, A., Uhlenbusch-Körwer, I., & Mann, H. (2001, September). A critical review of sodium profiling

for hemodialysis. In *Seminars in dialysis* (Vol. 14, No. 5, pp. 337-347). Blackwell Science Inc.

54. Moret, K., Aalten, J., van den Wall Bake, W., Gerlag, P., Beerenhout, C., van der Sande, F., ... & Kooman, J. (2006). The effect of sodium profiling and feedback technologies on plasma conductivity and ionic mass balance: a study in hypotension-prone dialysis patients. *Nephrology Dialysis Transplantation*, *21*(1), 138-144.
55. Davenport, A. (2009, May). Can advances in hemodialysis machine technology prevent intradialytic hypotension?. In *Seminars in dialysis* (Vol. 22, No. 3, pp. 231-236). Blackwell Publishing Ltd.
56. Ion Titapiccolo, J., Ferrario, M., Garzotto, F., Cruz, D., Moissl, U., Tetta, C., … Cerutti, S. (2010). Relative blood volume monitoring during hemodialysis in end stage renal disease patients. *Conference Proceedings :* ... Annual International Conference of the IEEE Engineering in Medicine and Biology Society. IEEE Engineering in Medicine and Biology Society. Annual Conference, *2010*, 5282–5.
57. Eftimovska–Otovic, N., Stojceva-Taneva, O., Grozdanovski, R., & Stojcev, S. (2016). Clinical Effects of Standard and Individualized Dialysate Sodium in Patients on Maintenance Hemodialysis. *Open Access Macedonian Journal of Medical Sciences*, *4*(2), 248.
58. Stiller, S., Bonnie-Schorn, E., Grassmann, A., Uhlenbusch-Körwer, I., & Mann, H. (2001, September). A critical review of sodium profiling for hemodialysis. In *Seminars in dialysis* (Vol. 14, No. 5, pp. 337-347). Blackwell Science Inc.
59. Selby, N. M., & McIntyre, C. W. (2006). A systematic review of the clinical effects of reducing dialysate fluid temperature. Nephrology Dialysis Transplantation, 21(7), 1883-1898.
60. Moret, K., Aalten, J., van den Wall Bake, W., Gerlag, P., Beerenhout, C., van der Sande, F., ... & Kooman, J. (2006). The effect of sodium profiling and feedback technologies on plasma conductivity and ionic mass balance: a study in hypotension-prone dialysis patients. Nephrology Dialysis Transplantation, 21(1), 138-144.
61. Locatelli, F., Manzoni, C., Pontoriero, G., Cavalli, A., Di Filippo, S., & Azar, A. (2013). Ionic Dialysance and Conductivity Modeling. Modeling and Control of Dialysis Systems, 811-865.
62. Davenport, A. (2011). Using dialysis machine technology to reduce intradialytic hypotension. Hemodialysis International, 15(S1), S37-S42.
63. van der Sande, F. M., Kooman, J. P., & Leunissen, K. M. (2000). Intradialytic hypotension—new concepts on an old problem. Nephrology Dialysis Transplantation, 15(11), 1746-1748.
64. Santoro A. On-line monitoring (Editorial). Nephrol Dial Transplant 1995; 10: 615-8
65. Locatelli, F., Di Filippo, S., Manzoni, C., Corti, M., Andrulli, S., & Pontoriero, G. (1995). Monitoring sodium removal and delivered dialysis by conductivity. The International journal of artificial organs, 18(11), 716-721.
66. Daugirdas, J. T., & Ing, T. S. (2007). Handbook of dialysis. Philadelphia: Lippincott Williams & Wilkins.
67. Selby, N. M., & McIntyre, C. W. (2007, May). The acute cardiac effects of dialysis. In Seminars in dialysis (Vol. 20, No. 3, pp. 220-228). Blackwell Publishing Ltd.
68. Sornmo, L., Sandberg, F., Gil, E., & Solem, K. (2012). Noninvasive techniques for prevention of intradialytic hypotension. IEEE reviews in biomedical engineering, 5, 45-59.

69. Burton, J. O., Korsheed, S., Grundy, B. J., & McIntyre, C. W. (2008). Hemodialysis-induced left ventricular dysfunction is associated with an increase in ventricular arrhythmias. Renal failure, 30(7), 701-709.
70. Mandolfo, S., Farina, M., & Imbasciati, E. (1995). Bioelectrical impedance and hemodialysis. The International journal of artificial organs, 18(11), 700-704.
71. Kyle, U. G., Bosaeus, I., De Lorenzo, A. D., Deurenberg, P., Elia, M., Gómez, J. M., ... & Scharfetter, H. (2004). Bioelectrical impedance analysis—part I: review of principles and methods. Clinical nutrition, 23(5), 1226-1243.
72. Foster, K. R., & Lukaski, H. C. (1996). Whole-body impedance--what does it measure?. The American journal of clinical nutrition, 64(3), 388S-396S.
73. Selby, N. M., Burton, J. O., Chesterton, L. J., & McIntyre, C. W. (2006). Dialysis-induced regional left ventricular dysfunction is ameliorated by cooling the dialysate. Clinical Journal of the American Society of Nephrology, 1(6), 1216-1225.
74. Casagrande, G., Teatini, U., Romei, L. G., Miglietta, F., Fumero, R., & Costantino, M. L. (2007). A new method to evaluate patient characteristic response to ultrafiltration during hemodialysis. The International journal of artificial organs, 30(5), 377-384.
75. Kyriazis, J., Kalogeropoulou, K., Bilirakis, L., Smirnioudis, N., Pikounis, V., Stamatiadis, D., & Liolia, E. (2004). Dialysate magnesium level and blood pressure. Kidney international, 66(3), 1221-1231.
76. Burton, J. O., Korsheed, S., Grundy, B. J., & McIntyre, C. W. (2008). Hemodialysis-induced left ventricular dysfunction is associated with an increase in ventricular arrhythmias. Renal failure, 30(7), 701-709.
77. Chebbi, R. (2015). Dynamics of blood flow: modeling of the Fåhræus–Lindqvist effect. *Journal of biological physics*, *41*(3), 313-326.
78. Andrulli, S., Colzani, S., Mascia, F., Lucchi, L., Stipo, L., Bigi, M. C., & Locatelli, F. (2002). The role of blood volume reduction in the genesis of intradialytic hypotension. American journal of kidney diseases, 40(6), 1244-1254.
79. Mitra, S., Chamney, P., Greenwood, R., & Farrington, K. (2017). Linear decay of relative blood volume during ultrafiltration predicts hemodynamic instability. American Journal of Kidney Diseases, 40(3),.
80. Barnas, M. G., Boer, W. H., & Koomans, H. A. (1999). Hemodynamic patterns and spectral analysis of heart rate variability during dialysis hypotension. Journal of the American Society of Nephrology, 10(12), 2577-2584.
81. Floras, J. S., & Ponikowski, P. (2015). The sympathetic/parasympathetic imbalance in heart failure with reduced ejection fraction. European heart journal.
82. Doret, M., Spilka, J., Chudáček, V., Gonçalves, P., & Abry, P. (2015). Fractal analysis and hurst parameter for intrapartum fetal heart rate variability analysis: a versatile alternative to frequency bands and LF/HF ratio. PloS one, 10(8).
83. Solem, K., Nilsson, A., & Sornmo, L. (2004, September). Detection of hypotension during hemodialysis using the ECG. In Computers in Cardiology, 2004 (pp. 717-720). IEEE..
84. Solem, K., Nilsson, A., & Sörnmo, L. (2006). An electrocardiogram-based method for early detection of abrupt changes in blood pressure during hemodialysis. ASAIO journal, 52(3), 282-290.
85. Santoro, A., Mancini, E., Gaggi, R., Cavalcanti, S., Severi, S., Cagnoli, L., & Mercadal, L. (2005). Electrophysiological response to dialysis:

the role of dialysate potassium content and profiling. In Cardiovascular Disorders in Hemodialysis (Vol. 149, pp. 295-305). Karger Publishers.
86. 3-3043. Hemodialysi-Induced Left Ventricular Dysfunction Is associated with an Increase in Ventricular Arrhythmias. Burton, James O, et al., et al. 7, 2008, Renal failure, Vol. 30, p. 701-709
87. Solem, K., Laguna, P., & Sornmo, L. (2006). An efficient method for handling ectopic beats using the heart timing signal. IEEE transactions on biomedical engineering, 53(1), 13-20..
88. Sörnmo, L., & Laguna, P. (2005). Bioelectrical signal processing in cardiac and neurological applications (Vol. 8). Academic Press.
89. Schmidt, G., Malik, M., Barthel, P., Schneider, R., Ulm, K., Rolnitzky, L.,& Schömig, A. (1999). Heart-rate turbulence after ventricular premature beats as a predictor of mortality after acute myocardial infarction. The Lancet, 353(9162), 1390-1396..
90. Bauer, A., Malik, M., Schmidt, G., Barthel, P., Bonnemeier, H., Cygankiewicz, I., ... & Schneider, R. (2008). Heart rate turbulence: standards of measurement, physiological interpretation, and clinical use: International Society for Holter and Noninvasive Electrophysiology Consensus. Journal of the American College of Cardiology, 52(17), 1353-1365.
91. Yamanaka, N., Aoyama, T., Ikeda, N., Higashihara, M., & Kamata, K. (2005). Characteristics of heart rate variability entropy and blood pressure during hemodialysis in patients with end-stage renal disease. Hemodialysis International, 9(3), 303-308.
92. Di Rienzo, M., Castiglioni, P., Mancia, G., Pedotti, A., & Parati, G. (2001). Advancements in estimating baroreflex function. IEEE Engineering in Medicine and Biology Magazine, 20(2), 25-32.
93. Chesterton, L. J., Selby, N. M., Burton, J. O., & McINTYRE, C. W. (2009). Cool dialysate reduces asymptomatic intradialytic hypotension and increases baroreflex variability. Hemodialysis International, 13(2), 189-196.
94. Chesterton, L. J., Selby, N. M., Burton, J. O., Fialova, J., Chan, C., & McIntyre, C. W. (2010). Categorization of the hemodynamic response to hemodialysis: the importance of baroreflex sensitivity. Hemodialysis International, 14(1), 18-28.
95. Hernando, D., Bailón, R., Laguna, P., & Sörnmo, L. (2011, September). Heart rate variability during hemodialysis and its relation to hypotension. In Computing in Cardiology, 2011 (pp. 189-192). IEEE.
96. Laude, D., Elghozi, J. L., Girard, A., Bellard, E., Bouhaddi, M., Castiglioni, P., ... & Janssen, B. (2004). Comparison of various techniques used to estimate spontaneous baroreflex sensitivity (the EuroBaVar study). American Journal of Physiology-Regulatory, Integrative and Comparative Physiology, 286(1), R226-R231.
97. Diercks, D. B., Shumaik, G. M., Harrigan, R. A., Brady, W. J., & Chan, T. C. (2004). Electrocardiographic manifestations: electrolyte abnormalities. The Journal of emergency medicine, 27(2), 153-160.
98. Brancati M, Coluccia V, Schiavoni G. (2011). Il potassio nella pratica clinica. Cardiology Science; (9)13-20
99. Blumberg, A., Roser, H. W., Zehnder, C., & Müller-Brand, J. (1997). Plasma potassium in patients with terminal renal failure during and after haemodialysis; relationship with dialytic potassium removal and total body potassium. Nephrology Dialysis Transplantation, 12(8), 1629-1634.
100. Paleari, R., Ivaldi, G., Leone, D., Amato, A., & Mosca, A. (2009). Utilità clinica della misura dell'emoglobina fetale. biochimica clinica, 33(6), 527.

101. Shapira, O. M., & Bar-Khayim, Y. (1992). ECG changes and cardiac arrhythmias in chronic renal failure patients on hemodialysis. Journal of electrocardiology, 25(4), 273-279..
102. Di Iorio, B., & Bellasi, A. (2013). QT interval in CKD and haemodialysis patients. Clinical kidney journal, sfs183.
103. Kyriazis, J., Kalogeropoulou, K., Bilirakis, L., Smirnioudis, N., Pikounis, V., Stamatiadis, D., & Liolia, E. (2004). Dialysate magnesium level and blood pressure. Kidney international, 66(3), 1221-1231..
104. 3-54 Barnas, M. G., Boer, W. H., & Koomans, H. A. (1999). Hemodynamic patterns and spectral analysis of heart rate variability during dialysis hypotension. Journal of the American Society of Nephrology, 10(12), 2577-2584.
105. Hoyer, D., Schmidt, K., Bauer, R., Zwiener, U., Kohler, M., Luthke, B., & Eiselt, M. (1997). Nonlinear analysis of heart rate and respiratory dynamics. IEEE engineering in medicine and biology magazine, 16(1), 31-39.
106. Cupisti, A., Galetta, F., Caprioli, R., Morelli, E., Tintori, G. C., Franzoni, F., ... & Barsotti, G. (1999). Potassium removal increases the QTc interval dispersion during hemodialysis. Nephron, 82(2), 122-126.
107. Locati, E. H., Bagliani, G., StrambaBadiale, M., Saronio, P., & Timio, M. (1997, February). Increased QT interval dispersion following post-dialytic decrease of potassium and magnesium: A model to study the repolarization changes associated to electrolyte abnormalities. In JOURNAL OF THE AMERICAN COLLEGE OF CARDIOLOGY (Vol. 29, No. 2, pp. 7376-7376). 655 AVENUE OF THE AMERICAS, NEW YORK, NY 10010: ELSEVIER SCIENCE INC.
108. Akiyama, T., Batchelder, J., Worsman, J., Moses, H. W., & Jedlinski, M. (1989). Hypocalcemic torsades de pointes. Journal of Electrocardiology, 22(1), 89–92.
109. Mayet, J., Shahi, M., McGrath, K., Poulter, N. R., Sever, P. S., Foale, R. A., & Thom, S. A. M. (1996). Left ventricular hypertrophy and QT dispersion in hypertension. Hypertension, 28(5), 791-796.
110. Rombola, G., Colussi, G., De Ferrari, M. E., Frontini, A., & Minetti, L. (1992). Cardiac arrhythmias and electrolyte changes during haemodialysis. Nephrology Dialysis Transplantation, 7(4), 318-322..
111. Näppi, S. E., Virtanen, V. K., Saha, H. H., Mustonen, J. T., & Pasternack, A. I. (2000). QT c dispersion increases during hemodialysis with low-calcium dialysate. Kidney international, 57(5), 2117-2122.
112. Floccari, F., Aloisi, E., Nostro, L., Caccamo, C., Crisafulli, A., Barilla, A& Frisina, N. (2004). QTc interval and QTc dispersion during haemodiafiltration. Nephrology, 9(6), 335-340..
113. Redaelli, B. (1996). Electrolyte modelling in haemodialysis—potassium. Nephrology Dialysis Transplantation, 11(supp2), 39-41.
114. Näppi, S. E., Virtanen, V. K., Saha, H. H., Mustonen, J. T., & Pasternack, A. I. (2000). QT c dispersion increases during hemodialysis with low-calcium dialysate. Kidney international, 57(5), 2117-2122.
115. Hemmett, J., & McIntyre, C. W. (2017, January). A Dialysis Patient's Choice and a Nephrologist's Obligation: The Need to Understand and Value the Patient's Perspective. In Seminars in Dialysis (Vol. 30, No. 1, pp. 3-5).

116. Vito, D., Casagrande, G., Bianchi, C., & Costantino, M. L. (2016, May). An interoperable common storage system for shared dialysis clinical data. In Student Conference (ISC), 2016 IEEE EMBS International (pp. 1-4). IEEE.
117. Hudson, D. L., Cohen, M. E., & Hudson, S. E. (2015, August). Development of health diagnostics based on personalized medical models. In Engineering in Medicine and Biology Society (EMBC), 2015 37th Annual International Conference of the IEEE (pp. 1413-1416). IEEE.
118. Vito, D., Casagrande, G., Bianchi, C., & Costantino, M. L. (2015, August). How to extract clinically useful information from large amount of dialysis related stored data. In Engineering in Medicine and Biology Society (EMBC), 2015 37th Annual International Conference of the IEEE (pp. 6812-6815). IEEE.
119. Vianello, M. (2013). Smart cities: gestire la complessità urbana nell'era di Internet (Vol. 1). Maggioli Editore.
120. 4-6 Legido-Quigley, H., Glinos, I., Baeten, R., & McKee, M. (2007). Patient mobility in the European Union. Bmj, 334(7586), 188-90.
121. Wismar, M., Palm, W., van Ginneken, E., Busse, R., Ernst, K., & Figueras, J. (2011). The Health Service Initiative: supporting the construction of a framework for cross-border health care. Cross-border health care in the European Union,
122. Footman, K., Knai, C., Baeten, R., Ketevan, G., & McKee, M. (2014). Cross Border Health Care in Europe. *Copenaghen: Who Regional Office for Europe and European Observatory on Health Systems and Policie*
123. Koivusalo, M. (2015). Health Systems and Policy Space for Health in the Context of European Union Trade Policies. In *Services of General Interest Beyond the Single Market* (pp. 371-396). TMC Asser Press.
124. Malin, B. A., El Emam, K., & O'keefe, C. M. (2013). Biomedical data privacy: problems, perspectives, and recent advances.
125. Kautsch, M., Lichoń, M., & Matuszak, N. (2016). Setting the scene for the future: implications of key legal regulations for the development of e-health interoperability in the EU. The International Journal of Health Planning and Management.
126. Kushida, C. A., Nichols, D. A., Jadrnicek, R., Miller, R., Walsh, J. K., & Griffin, K. (2012). Strategies for de-identification and anonymization of electronic health record data for use in multicenter research studies. Medical care, 50, S82-S101.
127. Fernández-Alemán, J. L., Señor, I. C., Lozoya, P. Á. O., & Toval, A. (2013). Security and privacy in electronic health records: A systematic literature review. Journal of biomedical informatics, 46(3), 541-562.
128. Joly, Y., Dyke, S. O., Knoppers, B. M., & Pastinen, T. (2016). Are Data Sharing and Privacy Protection Mutually Exclusive?. Cell, 167(5), 1150-1154.
129. Allard, T., Anciaux, N., Bouganim, L., Guo, Y., Le Folgoc, L., Nguyen, B., ... & Yin, S. (2010). Secure personal data servers: a vision paper. Proceedings of the VLDB Endowment, 3(1-2), 25-35.
130. Labrinidis, A., & Jagadish, H. V. (2012). Challenges and opportunities with big data. Proceedings of the VLDB Endowment, 5(12), 2032-2033.
131. Howe, D., Costanzo, M., Fey, P., Gojobori, T., Hannick, L., Hide, W& Twigger, S. (2008). Big data: The future of biocuration. Nature, 455(7209), 47-50.
132. Sargent, J. A. (2001). Identifying the Value of Computers in Dialysis Part II: Clinical Applications. *Nephrology news & issues*,
133. De Mauro, A., Greco, M., & Grimaldi, M. (2015, February). What is

big data? A consensual definition and a review of key research topics. In G. Giannakopoulos, D. P. Sakas, & D. Kyriaki-Manessi (Eds.), *AIP conference proceedings* (Vol. 1644, No. 1, pp. 97-104). AIP.

134. Sadler, J. H. (2006). Computers in Hemodialysis Facilities. Hemodialysis Horizon, Washington.
135. Malin, B. A., El Emam, K., & O'keefe, C. M. (2013). Biomedical data privacy: problems, perspectives, and recent advances.
136. Higham, D. J., & Higham, N. J. (2005). MATLAB guide. Society for Industrial and Applied Mathematics..
137. Tislér, A., Akócsi, K., Borbás, B., Fazakas, L., Ferenczi, S., Görögh, S., & Tóth, E. (2003). The effect of frequent or occasional dialysis-associated hypotension on survival of patients on maintenance haemodialysis. Nephrology Dialysis Transplantation, 18(12), 2601-2605.
138. Ketchersid, T. (2013). Big data in nephrology: friend or foe?. Blood purification, 36(3-4), 160-164.
139. Himss (2017). Himss Dictionary of Healthcare Information Technology Term, Acronyms and Organizations. CRC Press Book
140. Downey, A. S., & Olson, S. (Eds.). (2013). Sharing clinical research data: workshop summary. National Academies Press.
141. Cios, K. J., & Moore, G. W. (2002). Uniqueness of medical data mining. Artificial intelligence in medicine, 26(1), 1-24.
142. Sargent, J. A. (2001). Identifying the Value of Computers in Dialysis Part II: Clinical Applications. Nephrology news & issues, 2.
143. Wang, W., Tolk, A., & Wang, W. (2009, March). The levels of conceptual interoperability model: applying systems engineering principles to M&S. In Proceedings of the 2009 Spring Simulation Multiconference (p. 168). Society for Computer Simulation International.
144. Hammer M., McLeod D. (1979) "On the Architecture of Database Management Systems", Technical Report 79-4, Computer Science Department, University of Southern California, Los Angeles CA, April.
145. Heimbigner, D., & McLeod, D. (1985). A federated architecture for information management. ACM Transactions on Information Systems (TOIS), 3(3), 253-278.
146. Sheth, A. P., & Larson, J. A. (1990). Federated database systems for managing distributed, heterogeneous, and autonomous databases. ACM Computing Surveys (CSUR), 22(3), 183-236.
147. Alonso-Calvo, R., Perez-Rey, D., Paraiso-Medina, S., Claerhout, B., Hennebert, P., & Bucur, A. (2015). Enabling semantic interoperability in multi-centric clinical trials on breast cancer. Computer methods and programs in biomedicine, 118(3), 322-329.
148. Dumontier, M., Baker, C. J., Baran, J., Callahan, A., Chepelev, L., Cruz-Toledo, J., & Klassen, D. (2014). The Semantics cience Integrated Ontology (SIO) for biomedical research and knowledge discovery. Journal of biomedical semantics, 5(1), 14.
149. Golbreich, C., & Mercier, S. (2004). Construction of the dialysis and transplantation ontology: advantages, limits, and questions about Protege OWL. In *Workshop on Medical Applications of Protégé, 7th International Protégé Conference, Bethesda*.
150. Judd, C. M., McClelland, G. H., & Ryan, C. S. (2011). Data analysis: A model comparison approach. Routledge.
151. Weiss, S. M., & Indurkhya, N. (1998). Predictive data mining: a practical guide. Morgan Kaufmann
152. Prather, J. C., Lobach, D. F., Goodwin, L. K., Hales, J. W., Hage, M. L., & Hammond, W. E. (1997). Medical data mining: knowledge discovery in a clinical data warehouse. In Proceedings of the AMIA annual fall symposium (p. 101). American Medical Informatics Association.

153. Berson, A., & Smith, S. J. (2002). Building data mining applications for CRM, New York, NY:McGraw-Hill, Inc.
154. Armitage, P., Berry, G., & Matthews, J. N. S. (2008). Statistical methods in medical research. John Wiley & Sons.
155. Vickers, A. J. (2005). Parametric versus non-parametric statistics in the analysis of randomized trials with non-normally distributed data. BMC medical research methodology, 5(1), 35.
156. Cox, D. R. (2006). Principles of statistical inference, New York, NY: Cambridge University Press.
157. Hirose, H., Takayama, T., Hozawa, S., Hibi, T., & Saito, I. (2011). Prediction of metabolic syndrome using artificial neural network system based on clinical data including insulin resistance index and serum adiponectin. Computers in biology and medicine, 41(11), 1051-1056.
158. Shalev-Shwartz, S., & Ben-David, S. (2014). Understanding machine learning: From theory to algorithms. Cambridge university press.
159. Kodratoff, Y. (2014). Introduction to machine learning. Morgan Kaufmann.
160. Parmigiani, G., & Inoue, L. (2009). Decision theory: principles and approaches (Vol. 812). John Wiley & Sons
161. Wu, X., & Kumar, V. (2009). The top ten algorithm in data mining. International Standard Book, 13, 978-1.
162. Mitchell, T. M. (1999). Machine learning and data mining. Communications of the ACM, 42(11), 30-36.
163. Cucker, F., & Smale, S. (2002). Best choices for regularization parameters in learning theory: on the bias-variance problem. Foundations of Computational Mathematics, 2(4), 413-428.
164. Domingos, P. (2012). A few useful things to know about machine learning. Communications of the ACM, 55(10), 78-87.
165. A. Verikas, A. Gelzinis, and M. Bacauskiene, "Mining data with random forests: A survey and results of new tests," Pattern Recognit., vol. 44, no. 2, pp. 330–349, 2011
166. Breiman, L. (2001). Random forests. *Machine learning*, *45*(1), 5-32.
167. Steinberg, D., & Colla, P. (2009). CART: classification and regression trees. The top ten algorithms in data mining, 9, 179.
168. Temkin, N. R., Holubkov, R., Machamer, J. E., Winn, H. R., & Dikmen, S. S. (1995). Classification and regression trees (CART) for prediction of function at 1 year following head trauma. *Journal of neurosurgery*, *82*(5), 764-771.
169. Nguyen, C., Wang, Y., & Nguyen, H. N. (2013). Random forest classifier combined with feature selection for breast cancer diagnosis and prognostic.
170. Qi, Y. (2012). Random forest for bioinformatics. In Ensemble machine learning (pp. 307-323). Springer US.
171. Pauly, O. (2012). Random forests for medical applications (Doctoral dissertation, München, Technische Universität München, Diss., 2012).
172. Breiman, L. (1996). Bagging predictors. *Machine learning*, *24*(2), 123-140.
173. Chen, X., & Ishwaran, H. (2012). Random forests for genomic data analysis. Genomics, 99(6), 323-329.
174. Oshiro, T. M., Perez, P. S., & Baranauskas, J. A. (2012, July). How many trees in a random forest?. In International Workshop on Machine Learning and Data Mining in Pattern Recognition (pp. 154-168). Springer Berlin Heidelberg.
175. Jiang, W., & Simon, R. (2007). A comparison of bootstrap methods and an adjusted bootstrap approach for estimating the prediction error in microarray classification. Statistics in medicine, 26(29), 5320-5334.
176. Wang, S. C. (2003). Artificial neural network. In Interdisciplinary computing in java programming (pp. 81-100). Springer

177. Vijayasaradhi I. Recognising Handwritten Digits using Artificial Neural Networks. Retrieved December 8, 2015, from https://www.linkedin.com/pulse/recognising-handwritten-digits-using-artificial-neural-indurthi
178. Cross, S. S., Harrison, R. F., & Kennedy, R. L. (1995). Introduction to neural networks. The Lancet, 346(8982), 1075-1079.
179. Malmgren, H., Borga, M., & Niklasson, L. (Eds.). (2012). Artificial Neural Networks in Medicine and Biology: Proceedings of the ANNIMAB-1 Conference, Göteborg, Sweden, 13–16 May 2000. Springer Science & Business Media..
180. Rosenblatt, F. (1958). The perceptron: A probabilistic model for information storage and organization in the brain. *Psychological review*, *65*(6), 386.
181. N. Subramanian, A. Yajnik, and R. S. R. Murthy, "Artificial neural network as an alternative to multiple regression analysis in optimizing formulation parameters of cytarabine liposomes.," AAPS PharmSciTech, vol. 5, no. 1, p. E4, 2004
182. Retrieved from. https://www.quora.com/What-does-support-vector-machine-SVM-mean-in-laymans-terms
183. Ben-Hur, A., Ong, C. S., Sonnenburg, S., Schölkopf, B., & Rätsch, G. (2008). Support vector machines and kernels for computational biology. PLoS Comput Biol, 4(10), e1000173.
184. Chapelle, O., Vapnik, V., Bousquet, O., & Mukherjee, S. (2002). Choosing multiple parameters for support vector machines. Machine learning, 46(1), 131-159.
185. Yu, W., Liu, T., Valdez, R., Gwinn, M., & Khoury, M. J. (2010). Application of support vector machine modeling for prediction of common diseases: the case of diabetes and pre-diabetes. BMC Medical Informatics and Decision Making, 10(1), 16.
186. Barakat, N., & Bradley, A. P. (2010). Rule extraction from support vector machines: a review. Neurocomputing, 74(1), 178-190.
187. Martens, D., Huysmans, J., Setiono, R., Vanthienen, J., & Baesens, B. (2008). Rule extraction from support vector machines: an overview of issues and application in credit scoring. In *Rule extraction from support vector machines* (pp. 33-63). Springer Berlin Heidelberg.
188. Barakat, N., & Diederich, J. (2005). Eclectic rule-extraction from support vector machines. *International Journal of Computational Intelligence*, *2*(1), 59-62.
189. Martens, D., Baesens, B. B., & Van Gestel, T. (2009). Decompositional rule extraction from support vector machines by active learning. IEEE Transactions on Knowledge and Data Engineering, 21(2), 178-191.
190. Casari, P., Nati, M., Petrioli, C., & Zorzi, M. (2006, October). ALBA: an adaptive load-balanced algorithm for geographic forwarding in wireless sensor networks. In Military Communications Conference, 2006. MILCOM 2006. IEEE (pp. 1-9). IEEE.
191. Bradley, A. P. (1997). The use of the area under the ROC curve in the evaluation of machine learning algorithms. Pattern recognition, 30(7), 1145-1159
192. Tom Fawcett. An introduction to roc analysis. Pattern recognition letters, 27(8):861{874, 2006
193. Buckland, M., & Gey, F. (1994). The relationship between recall and precision. Journal of the American society for information science, 45(1), 12.
194. Powers, D. M. (2011). Evaluation: from precision, recall and F-measure to ROC, informedness, markedness and correlation.
195. Vito D, Casagrande G, Cappoli G, et al.(2015) A predictive index of intra-dialysis IDH A statistical clinical data mining approach. IJSERM.;2(2):53-57

196. Vito D., Bianchi C., Casagrande G., Costantino M.L.,(2014)A novel database approach to gather clinical data on dialysis treatments" - Proceeding of 1st International Conference Recent Trends and Applications in Computer Science and Information Technology", pp 12-26.
197. Henry, S., Hoon, S., Hwang, M., Lee, D., & DeVore, M. D. (2005, April). Engineering trade study: extract, transform, load tools for data migration. In Systems and Information Engineering Design Symposium, 2005 IEEE (pp. 1-8). IEEE.
198. Berger, D., & Takala, J. (2016). Hypotension and hypovolemia during hemodialysis: is the usual suspect innocent?. Critical care, 20(1), 140.
199. Damasiewicz, M. J., & Polkinghorne, K. R. (2011). Intra-dialytic hypotension and blood volume and blood temperature monitoring. Nephrology, 16(1), 13-18.
200. Shapiro, S. S., & Wilk, M. B. (1965). An analysis of variance test for normality (complete samples). Biometrika, 52(3-4), 591-611.
201. Razali, N. M., & Wah, Y. B. (2011). Power comparisons of shapiro-wilk, kolmogorov-smirnov, lilliefors and anderson-darling tests. Journal of statistical modeling and analytics, 2(1), 21-33.
202. Marusteri, M., & Bacarea, V. (2010). Comparing groups for statistical differences: how to choose the right statistical test?. Biochemia medica, 20(1), 15-32.
203. Kruskal, W. H., & Wallis, W. A. (1952). Use of ranks in one-criterion variance analysis. Journal of the American statistical Association, 47(260), 583-621
204. Benjamini, Y., & Leshno, M. (2005). Statistical methods for data mining. Data Mining and Knowledge Discovery Handbook, 565-587..
205. Palatini, P., & Rizzoni, D. (2008). Linee Guida della Società Italiana dell'Ipertensione Arteriosa sulla misurazione convenzionale e automatica della pressione arteriosa nello studio medico, a domicilio e nelle 24 ore. Ipertensione e Prevenzione Cardiovascolare, 15, 63-115.
206. Sands, J. J., Usvyat, L. A., Sullivan, T., Segal, J. H., Zabetakis, P., Kotanko, P., ... & Diaz-Buxo, J. A. (2014). Intradialytic hypotension: frequency, sources of variation and correlation with clinical outcome. Hemodialysis International, 18(2), 415-422.
207. Schafer, R. W. (2011). What is a Savitzky-Golay filter?[lecture notes]. IEEE Signal processing magazine, 28(4), 111-117.
208. Kinet, J. P., Soyeur, D., Balland, N., Saint-Remy, M., Collignon, P., & Godon, J. P. (1982). Hemodynamic study of hypotension during hemodialysis. Kidney international, 21(6), 868-876.
209. Poldermans, D., In't Veld, A. J. M., Rambaldi, R., Van Den Meiracker, A. H., Van Den Dorpel, M. A., Rocchi, G., ... & Zietse, R. (1999). Cardiac evaluation in hypotension-prone and hypotension-resistant hemodialysis patients. Kidney international, 56(5), 1905-1911.
210. Brain, D., & Webb, G. (1999). On the effect of data set size on bias and variance in classification learning. In Proceedings of the Fourth Australian Knowledge Acquisition Workshop, University of New South Wales (pp. 117-128).
211. Figueroa, R. L., Zeng-Treitler, Q., Kandula, S., & Ngo, L. H. (2012). Predicting sample size required for classification performance. BMC medical informatics and decision making, 12(1), 8.
212. Saar-Tsechansky, M., & Provost, F. (2007). Handling missing values when applying classification models. Journal of machine learning research, 8(Jul), 1623-1657.
213. Bengio, Y., & Grandvalet, Y. (2004). No unbiased estimator of the variance of k-fold cross-validation. Journal of machine learning research, 5(Sep), 1089-1105.

214. Wu, G., & Chang, E. Y. (2003, August). Class-boundary alignment for imbalanced dataset learning. In ICML 2003 workshop on learning from imbalanced data sets II, Washington, DC (pp. 49-56).
215. Akbani, R., Kwek, S., & Japkowicz, N. (2004, September). Applying support vector machines to imbalanced datasets. In European conference on machine learning (pp. 39-50). Springer Berlin Heidelberg.
216. Mena, L., & Gonzalez, J. A. (2006, May). Machine Learning for Imbalanced Datasets: Application in Medical Diagnostic. In Flairs Conference (pp. 574-579).
217. Pazzani, M., Merz, C., Murphy, P., Ali, K., Hume, T., & Brunk, C. (1994). Reducing misclassification costs. In Proceedings of the Eleventh International Conference on Machine Learning (pp. 217-225).
218. Kubat, M., & Matwin, S. (1997, July). Addressing the curse of imbalanced training sets: one-sided selection. In ICML (Vol. 97, pp. 179-186).
219. Kohavi, R. (1995, August). A study of cross-validation and bootstrap for accuracy estimation and model selection. In Ijcai (Vol. 14, No. 2, pp. 1137-1145).
220. Chawla, N. V., Bowyer, K. W., Hall, L. O., & Kegelmeyer, W. P. (2002). SMOTE: synthetic minority over-sampling technique. Journal of artificial intelligence research, 16, 321-357.
221. Klinkenberg, R. (Ed.). (2013). RapidMiner: Data mining use cases and business analytics applications. Chapman and Hall/CRC.Kohavi, R. (1995, August). A study of cross-validation and bootstrap for accuracy estimation and model selection. In Ijcai (Vol. 14, No. 2, pp. 1137-1145).
222. Rodriguez, J. D., Perez, A., & Lozano, J. A. (2010). Sensitivity analysis of k-fold cross validation in prediction error estimation. IEEE transactions on pattern analysis and machine intelligence, 32(3), 569-575.
223. Bengio, Y., & Grandvalet, Y. (2004). No unbiased estimator of the variance of k-fold cross-validation. Journal of machine learning research, 5(Sep), 1089-1105.
224. Rodriguez, J. D., Perez, A., & Lozano, J. A. (2010). Sensitivity analysis of k-fold cross validation in prediction error estimation. IEEE transactions on pattern analysis and machine intelligence, 32(3), 569-575.
225. Davison, A. C., & Hinkley, D. V. (1997). Bootstrap methods and their application (Vol. 1). Cambridge university press.ISO 690
226. Bengio, Y., & Grandvalet, Y. (2004). No unbiased estimator of the variance of k-fold cross-validation. Journal of machine learning research, 5(Sep), 1089-1105.
227. Karaboga, D., Akay, B., & Ozturk, C. (2007, August). Artificial bee colony (ABC) optimization algorithm for training feed-forward neural networks. In International Conference on Modeling Decisions for Artificial Intelligence (pp. 318-329). Springer Berlin Heidelberg ISO 690.
228. Ben-Hur, A., Ong, C. S., Sonnenburg, S., Schölkopf, B., & Rätsch, G. (2008). Support vector machines and kernels for computational biology. PLoS Comput Biol, 4(10), e1000173.
229. Zhang, K., Lan, L., Wang, Z., & Moerchen, F. (2012). Scaling up Kernel SVM on Limited Resources: A Low-rank Linearization Approach. In AISTATS (Vol. 22, pp. 1425-1434).
230. Marti34nez, W. L., & Martinez, A. R. (2005). Exploratory data analysis with MATLAB/Wendy L. Martinez, Angel R. Martinez., Boca Raton, Fla.: Chapman & Hall/CRC.
231. Casagrande G., Vito D., Bianchi C., Carfagna F., Minoretti C.,

Pontoriero G., Schoenholzer C., Minoretti C., Rombolà G., Costantino M.L (2017), Data Mining Analysis Over a Clinical Database for the Prediction of Intradialysis Hypotension" IEEE Transactions on Pattern Analysis and Machine Intelligence (Submitted).

232. Casagrande G., Vito D., Bianchi C., Carfagna F., Minoretti C., Pontoriero G., Schoenholzer C., Minoretti C., Rombolà G., Costantino M.L, (2016).IDH risk prediction at dialysis session start using J index: index optimization and prediction accuracy evaluation.", Int J Artif Organs (Submitted).
233. Morfin, J. A., Fluck, R. J., Weinhandl, E. D., Kansal, S., McCullough, P. A., & Komenda, P. (2016). Intensive hemodialysis and treatment complications and tolerability. American Journal of Kidney Diseases, 68(5), S43-S50.
234. Daugirdas, J. T. (2001). Pathophysiology of dialysis hypotension: an update. American journal of kidney diseases, 38(4), S11-S17.
235. Zhou, Y. L., Liu, H. L., Duan, X. F., Yao, Y., Sun, Y., & Liu, Q. (2006). Impact of sodium and ultrafiltration profiling on haemodialysis-related hypotension. Nephrology Dialysis Transplantation, 21(11), 3231-3237.
236. Platt, J. (1999). Probabilistic outputs for support vector machines and comparisons to regularized likelihood methods. Advances in large margin classifiers, 10(3), 61-74.
237. Titapiccolo, J. I., Ferrario, M., Cerutti, S., Signorini, M. G., Barbieri, C., Mari, F., & Gatti, E. (2012). Mining Medical Data to Develop Clinical Decision Making Tools in Hemodialysis. 2012 IEEE 12th International Conference on Data Mining Workshops, 99–106.
238. Shahabi, M., Nafisi, V. R., & Pak, F. (2015, November). Prediction of intradialytic hypotension using PPG signal features. In Biomedical Engineering (ICBME), 2015 22nd Iranian Conference on (pp. 399-404). IEEE.
239. Sandberg F., Bail´on R., Hernando D., Laguna P.,Martınez J. P., Solem K., & Sornmo L. (2014) Prediction of Hypotension in Hemodialysis Patients Physiological Measurement. Physiol. Meas. vol. 35, pp. 1885–1898.
240. Fogel, D. B. (1994). An introduction to simulated evolutionary optimization. IEEE transactions on neural networks, 5(1), 3-14.
241. Snoek, J., Larochelle, H., & Adams, R. P. (2012). Practical bayesian optimization of machine learning algorithms. In Advances in neural information processing systems (pp. 2951-2959).
242. Quinlan, J. R., & Cameron-Jones, R. M. (1995). Induction of logic programs: FOIL and related systems. New Generation Computing, 13(3-4), 287-312.
243. Analisi dei fattori predisponenti all'ipotensione intra-dialitica valutabilit a inizio trattamento - Final Master Thesis G.Cappoli (2014)
244. Supervisor: Giustina Casagrande, Maria Laura Costantino, Domenico Vito, Politecnico di Milano
245. Statistical and Data Mining Analysis Over a Clinical Database for the Prediction of Intradialytic Hypotension Final Master Thesis S. Gritti, A.Canovi (2014) Supervisor: Giustina Casagrande, Maria Laura Costantino, Domenico Vito, Politecnico di Milano AA:(2015/2016)
246. Statistical and Data Mining Analysis Over a Clinical Database for the Prediction of Intradialytic Hypotension Final Master Thesis S. Gritti, A.Canovi (2014) Supervisor: Giustina Casagrande, Maria Laura Costantino, Domenico Vito, Politecnico di Milano AA:(2015/2016)
247. Analisi multiparametrica di episodi ipotensivi intradialialitici- Final Master Thesis E.Merlo, S. Panzeri
    Supervisor: Giustina Casagrande, Maria Laura Costantino, Domenico Vito, Politecnico di Milano AA:(2014/2015)
248. Analisi dei fattori predisponenti all'ipotensione intra-dialitica valutati .a inizio trattamento - Final Master Thesis G.Cappoli

Supervisor: Giustina Casagrande, Maria Laura Costantino, Domenico Vito, Politecnico di Milano AA:(2014/2015)

Annex A

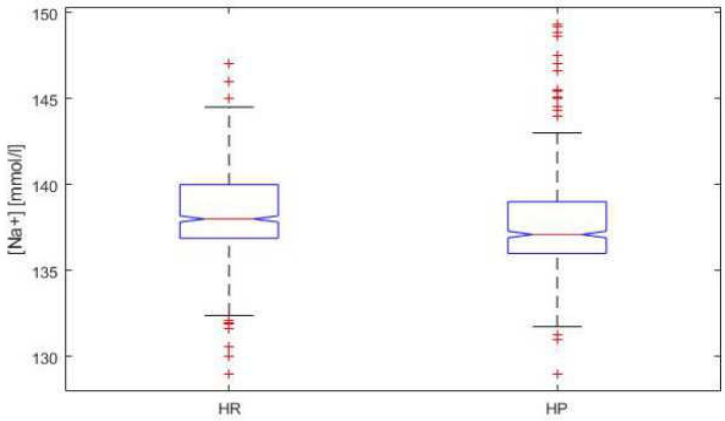

Figure A.1: Box plot Sodium Blood Concentration HR/HP

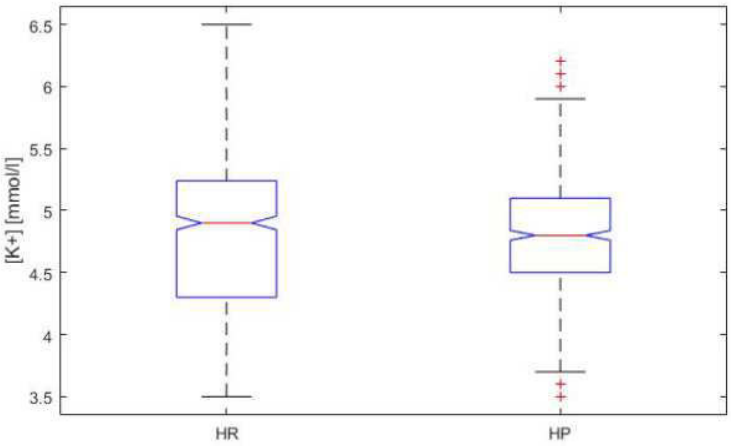

Figure A.2: Box plot Potassium Blood Concentration HR/HP, Dataset 1

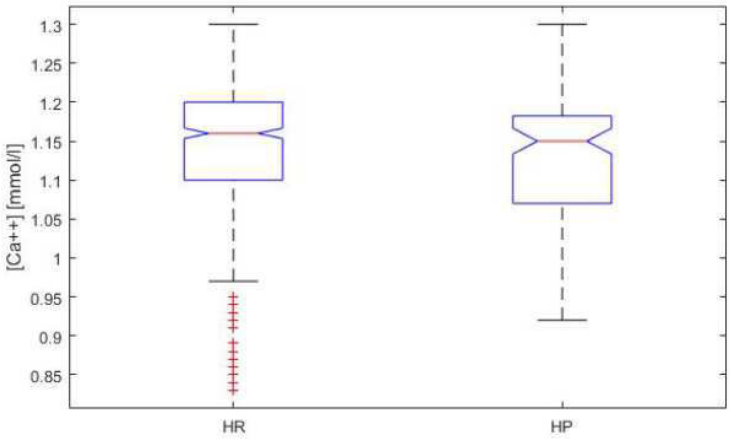

Figure A.3: Box plot Calcium Blood Concentration HR/HP, Dataset 1

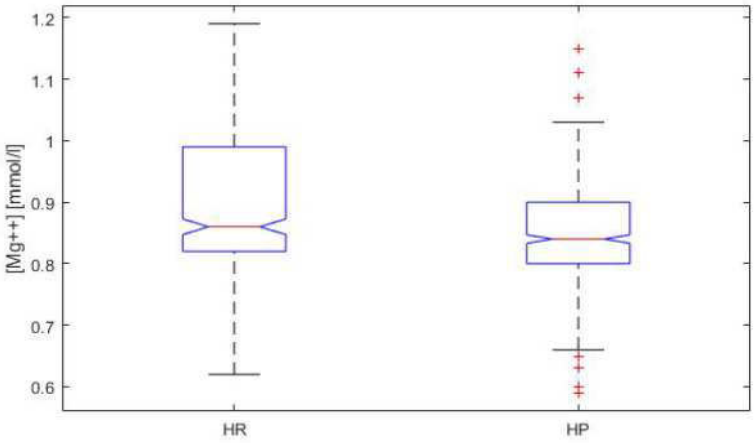

Figure A.4: Box plot Magnesium Blood Concentration HR/HP, Dataset 1

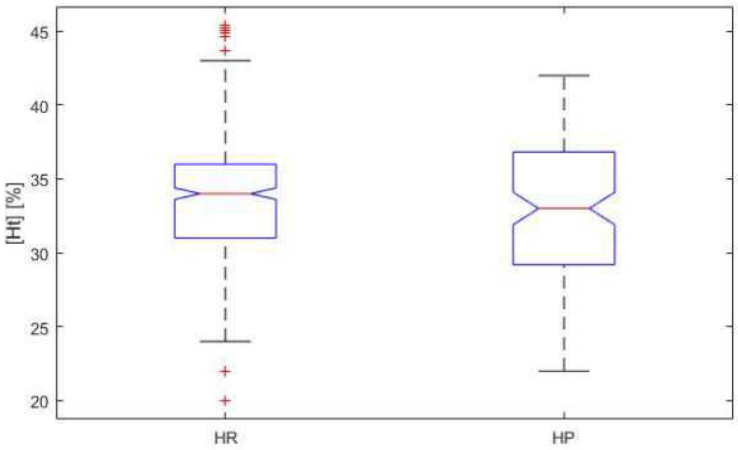

Figure A.5: Box plot Hematocrit HR/HP, Dataset 1

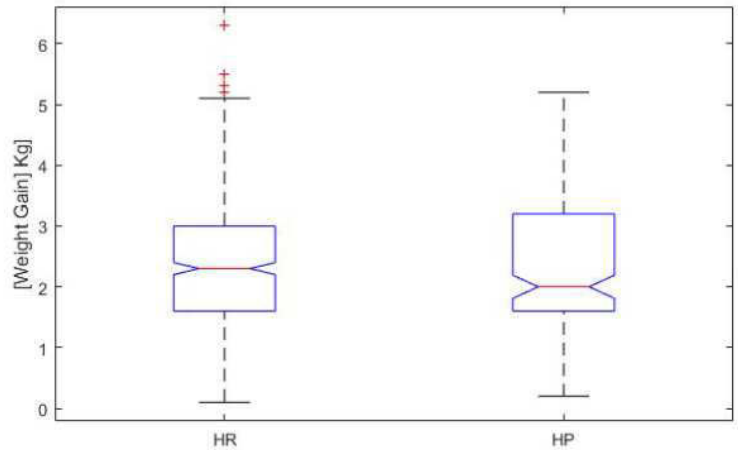

Figure A.6: Box plot Weight Gain HR/HP, Dataset 1

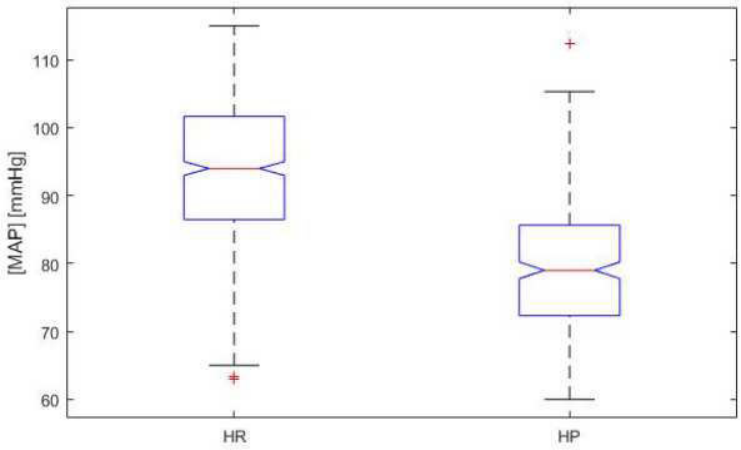

Figure A.7: Box plot MAP HR/HP, Dataset 1

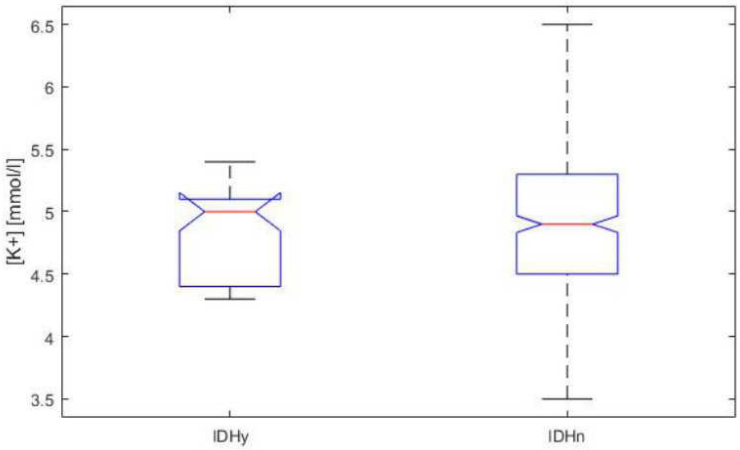

Figure A.8: Box plot MAP HR/HP, Dataset 1

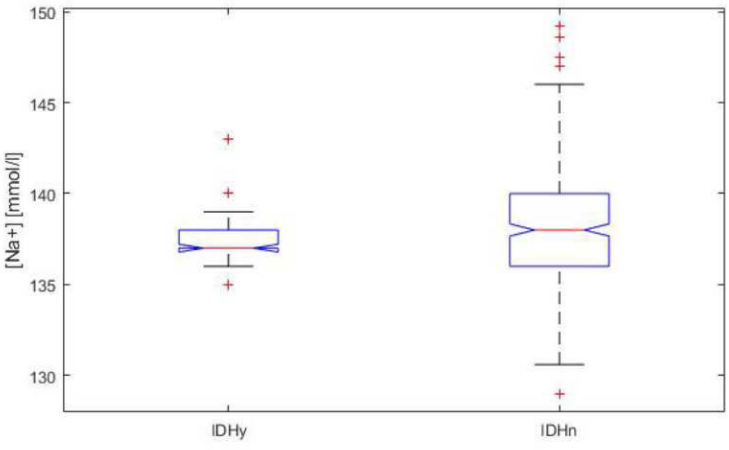

Figure A.9: Box plot Sodium Blood Concentration IDHy/IDHn, Dataset2

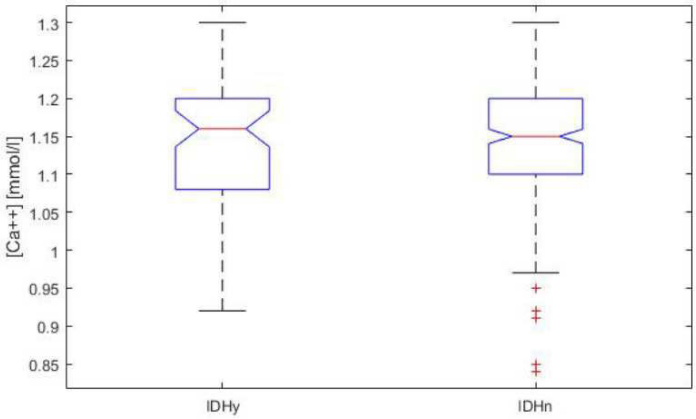

Figure A.10: Box plot Calcium Blood Concentration IDHy/IDHn, Dataset2

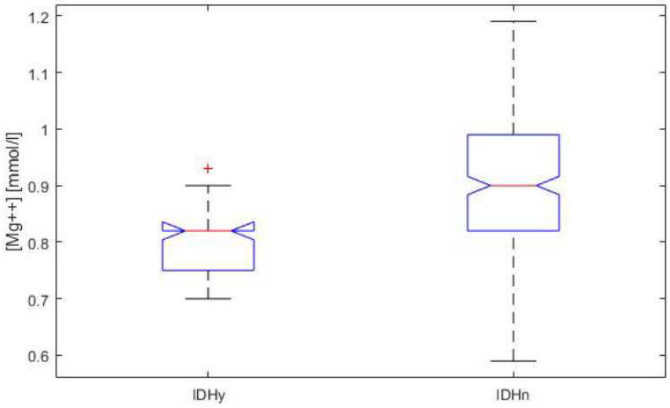

Figure A.11: Box plot Magnesium Blood Concentration IDHy/IDHn, Dataset2

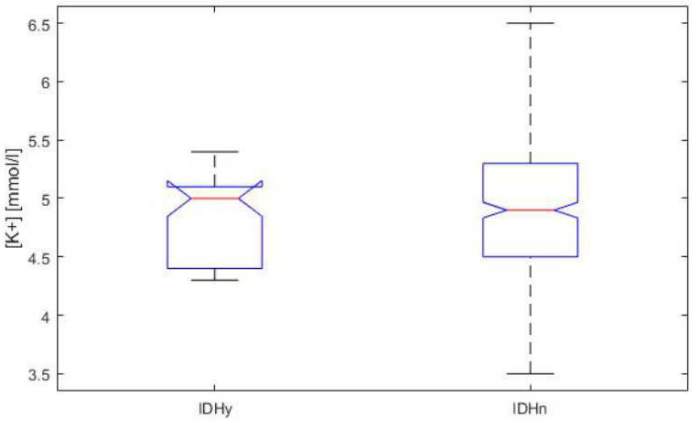

Figure A.12: Box plot Potassium Blood Concentration IDHy/IDHn, Dataset2

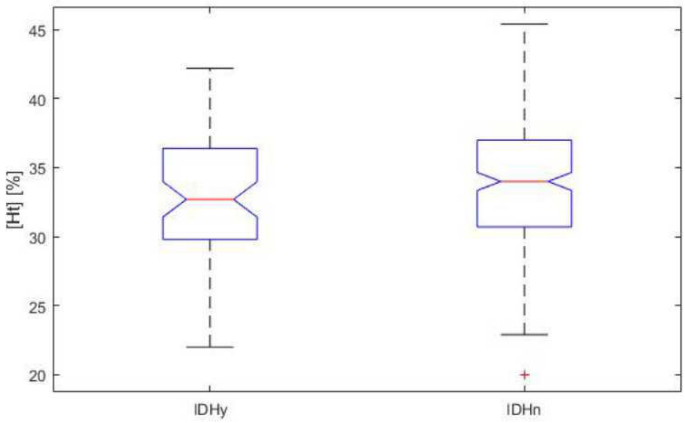

Figure A.13: Box plot Hematocrit IDHy/IDHn, Dataset2

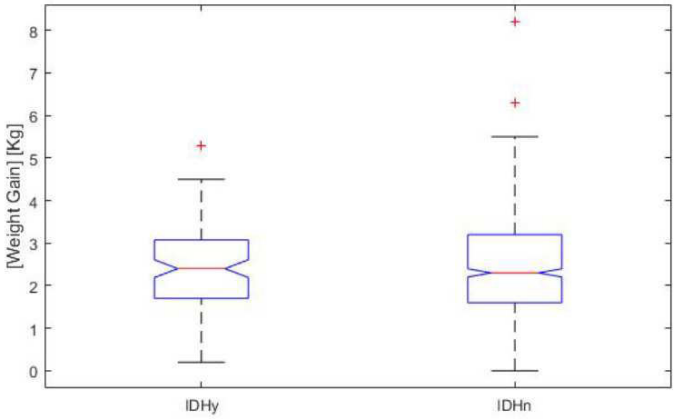

Figure A.14: Box plot Weight Gain IDHy/IDHn, Dataset2

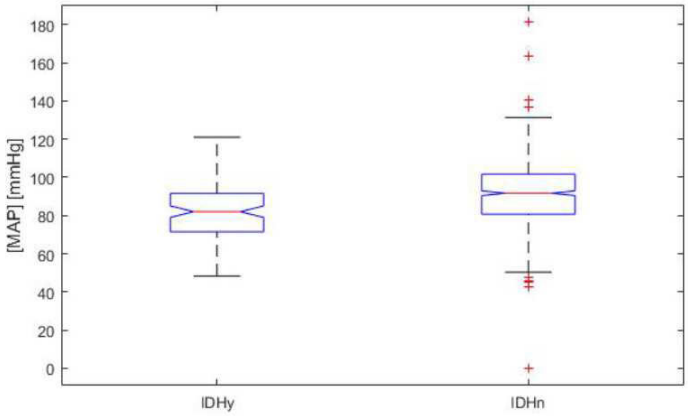

Figure A.15: Box plot MAP IDHy/IDHn, Dataset2

ANNEX B

Table B1.1: Result of the application of $SAP(0)_{140}$ Criterion

Legend:

#SAP_IDH/Tot = number of session identified as IDH by $SAP(0)_{140}$ / total sessio
%SAP_IDH/Tot = percentage of sessions identified as IDH by $SAP(0)_{140}$/ total session
#SAP_IDH/#Syntom = number of session identified as IDH by $SAP(0)_{140}$ / number of session with syntoms
%SAP_IDH/Tot = percentage of session identified as IDH by $SAP(0)_{140}$ / number of session with syntoms
#Pz_IDH/Pz_Tot = n° of patients with IDH by $SAP(0)_{140}$ / Total_patients
%Pz_IDH/Tot = % of patients with IDH by $SAP(0)_{140}$/ Total_patients
#Pz_IDH/Pz_Synt =n° of patients with IDH by $SAP(0)_{140}$ / Patient_ Patient with registered symptoms on medical records
%iPz_IDH/Pz_Synt = n° of patients with IDH by $SAP(0)_{140}$ / Patient with registered symptoms on medical records

A. Application to EOC Lugano

E.O.C LUGANO	#SAP_IDH/Tot	%SAP_IDH/Tot	#SAP_IDH/#Synt	%SAP_IDH/Synt
SAP(0)<140	43/150	**28,67%**	2/4	**50%**
SAP(0)≥140	22/150	**14,67%**	0/4	**0%**
$SAP(0)_{140}$	65/150	**43,33**	2/4	**50%**
	#Pz_IDH/P_Tot	**%Pz_IDH/Tot**	**#Pz_IDH/ #Pz_Synt**	**%i_IDH/Tot**
SAP(0)<140	18/20	**90%**	2/4	**50%**
SAP(0)≥140	11/20	**55%**	0/4	**0%**
$SAP(0)_{140}$	20/20	**100%**	2/4	**50%**

B. Application to A.O. Provincia di Lecco

A.O. LECCO	#SAP_IDH/Tot	%SAP_IDH/Tot	#SAP_IDH/#Synt	%SAP_IDH/Synt
SAP(0)<140	20/284	**7,04%**	2/11	**18,19%**
SAP(0)≥140	27/284	**9,05%**	5/11	**45,46%**
$SAP(0)_{140}$	47/284	**16,55%**	7/11	**60,64%**
	#Pz_IDH/P_Tot	**%Pz_IDH/Tot**	**##Pz_IDH/ #Pz_Synt**	**%Pz_IDH/Tot**
SAP(0)<140	14/48	**29,17%**	2/5	**40%**
SAP(0)≥140	16/48	**33,34%**	3/5	**60%**
$SAP(0)_{140}$	25/48	**52,1%**	4/5	**80%**

Table B1.2: Result of the comparison between SAP_{0_140} and IDH-D

Legend:

For both Sessions and Patients

 # SAP(0)$_{140}$∧ IDH D = number of detections by both SAP(0)$_{140}$ criterion and IDH-D

 # SAP(0)$_{140}$∧ IDH D)/ IDH-D = fraction of detections by both SAP(0)$_{140}$ criterion and IDH-D on the total of IDH-D detections

 # SAP(0)$_{140}$∧ IDH D)/ IDH-D = percentages of detections by both SAP(0)$_{140}$ criterion and IDH-D on the total of IDH-D detections

A. SAP(0)140: SAP(0)<140 mmHg

SESSIONS	**# SAP(0)$_{140}$∧ IDH D**	**# (SAP(0)$_{140}$∧ IDH D)/ IDH-D**	**%(SAP(0)$_{140}$∧ IDH D)/ IDH-D**
EOC LUGANO	22	22/45	**48,89%**
A:O. LECCO	11	11/29	**37,93%**
PATIENTS	**# SAP(0)$_{140}$∧ IDH D**	**# (SAP(0)$_{140}$∧ IDH D)/ IDH-D**	**%(SAP(0)$_{140}$∧ IDH D)/ IDH-D**
EOC LUGANO	13	13/15	**86,67%**
A:O. LECCO	6	6/11	**54,55%**

B. SAP(0)140: SAP(0)≥140 mmHg

SESSIONS	**# SAP(0)$_{140}$∧ IDH D**	**# (SAP(0)$_{140}$∧ IDH D)/ IDH-D**	**%(SAP(0)$_{140}$∧ IDH D)/ IDH-D**
EOC LUGANO	8	8/45	**17,78%**
A:O. LECCO	7	7/29	**24,13%**
PATIENTS	**# SAP(0)$_{140}$∧ IDH D**	**# (SAP(0)$_{140}$∧ IDH D)/ IDH-D**	**%(SAP(0)$_{140}$∧ IDH D)/ IDH-D**
EOC LUGANO	5	5/15	**45,45%**
A:O. LECCO	3	3/11	**27,27%**

Table B2.1: Result of the application of MAP_{30} Criterion

MAP_{30}_IDH/Tot = number of session identified as IDH by MAP_{30}/ total sessio
% MAP_{30}_IDH/Tot = percentage of sessions identified as IDH by MAP_{30}total session
# MAP_{30}_IDH/#Synt = number of session identified as IDH by MAP_{30}/ number of session with syntoms
%MAP_{30}_IDH/Tot = percentage of session identified as IDH by MAP_{30}/ number of session with syntoms
#Pz_IDH/Pz_Tot = n° of patients with IDH by MAP_{30}/ Total_patients
%Pz_IDH/Totv = % of patients with IDH by MAP_{30}/ Total_patients
#Pz_IDH/Pz_Synt =n° of patients with IDH by MAP_{30}/ Patient_ Patient with registered symptoms on medical records
%Pz_IDH/Pz_Synt = n° of patients with IDH by MAP_{30}/ Patient with registered symptoms on medical records

SESSIONS	#MAP_{30}_IDH/Tot	%MAP_{30}_IDH/Tot	# MAP_{30}IDH/#Synt	% MAP_{30}IDH/Synt
EOC LUGANO	16/150	**10,67%**	1/4	**25%**
A:O. LECCO	28/284	**9,86%**	5/11	**45,45%**
PATIENTS	#Pz_IDH/P_Tot	%Pz_IDH/Tot	#Pz_IDH/ #Pz_Synt	%Pz_IDH/Tot
EOC LUGANO	8/20	**40%**	1/4	**25%**
A:O. LECCO	16/48	**33,34%**	4/5	**80%**

Table B2.2: Result of the comparison between MAP_{30} and IDH-D

Legend:

For both Sessions and Patients

 # MAP_{30}∧ IDH D = number of detections by both MAP_{30}criterion and IDH-D
 # MAP_{30}∧ IDH D)/ IDH-D = fraction of detections by both MAP_{30}criterion and IDH-D on the total of IDH-D detections
% MAP_{30}∧ IDH D)/ IDH-D = percentages of detections by both MAP_{30} criterion and IDH-D on the total of IDH-D detections

SESSIONS	# MAP_{30}∧ IDH D	# (MAP_{30}∧ IDH D)/ IDH-D	%(MAP_{30}∧ IDH D)/ IDH-D
EOC LUGANO	6	6/45	**13,33%**
A:O. LECCO	9	9/29	**31,03%**
PATIENTS	# MAP_{30}∧ IDH D	# (MAP_{30}∧ IDH D)/ IDH-D	%(MAP_{30}∧ IDH D)/ IDH-D
EOC LUGANO	4	4/15	**26,67%**
A:O. LECCO	6	6/11	**54,55%**

Table B3.1: Result of the application of RBV_{13} Criterion

Legend:

#RBV_{13}_IDH /Tot = number of session identified as IDH by RBV_{13}/ total sessio
%RBV_{13}_IDH /Tot = percentage of sessions identified as IDH by RBV_{13}/ total session
#RBV_{13}_IDH /#Synt = number of session identified as IDH by RBV_{13}/ number of session with syntoms
%RBV_{13}_IDH /Tot = percentage of session identified as IDH by RBV_{13}/ number of session with syntoms
Pz _IDH /Pz_Tot = n° of patients with IDH by RBV_{13}/ Total_patients
%Pz_IDH/Tot = % of patients with IDH by RBV_{13}/ Total_patients
#Pz_IDH/Pz_Synt =n° of patients with IDH by RBV_{13}/ Patient_ Patient with registered symptoms on medical records
%iPz_IDH/Pz_Synt = n° of patients with IDH by RBV_{13} / Patient with registered symptoms on medical records

SESSIONS	#RBV_{13}_IDH/Tot	% RBV_{13}_IDH/Tot	# RBV_{13}IDH/#Synt	% RBV_{13} IDH/Synt
EOC LUGANO	46/140	**33,45%**	1/4	**25%**
A:O. LECCO	92/275	**32,62%**	5/9	**55,56%**
PATIENTS	#Pz_IDH/P_Tot	%Pz_IDH/Tot	#Pz_IDH/ #Pz_Synt	%i_IDH/Tot
EOC LUGANO	11/20	**55%**	1/4	**25%**
A:O. LECCO	50/50	**100%**	3/5	**60%**

Table B3.2: Result of the comparison between RBV_{13} Criterion

Legend:

For both Sessions and Patients

#RBV_{13}∧ IDH-D = number of detections by both RBV13 criterion and IDH-D
 # RBV_{13}∧ IDH-D / IDH-D = fraction of detections by both RBV13 criterion and IDH-D on the total of IDH-D detections
% RBV_{13}∧ IDH-D/ IDH-D = percentages of detections by both RBV_{13} criterion and IDH-D on the total of IDH-D detections

SESSIONS	# RBV_{13}∧ IDH D	# (RBV_{13}∧ IDH D)/ IDH-D	%(RBV_{13}∧ IDH D)/ IDH-D
EOC LUGANO	20	20/42	**47,62%**
A:O. LECCO	14	14/27	**51,85%**
PATIENTS	# RBV_{13}∧ IDH D	# (RBV_{13}∧ IDH D)/ IDH-D	%(RBV_{13}∧ IDH D)/ IDH-D
EOC LUGANO	8	8 /15	**55,33%**
A:O. LECCO	7	7 /11	**63,64%**

Table B4.1: Result of the application of ΔK^+ Criterion

Legend:

#ΔK^+_IDH /Tot = number of session identified as IDH by ΔK^+/ total session
%ΔK^+ _IDH /Tot = percentage of sessions identified as IDH by ΔK^+/ total session
#ΔK^+_IDH /#Synt = number of session identified as IDH by ΔK^+ / number of session with syntoms
%ΔK^+_IDH /Tot = percentage of session identified as IDH by ΔK^+/ number of session with syntoms
#Pz_Tot = n° of patients with IDH by ΔK^+/ Total patients
%Pz_IDH/Tot = % of patients with IDH by ΔK^+/ Total patients
#Pz_IDH/Pz_Synt =n° of patients with IDH by ΔK^+ / Patient with registered symptoms on medical records
%Pz_IDH/Pz_Synt = n° of patients with IDH by ΔK^+ / Patient with registered symptoms on medical records

A. Application to EOC Lugano

EOC LUGANO	# ΔK^+_IDH /Tot	% ΔK^+_IDH /Tot	# ΔK^+_IDH/#Synt	% ΔK^+_IDH/Synt
dK1	20/150	**13,34%**		
dK2	65/150	**43,43%**		
dK3	80/150	**53,34%**		
dKtot	112/150	**74.67%**	4/4	**100%**
	#Pz_IDH/P_Tot	**%Pz_IDH/Tot**	**#Pz_IDH/ #Pz_Synt**	**%i_IDH/Tot**
dK1	20/20	**100%**		
dK2	17/20	**85%**		
dK3	17/20	**85%**		
dKtot	20/20	**100%**	4/4	100%

B. Application to A.O. Provincia di Lecco

A.O. LECCO	#ΔK⁺_IDH /Tot	%ΔK⁺_IDH /Tot	#ΔK⁺_IDH/#Synt	%ΔK⁺_IDH/Synt
dK1	43/296	**14,53%**		
dK2	117/296	**39,53%**		
dK3	88/296	**29,73%**		
dKtot	169/296	**57,09%**	4/11	**36.36%**
	#Pz_IDH/P_Tot	**%Pz_IDH/Tot**	**##Pz_IDH/ #Pz_Synt**	**%Pz_IDH/Tot**
dK1	20/50	**40%**		
dK2	39/50	**78%**		
dK3	22/50	**44%**		
dKtot	43/50	86%	4/5	**80%**

Table B4.2: Result of the comparison between Criterion

Legend:

For both Sessions and Patients

#ΔK⁺ ∧ IDH-D = number of detections by both ΔK^+/ criterion and IDH-D

#ΔK⁺ ∧ IDH-D / IDH-D = fraction of detections by both ΔK^+/ $_3$criterion and IDH-D on the total of IDH-D detections

% RBV$_{13}$∧ IDH-D/ IDH-D = percentages of detections by both ΔK^+/ criterion and IDH-D on the total of IDH-D detections

SESSIONS	#ΔK⁺ ∧ IDH D	#(ΔK⁺ ∧ IDH D)/ IDH-D	%(ΔK⁺ ∧ IDH D)/ IDH-D
EOC LUGANO	31	31/45	**68,88%**
A:O. LECCO	13	13/29	**44,83%**
PATIENTS	#ΔK⁺ ∧ IDH D	# (ΔK⁺ ∧ IDH D)/ IDH-D	%(ΔK⁺ ∧ IDH D)/ IDH-D
EOC LUGANO	14	14/15	**93,33%**
A:O. LECCO	8	8/11	**72,73%**

Table B5.1: Result of the application of Dysritmia Criterion

Legend:

Dim20IDH /Tot = number of session identified as IDH by Dysritmia Criterion / total session
% Dim20IDH /Tot = percentage of sessions identified as IDH by Dysritmia Criterion/ total session
# Dim20IDH /#Synt = number of session identified as IDH by Dysritmia Criterion / number of session with syntoms
%Dim20IDH /Tot = percentage of session identified as IDH by Dysritmia Criterion / number of session with syntoms
#Pz_Tot = n° of patients with IDH by Dysritmia Criterion / Total patients
%Pz_IDH/Tot = % of patients with IDH by Dysritmia Criterion / Total patients
#Pz_IDH/Pz_Synt =n° of patients with IDH by Dysritmia Criterion / Patient with registered symptoms on medical records
%Pz_IDH/Pz_Synt = n° of patients with IDH by Dysritmia Criterion / Patient with registered symptoms on medical records

A. Application to EOC Lugano

EOC LUGANO	# Dim20IDH /Tot	%Dim20IDH /Tot	#Dim20IDH/#Synt	% Dim20IDH +_IDH/Synt
HRate(t) ≤ 20	62/150	**41,34%**		
HRate(t) > 20	26/150	**17,34%**		
Dim20	88/150	**58,67%**	3/4	**75%**
	#Pz_IDH/P_Tot	**%Pz_IDH/Tot**	**#Pz_IDH/ #Pz_Synt**	**%Pz_IDH/Tot**
HRate(t) ≤ 20	17	**85,00%**		
HRate(t) > 20	8	**40,00%**		
Dim20	17/20	**85%**	1./4	**25%**

B. Application to A.O. Provincia di Lecco

AO LECCO	# Dim20IDH /Tot	%Dim20IDH /Tot	#Dim20IDH/#Synt	%Dim20IDH/Synt
HRate(t) ≤ 20	63/284	**22,18%**		
HRate(t) > 20	64/284	**22,53%**		
Dim20	127/284	**44,72%**	10/11	**90,90%**
	#Pz_IDH/P_Tot	**%Pz_IDH/Tot**	**#Pz_IDH/ #Pz_Synt**	**%Pz _IDH/Tot**
HRate(t) ≤ 20	26	**54,17%**		
HRate(t) > 20	30	**62,50%**		
Dim20	41/48	**85,42%**	5/5	**100%**

Table B5.2: Result of the comparison between Dysritmia Criterion and IDH-D

Legend:

For both Sessions and Patients

Dim20∧ IDH-D = number of detections by both MAP30criterion and IDH-D

Dim20∧ IDH-D / IDH-D = fraction of detections by both MAP30criterion and IDH-D on the total of IDH-D detections

% Dim20∧ IDH-D/ IDH-D = percentages of detections by both MAP30criterion and IDH-D on the total of IDH-D detections

SESSIONS	**Dim2# Dim200^{+} ∧ IDH D**	**#(ΔK^{+} ∧ IDH D)/ IDH-D**	**%(ΔK^{+} ∧ IDH D)/ IDH-D**
EOC LUGANO	26	26/45	**57,78%**
A:O. LECCO	19	19/29	**65,52%**
PATIENTS	**#ΔK^{+} ∧ IDH D**	**# (ΔK^{+} ∧ IDH D)/ IDH-D**	**%(ΔK^{+} ∧ IDH D)/ IDH-D**
EOC LUGANO	15	15/15	**100%**
A:O. LECCO	10	10/11	**90,90%**

Table B6.1: Result of the application of Multiparametric Criterion

Legend:
#MC_IDH /Tot = number of session identified as IDH by Multiparametric Criterion
%IDH-D= number of sessions identified as IDH
FP= number of false positives
%FP = percentage of false positives

A. Application to EOC Lugano

LUGANO	# MC_IDH	#IDH-D	%TP (IDH-D)	FP	%FP
Cr1	10	8	**80,00%**	2	**20,00%**
Cr2	22	16	**72,72%**	6	**27,27%**
Cr3	20	17	**85,00%**	3	**15,00%**
TOT	52	41	**78,85%**	11	**21,15%**

B. Application to A.O Lecco

LECCO	# MC_IDH	#IDH-D	%TP (IDH-D)	FP	%FP
Cr1	11	7	**63,64%**	4	**36,36%**
Cr2	14	10	**71,43%**	4	**28,57%**
Cr3	13	10	**76,93%**	3	**23,07%**
TOT	11	7	**63,64%**	4	**36,36%**

C. Application to EOC Lugano and A.O Lecco

TOTAL	# MC_IDH	#IDH-D	%TP (IDH-D)	FP	%FP
Cr1	21	15	**71,43%**	6	**28,57%**
Cr2	36	26	**72,22%**	10	**27,78%**
Cr3	33	27	**81,82%**	6	**18,18%**
TOT	90	68	**75,56%**	22	**24,44%**

A.2 Machine Learning

A.2.1 Random Forest

Dataset A

	IDHn	IDHy	*PRC*
$\widehat{\text{IDHn}}$	348	71	83.05%
$\widehat{\text{IDHy}}$	157	429	73.21%
RCL	68.91%	85.80%	

Table A.9: Validation confusion matrix, Dataset A, RF

	IDHn	IDHy	*PRC*
$\widehat{\text{IDHn}}$	37	4	90.24%
$\widehat{\text{IDHy}}$	17	54	76.06%
RCL	68.52%	93.10%	

Table A.10: Independent test confusion matrix, Dataset A, RF

Sample	Accuracy	AUC	f-Measure
Validation	$77.31\% \pm 4.08\%$	0.833 ± 0.029	$79.01\% \pm 3.77\%$
Indipendent	81.25%	0.871	83.72%

Table A.11: Performance summary, Dataset A, RF

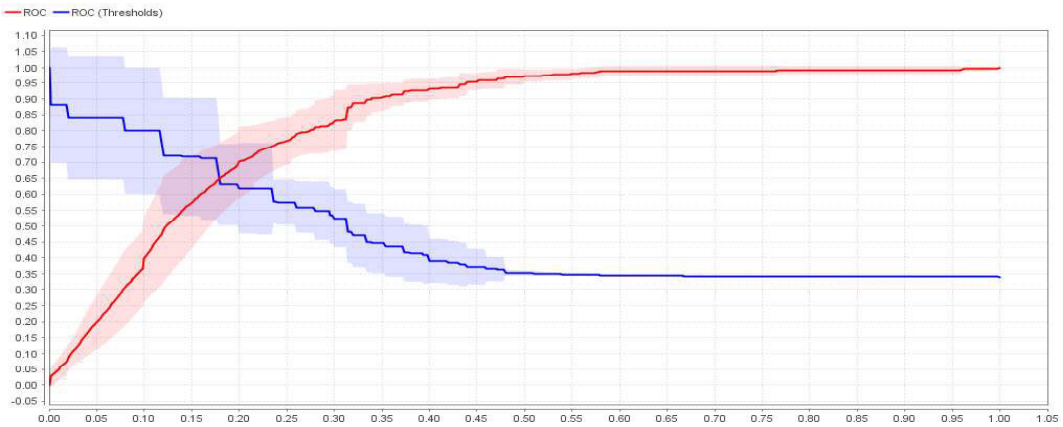

Figure A.16: Validation ROC, Dataset A, RF

Dataset B

	IDHn	IDHy	*PRC*
$\widehat{\textbf{IDHn}}$	241	49	83.10%
$\widehat{\textbf{IDHy}}$	109	271	71.32%
RCL	68.86%	84.69%	

Table A.12: Validation confusion matrix, Dataset B, RF

	IDHn	IDHy	*PRC*
$\widehat{\textbf{IDHn}}$	24	5	82.76%
$\widehat{\textbf{IDHy}}$	12	33	73.33%
RCL	66.67%	86.84%	

Table A.13: Independent test confusion matrix, Dataset B, RF

Sample	Accuracy	AUC	f-Measure
Validation	$76.42\% \pm 3.52\%$	0.844 ± 0.042	$77.42\% \pm 3.11\%$
Indipendent	77.03%	0.807	79.52%

Table A.14: Performance summary, Dataset B, RF

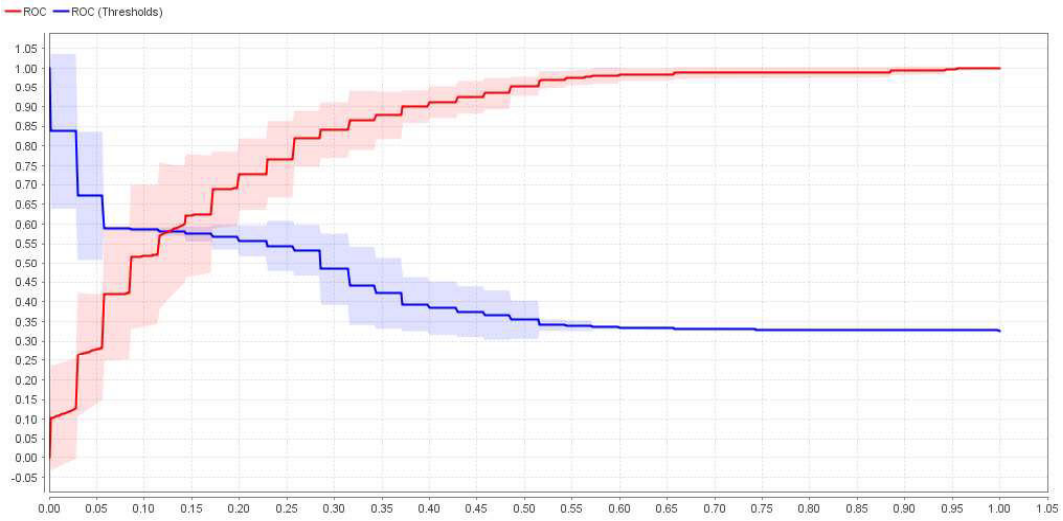

Figure A.17: Validation ROC, Dataset B, RF

Dataset C

	IDHn	IDHy	*PRC*
$\widehat{\text{IDHn}}$	128	49	72.32%
$\widehat{\text{IDHy}}$	49	103	67.76%
RCL	72.32%	67.76%	

Table A.15: Validation confusion matrix, Dataset C, RF

	IDHn	IDHy	*PRC*
$\widehat{\text{IDHn}}$	15	3	83.33%
$\widehat{\text{IDHy}}$	2	16	88.89%
RCL	88.24%	84.21%	

Table A.16: Independent test confusion matrix, Dataset C, RF

Sample	Accuracy	AUC	f-Measure
Validation	$70.21\% \pm 6.09\%$	0.818 ± 0.081	$66.95\% \pm 9.09\%$
Indipendent	86.11%	0.913	86.49%

Table A.17: Performance summary, Dataset C, RF

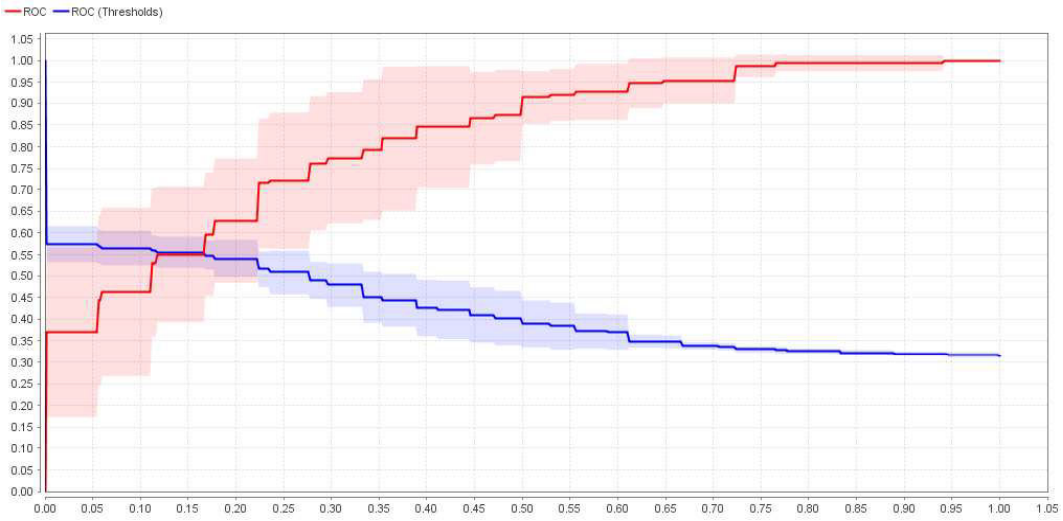

Figure A.18: Validation ROC, Dataset C, RF

Dataset D

	IDHn	IDHy	*PRC*
$\widehat{\text{IDHn}}$	142	25	85.03%
$\widehat{\text{IDHy}}$	37	131	77.98%
RCL	79.33%	83.97%	

Table A.18: Validation confusion matrix, Dataset D, RF

	IDHn	IDHy	*PRC*
$\widehat{\text{IDHn}}$	14	3	82.35%
$\widehat{\text{IDHy}}$	5	15	75.00%
RCL	76.68%	83.33%	

Table A.19: Independent test confusion matrix, Dataset D, RF

Sample	Accuracy	AUC	f-Measure
Validation	$81.52\% \pm 6.75\%$	0.913 ± 0.048	$80.70\% \pm 7.41\%$
Indipendent	78.38%	0.924	78.95%

Table A.20: Performance summary, Dataset D, RF

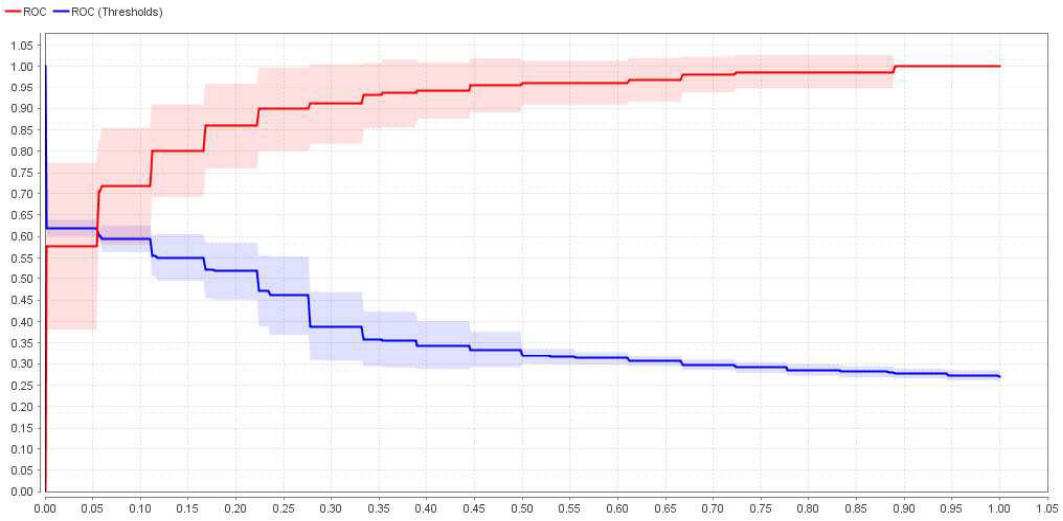

Figure A.19: Validation ROC, Dataset D, RF

Dataset E

	IDHn	IDHy	*PRC*
$\widehat{\textbf{IDHn}}$	105	16	86.79%
$\widehat{\textbf{IDHy}}$	24	106	81.54%
RCL	81.40%	86.89%	

Table A.21: Validation confusion matrix, Dataset E, RF

	IDHn	IDHy	*PRC*
$\widehat{\textbf{IDHn}}$	12	1	92.31%
$\widehat{\textbf{IDHy}}$	6	9	60.00%
RCL	66.67%	90.00%	

Table A.22: Independent test confusion matrix, Dataset E, RF

Sample	Accuracy	AUC	f-Measure
Validation	$84.05\% \pm 8.22\%$	0.923 ± 0.064	$84.01\% \pm 8.35\%$
Indipendent	75.00%	0.878	72.49%

Table A.23: Performance summary, Dataset E, RF

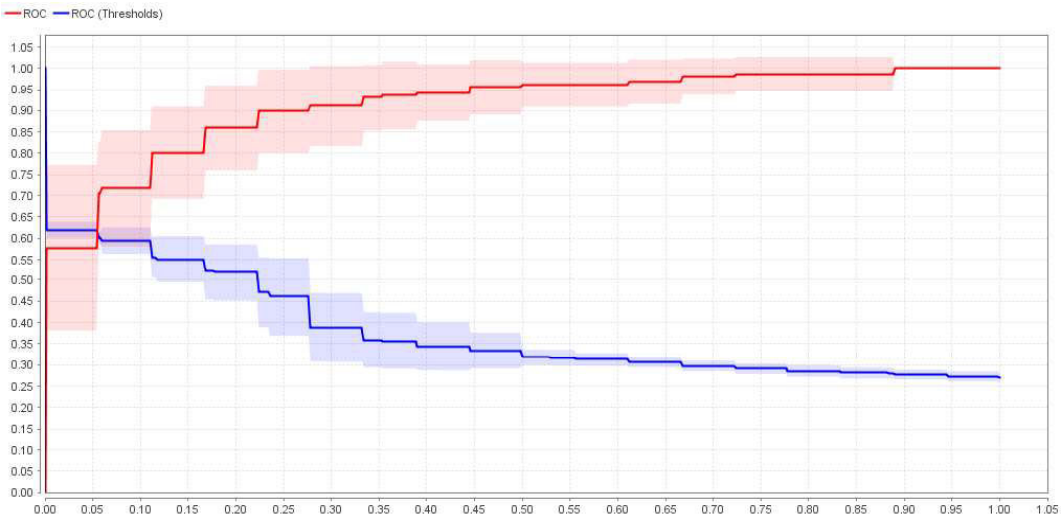

Figure A.20: Validation ROC, Dataset E, RF

8

A.2.2 Artificial Neural Network

Dataset A

	IDHn	IDHy	*PRC*
$\widehat{\text{IDHn}}$	387	76	83.59%
$\widehat{\text{IDHy}}$	118	424	78.23%
RCL	76.63%	84.80%	

Table A.24: Validation confusion matrix, Dataset A, ANN

	IDHn	IDHy	*PRC*
$\widehat{\text{IDHn}}$	49	12	80.33%
$\widehat{\text{IDHy}}$	5	46	90.20%
RCL	90.74%	79.31%	

Table A.25: Independent test confusion matrix, Dataset A, ANN

Sample	Accuracy	AUC	f-Measure
Validation	$80.69\% \pm 3.57\%$	0.869 ± 0.041	$81.41\% \pm 3.13\%$
Indipendent	84.82%	0.898	84.40%

Table A.26: Performance summary, Dataset A, ANN

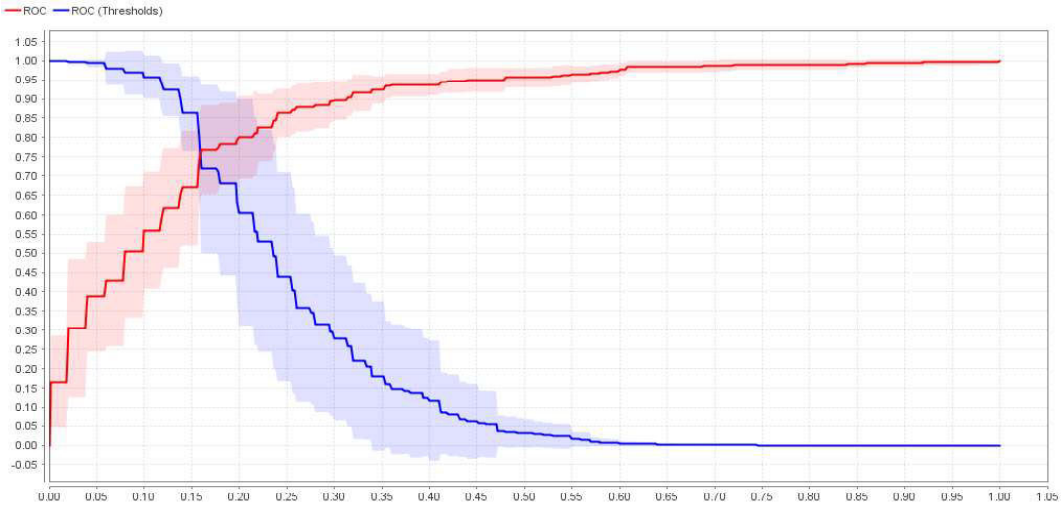

Figure A.21: Validation ROC, Dataset A, ANN

Dataset B

	IDHn	IDHy	*PRC*
$\widehat{\text{IDHn}}$	265	60	81.54%
$\widehat{\text{IDHy}}$	85	260	75.36%
RCL	75.71%	81.25%	

Table A.27: Validation confusion matrix, Dataset B, ANN

	IDHn	IDHy	*PRC*
$\widehat{\text{IDHn}}$	26	7	78.79%
$\widehat{\text{IDHy}}$	10	31	75.61%
RCL	72.22%	81.58%	

Table A.28: Independent test confusion matrix, Dataset A, ANN

Sample	Accuracy	AUC	f-Measure
Validation	$78.36\% \pm 3.61\%$	0.858 ± 0.024	$78.14\% \pm 3.92\%$
Indipendent	77.03%	0.846	78.48%

Table A.29: Performance summary, Dataset B, ANN

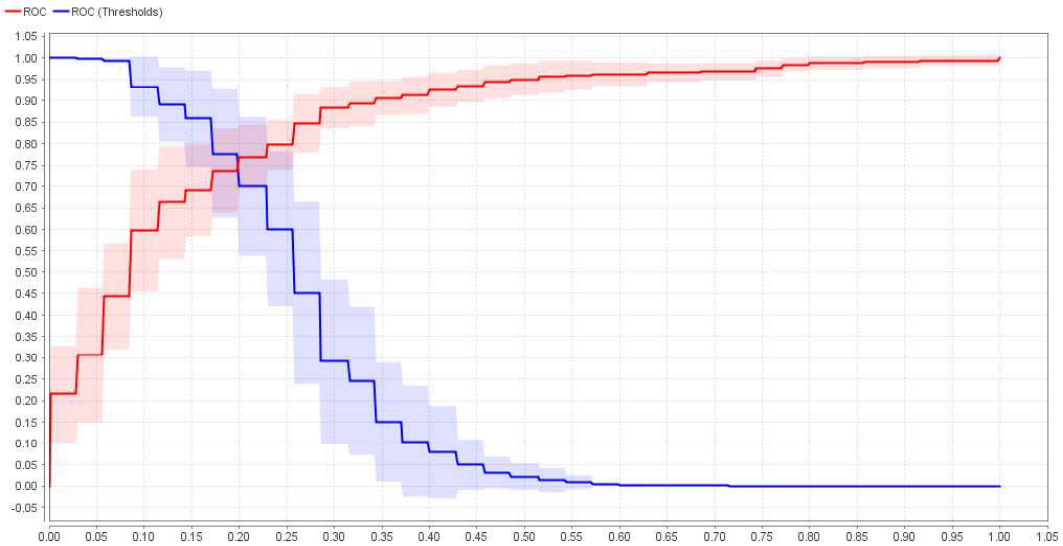

Figure A.22: Validation ROC, Dataset B, ANN

Dataset C

	IDHn	IDHy	*PRC*
$\widehat{\text{IDHn}}$	131	40	76.61%
$\widehat{\text{IDHy}}$	46	112	70.89%
RCL	74.01%	73.68%	

Table A.30: Validation confusion matrix, Dataset C, ANN

	IDHn	IDHy	*PRC*
$\widehat{\text{IDHn}}$	15	6	71.43%
$\widehat{\text{IDHy}}$	2	13	86.67%
RCL	88.24%	68.42%	

Table A.31: Independent test confusion matrix, Dataset C, ANN

Sample	Accuracy	AUC	f-Measure
Validation	73.86% ± 7.05%	0.829 ± 0.060	72.30% ± 7.23%
Indipendent	77.78%	0.882	76.47%

Table A.32: Performance summary, Dataset C, ANN

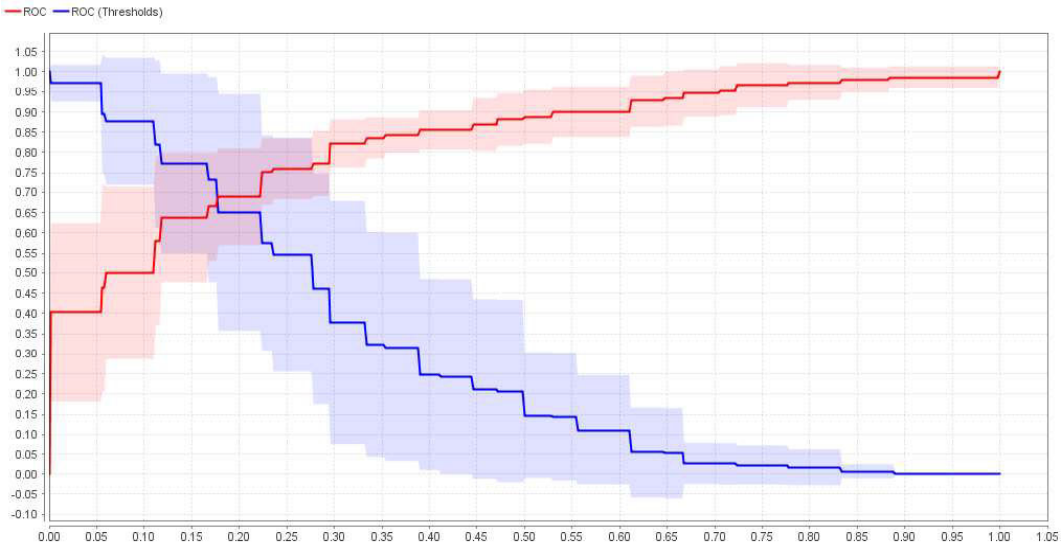

Figure A.23: Validation ROC, Dataset C, ANN

Dataset D

	IDHn	IDHy	*PRC*
$\widehat{\text{IDHn}}$	155	19	89.08%
$\widehat{\text{IDHy}}$	24	137	85.09%
RCL	86.59%	87.82%	

Table A.33: Validation confusion matrix, Dataset D, ANN

	IDHn	IDHy	*PRC*
$\widehat{\text{IDHn}}$	17	1	94.44%
$\widehat{\text{IDHy}}$	2	17	89.47%
RCL	89.47%	94.44%	

Table A.34: Independent test confusion matrix, Dataset D, ANN

Sample	Accuracy	AUC	f-Measure
Validation	$87.17\% \pm 4.39\%$	0.896 ± 0.061	$86.38\% \pm 4.63\%$
Indipendent	91.89%	0.921	91.89%

Table A.35: Performance summary, Dataset D, ANN

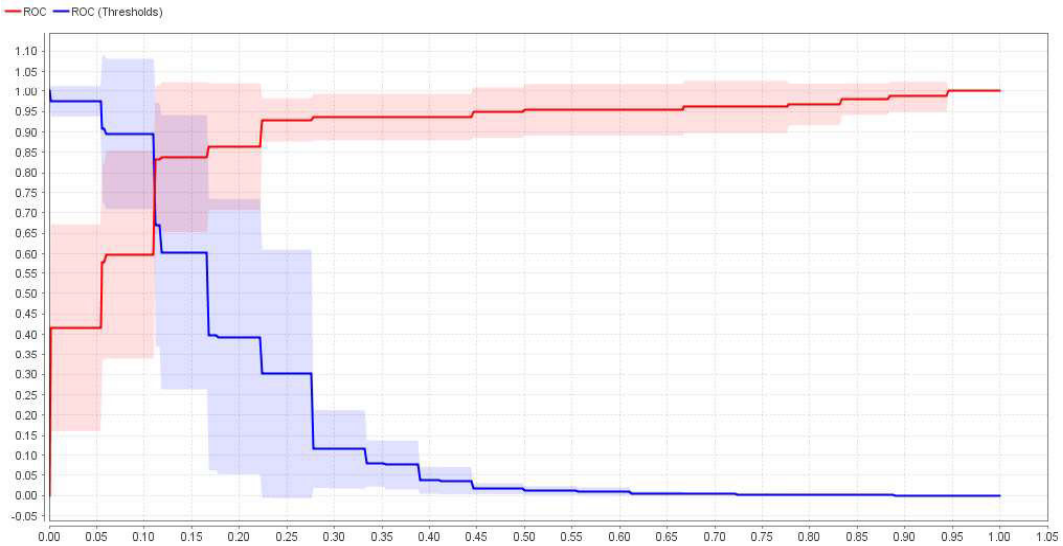

Figure A.24: Validation ROC, Dataset D, ANN

Dataset E

	IDHn	IDHy	*PRC*
$\widehat{\text{IDHn}}$	106	13	89.08%
$\widehat{\text{IDHy}}$	23	109	82.58%
RCL	82.17%	89.34%	

Table A.36: Validation confusion matrix, Dataset E, ANN

	IDHn	IDHy	*PRC*
$\widehat{\text{IDHn}}$	15	2	88.14%
$\widehat{\text{IDHy}}$	3	8	72.73%
RCL	88.33%	80.00%	

Table A.37: Independent test confusion matrix, Dataset E, ANN

Sample	Accuracy	AUC	f-Measure
Validation	$85.62\% \pm 5.15\%$	0.874 ± 0.045	$85.54\% \pm 5.64\%$
Indipendent	82.14%	0.856	76.19%

Table A.38: Performance summary, Dataset E, ANN

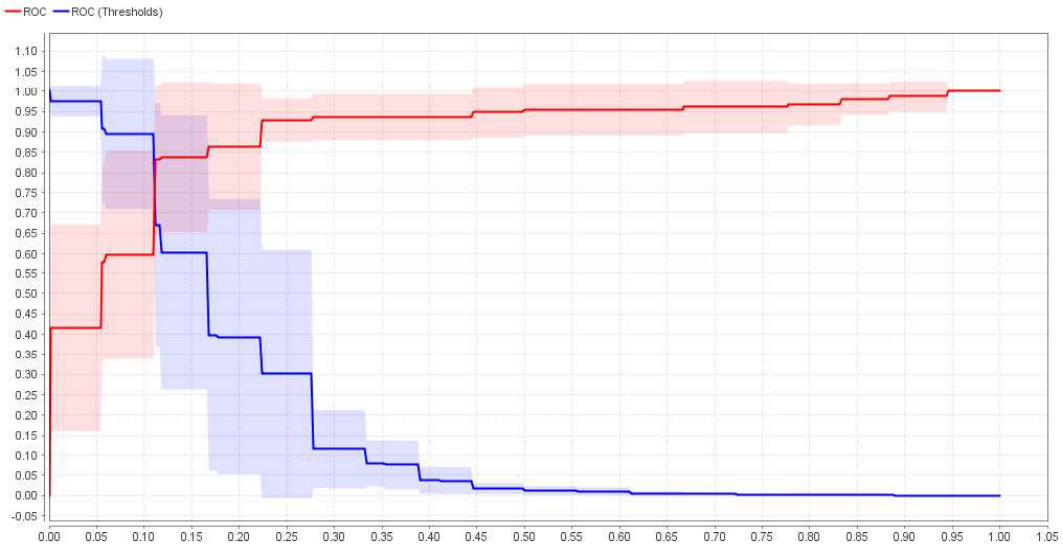

Figure A.25: Validation ROC, Dataset E, ANN

A.2.3 Support Vector Machine

Dataset A

	IDHn	IDHy	*PRC*
$\widehat{\text{IDHn}}$	433	51	83.59%
$\widehat{\text{IDHy}}$	67	454	78.23%
RCL	86.60%	89.90%	

Table A.39: Validation confusion matrix, Dataset A, SVM

	IDHn	IDHy	*PRC*
$\widehat{\text{IDHn}}$	52	2	96.30%
$\widehat{\text{IDHy}}$	7	51	87.93%
RCL	88.14%	96.23%	

Table A.40: Independent test confusion matrix, Dataset A, SVM

Sample	Accuracy	AUC	f-Measure
Validation	$88.26\% \pm 2.80\%$	0.948 ± 0.020	$88.52\% \pm 2.66\%$
Indipendent	91.96%	0.965	91.89%

Table A.41: Performance summary, Dataset A, SVM

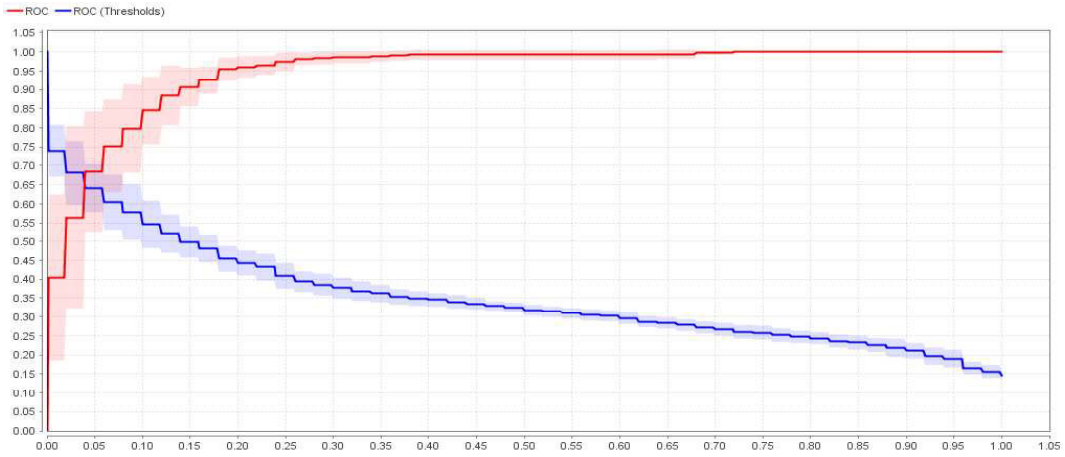

Figure A.26: Validation ROC, Dataset A, ANN

Dataset B

	IDHn	IDHy	*PRC*
$\widehat{\text{IDHn}}$	287	31	90.25%
$\widehat{\text{IDHy}}$	63	289	82.10%
RCL	82.00%	90.31%	

Table A.42: Validation confusion matrix, Dataset B, SVM

	IDHn	IDHy	*PRC*
$\widehat{\text{IDHn}}$	30	4	88.24%
$\widehat{\text{IDHy}}$	6	34	85.00%
RCL	83.33%	89.47%	

Table A.43: Independent test confusion matrix, Dataset B, SVM

Sample	Accuracy	AUC	f-Measure
Validation	$85.97\% \pm 4.96\%$	0.921 ± 0.039	$86.04\% \pm 4.71\%$
Indipendent	86.49%	0.937	87.18%

Table A.44: Performance summary, Dataset B, SVM

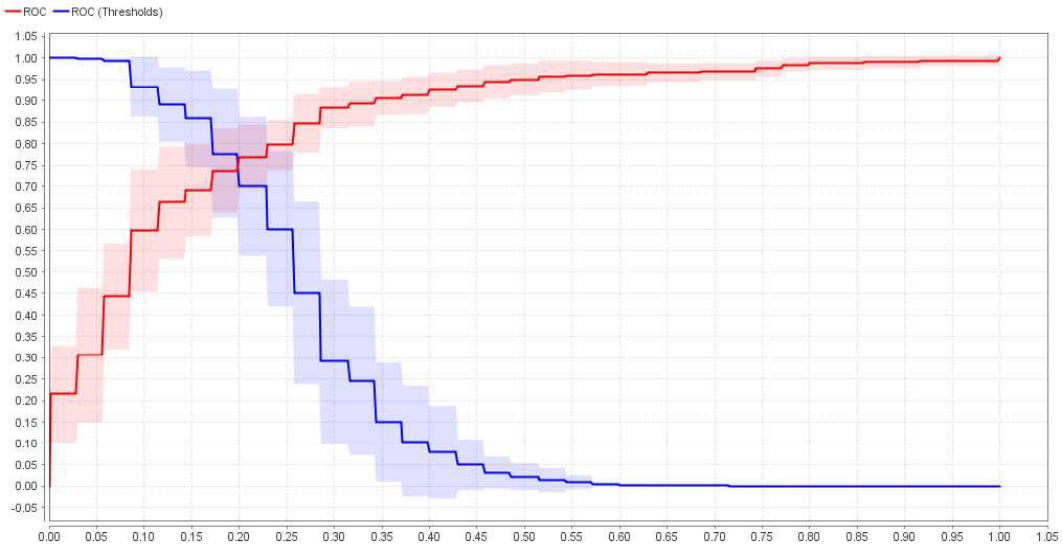

Figure A.27: Validation ROC, Dataset B, SVM

Dataset C

	IDHn	IDHy	*PRC*
$\widehat{\text{IDHn}}$	151	25	85.89%
$\widehat{\text{IDHy}}$	24	129	84.31%
RCL	86.29%	83.77%	

Table A.45: Validation confusion matrix, Dataset C, SVM

	IDHn	IDHy	*PRC*
$\widehat{\text{IDHn}}$	14	4	77.78%
$\widehat{\text{IDHy}}$	5	13	72.22%
RCL	73.68%	76.47%	

Table A.46: Independent test confusion matrix, Dataset C, SVM

Sample	Accuracy	AUC	f-Measure
Validation	$85.09\% \pm 8.01\%$	0.901 ± 0.073	$83.69\% \pm 8.97\%$
Indipendent	75.00%	0.836	74.29%

Table A.47: Performance summary, Dataset C, SVM

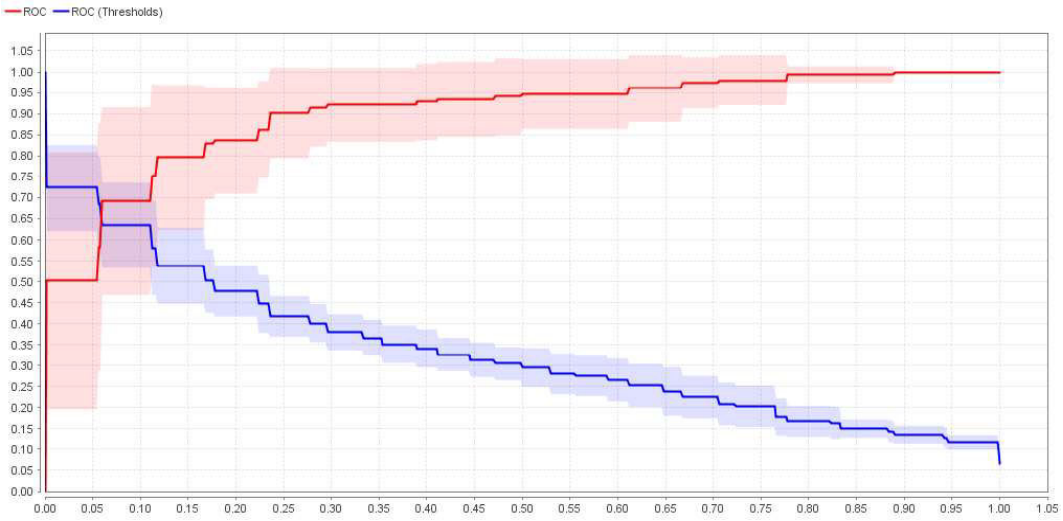

Figure A.28: Validation ROC, Dataset C, SVM

Dataset D

	IDHn	IDHy	*PRC*
$\widehat{\text{IDHn}}$	176	19	90.26%
$\widehat{\text{IDHy}}$	6	134	95.71%
RCL	96.70%	87.58%	

Table A.48: Validation confusion matrix, Dataset D, SVM

	IDHn	IDHy	*PRC*
$\widehat{\text{IDHn}}$	16	3	84.21%
$\widehat{\text{IDHy}}$	0	18	100.00%
RCL	100.00%	85.71%	

Table A.49: Independent test confusion matrix, Dataset D, SVM

Sample	Accuracy	AUC	f-Measure
Validation	$92.54\% \pm 5.02\%$	0.967 ± 0.044	$91.16\% \pm 6.21\%$
Indipendent	91.89%	0.958	92.31%

Table A.50: Performance summary, Dataset D, SVM

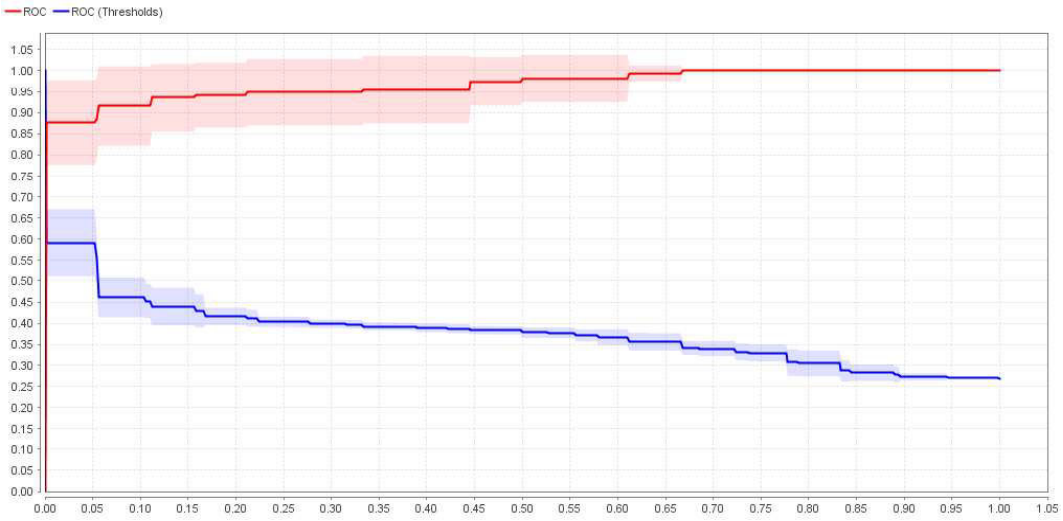

Figure A.29: Validation ROC, Dataset D, SVM

Dataset E

	IDHn	IDHy	*PRC*
$\widehat{\text{IDHn}}$	127	15	89.44%
$\widehat{\text{IDHy}}$	5	104	95.41%
RCL	96.21%	87.39%	

Table A.51: Validation confusion matrix, Dataset E, SVM

	IDHn	IDHy	*PRC*
$\widehat{\text{IDHn}}$	15	3	83.33%
$\widehat{\text{IDHy}}$	0	10	100.00%
RCL	100.00%	76.92%	

Table A.52: Independent test confusion matrix, Dataset E, SVM

Sample	Accuracy	AUC	f-Measure
Validation	$92.03\% \pm 4.38\%$	0.974 ± 0.033	$91.04\% \pm 5.28\%$
Indipendent	89.29%	0.867	89.96%

Table A.53: Performance summary, Dataset E, SVM

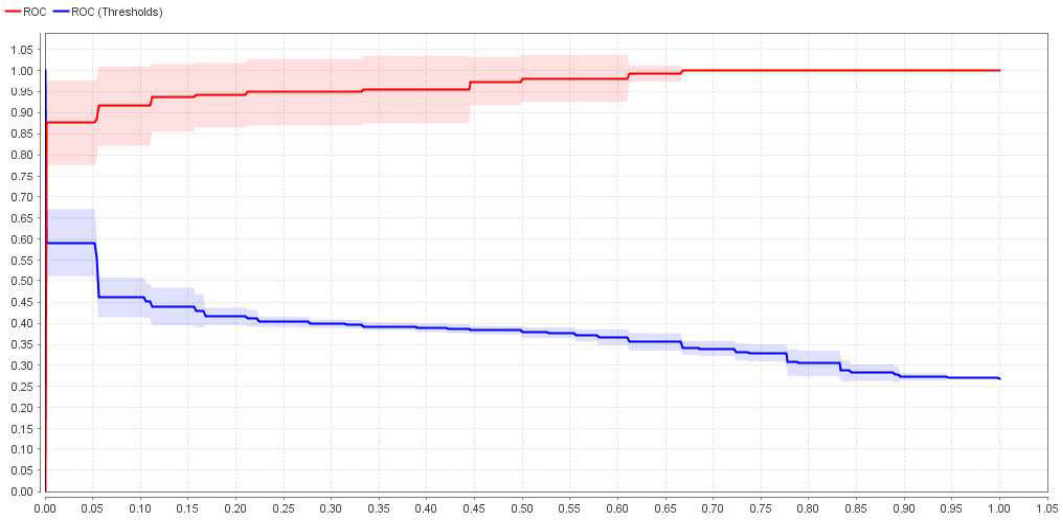

Figure A.30: Validation ROC, Dataset E, SVM

Rule Extraction

	IDHn	IDHy	*PRC*
$\widehat{\text{IDHn}}$	351	76	82.20%
$\widehat{\text{IDHy}}$	171	394	69.73%
RCL	67.24%	83.83%	

Table A.54: Confusion matrix, Synthetic Dataset, Extraction

	IDHn	IDHy	*PRC*
$\widehat{\text{IDHn}}$	148	34	81.32%
$\widehat{\text{IDHy}}$	41	157	79.29%
RCL	78.31%	82.20%	

Table A.55: Confusion matrix, Independent Dataset, Testing

Sample	Accuracy	AUC	f-Measure
RuleExtraction	$75.10\% \pm 4.31\%$	0.755 ± 0.042	$76.13\% \pm 3.92\%$
RuleTesting	80.26%	0.792	80.72%

Table A.56: Performance summary, Rule Extraction

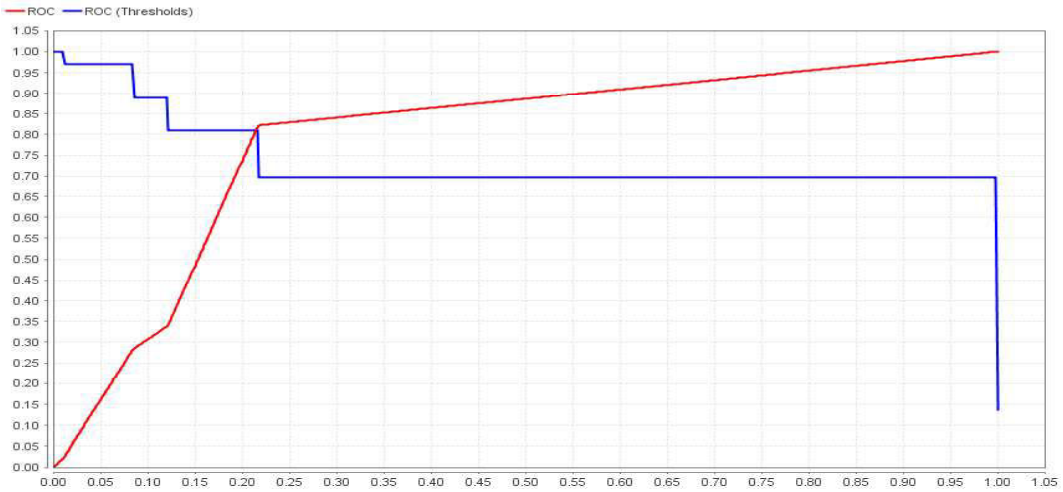

Figure A.31: Rule Testing, Independent Dataset